Electronic Supplementary Information

Molecular photo-charge-separators enabling single-pigment-driven multi-electron transfer and storage leading to H$_2$ evolution from water

Kyoji Kitamoto,[1,2] Makoto Ogawa,[1] Gopalakrishnan Ajayakumar,[1] Shigeyuki Masaoka,[1] Heinz-Bernhard Kraatz[3,4] and Ken Sakai[1,2,5]*

[1]Department of Chemistry, Faculty of Sciences, Kyushu University, 744 Motooka Nishi-ku, Fukuoka 819-0395, Japan.

[2]International Institute for Carbon-Neutral Energy Research (WPI-I2CNER), Kyushu University, 744 Motooka, Nishi-ku, Fukuoka 819-0395, Japan.

[3]Department of Physical and Environmental Sciences, University of Toronto Scarborough, 1265 Military Trail, Toronto, Ontario M1C 1A4, Canada.

[4]Department of Chemistry, University of Toronto, 80 St. George Street, Toronto, Ontario M5S 3H6, Canada.

[5]Center for Molecular Systems (CMS), Kyushu University, 744 Motooka Nishi-ku, Fukuoka 819-0395, Japan.

Experimental Section

Materials

A 2.0 M methylamine solution in tetrahydrofuran (THF) was purchased from Watanabe Chemical Industries. PVP-protected colloidal Pt (2 nm in particle size) was purchased from Tanaka Holdings Co., Ltd. All other chemicals and solvents were purchased from Kanto Chemicals Co., Inc. and used without further purification. **4,4'-MV4**$(PF_6)_8 \cdot 5H_2O$,[1] **5,5'-MV4**$(PF_6)_8 \cdot 3H_2O$,[2] [Ru(bpy)$_2$(**5,5'-MV4**)]$(PF_6)_{10} \cdot H_2O$,[2] 4,4'-dicarboxy-2,2'-bipyridine,[3] [Ru(**5,5'-ME2**)$_3$]$(PF_6)_2 \cdot H_2O$ (**5,5'-ME2** = 5,5'-bis(N-methylcarbamoyl)-2,2'-bipyridine),[4] cis-RuCl$_2$(DMSO)$_4$[5] (DMSO = dimethyl sulfoxide), [Ru(bpy)$_3$]$(NO_3)_2 \cdot 3H_2O$,[6] and MV$(NO_3)_2$[6] were synthesized as previously described.

Synthesis of [Ru(4,4'-MV4)$_3$]$(PF_6)_{26} \cdot 12H_2O$.

A solution of cis-RuCl$_2$(DMSO)$_4$ (24 mg, 0.050 mmol) and **4,4'-MV4**$(PF_6)_8 \cdot 5H_2O$ (0.490 mg, 0.195 mmol) in a water–ethanol mixture (1:1 v/v, 10 mL) was refluxed under Ar for 48 h, while the reaction progress was monitored spectrophotometrically. After cooling to room temperature, the reaction mixture was filtered to remove insoluble materials. To the filtrate was added water (ca. 5 mL), followed by concentration by evaporation in order to remove most of ethanol. To the resulting solution was added saturated aqueous NH$_4$PF$_6$, (ca. 0.5 mL), resulting in prompt deposition of the product as a reddish brown solid, which was collected by filtration. The crude product was purified on a Sephadex LH-20 column (ca. 60 cm) using acetonitrile:methanol (1:1 v/v) as an eluent. The first red band was collected and dried in vacuo to give a pure product as a dark red solid (yield: 251 mg, 63.7 %). ^{1}H NMR (CD$_3$CN/TMS (TMS = tetramethylsilane), 20 °C, ppm): δ 9.02 (s, 6H), 8.91-8.83 (m, 48H), 8.43-8.38 (m, 48H), 7.92-7.87 (m, 12H), 7.70 (s, 6H), 7.06 (s, 6H), 6.66 (s, 6H), 4.83-4.61 (m, 30H), 4.41 (s, 36H), 3.81-3.64 (m, 24H), 2.77-2.61 (m, 12H); Anal. Calcd for C$_{216}$H$_{234}$F$_{156}$N$_{48}$O$_{18}$P$_{26}$Ru·12H$_2$O (7876.79): C 32.94, H 3.30, N 8.54; found: C, 33.16; H, 3.21; N, 8.56, where the number of water solvate was calibrated based on the integrated intensity ratios of the ^{1}H NMR signals (averaged for three separately prepared samples).

Synthesis of [Ru(5,5'-MV4)$_3$]$(PF_6)_{26} \cdot 9H_2O$.

Prepared as described above for [Ru(**4,4'-MV4**)$_3$]$(PF_6)_{26} \cdot 12H_2O$ substituting **5,5'-MV4**$(PF_6)_8 \cdot 3H_2O$ (495 mg, 0.195 mmol) for **4,4'-MV4**$(PF_6)_8 \cdot 5H_2O$ (yield: 237 mg, 60.5 %). ^{1}H NMR (CD$_3$CN/TMS, 20 °C, ppm) : δ 8.99-8.86 (m, 48H), 8.66 (m, 6H), 8.39 (m, 54H), 8.11-7.95 (m, 6H), 7.71-7.06 (m, 6H), 6.96-6.87 (m, 6H), 6.68-6.61 (m, 6H), 4.84-4.63 (m, 30H), 4.41 (s, 36H), 3.78-3.60 (m, 24H), 2.56-2.50 (m, 12H); Anal. Calcd for C$_{216}$H$_{234}$F$_{156}$N$_{48}$O$_{19}$P$_{26}$Ru·9H$_2$O (7822.74): C 33.16, H 3.25, N 8.59; found: C 33.55, H 3.27, N 8.67, where the number of water solvate was calibrated based

on the integrated intensity ratios of the ^{1}H NMR signals (averaged for three separately prepared samples).

Synthesis of 4,4'-bis(N-methylcarbamoyl)-2,2'-bipyridine (4,4'-ME2). To a solution of 2,2'-bipyridine-4,4'-dicarboxylic acid (0.16 g, 0.655 mmol) in thionyl chloride (10 mL) was added a drop of dry dimethylformamide (DMF) followed by refluxing for 2 h with stirring. After the reaction mixture was cooled to room temperature, thionyl chloride and DMF were removed under reduced pressure to give the bis(chlorocarbonyl) derivative, which was dissolved in dry THF (25 mL) followed by addition of a 2.0 M methylamine solution in THF (2.0 mL). The solution was refluxed for 5 h. The resulting yellow precipitate was collected by filtration, washed several times with water, and dried in vacuo (yield: 145 mg, 79.2 %). ^{1}H NMR (DMSO-d_6/TMS, 20 °C, ppm): δ 8.92 (d, J = 4.1 Hz, 2H), 8.86 (d, J = 4.8 Hz, 2H), 8.79 (s, 2H), 7.84 (dd, J = 4.8, 2.0 Hz, 2H), 2.84 (d, J = 4.1 Hz, 6H); ESI-TOF MS: m/z = 271.20 [M + H]$^+$ (Calcd for $C_{14}H_{14}N_4O_2$: 271.29); Anal. Calcd for $C_{14}H_{14}N_4O_2 \cdot 0.5H_2O$ (279.30): C, 60.21; H, 5.41; N, 20.06; found: C, 60.50; H, 5.29; N, 19.78.

Synthesis of [Ru(4,4'-ME2)$_3$](PF$_6$)$_2$·2H$_2$O. Prepared as described above for [Ru(**4,4'-MV4**)$_3$](PF$_6$)$_{26}$·12H$_2$O by reacting cis-RuCl$_2$(DMSO)$_4$ (40.5 mg, 0.0836 mmol) and 4,4'-bis(N-methylcarbamoyl)-2,2'-bipyridine (**4,4'-ME2**) (93.4 mg, 0.334 mmol) in a water-ethanol mixture (1 : 1 v/v, 20 mL) under Ar for 20 h to give a product as a dark red solid (yield: 70.8 mg, 68.4 %). ^{1}H NMR (CD$_3$CN/TMS, 20 °C, ppm): δ 8.91 (d, J = 2.0 Hz, 6H), 7.82 (d, J = 6.2 Hz, 6H), 7.68 (dd, J = 5.5, 2.0 Hz, 6H), 2.93 (d, J = 4.9 Hz, 18H); ESI-TOF MS: m/z = 1057.42 [M − PF$_6$]$^+$ (Calcd for $C_{42}H_{42}F_6N_{12}O_6PRu$: 1057.19), m/z = 456.11 [M − 2PF$_6$]$^{2+}$ (Calcd for $C_{42}H_{42}N_{12}O_6Ru$: 912.38); Anal. Calcd for $C_{42}H_{42}F_{12}N_{12}O_6P_2Ru \cdot 2H_2O$ (1237.89): C, 40.75; H, 3.75; N, 13.58; found: C, 40.65; H, 3.73; N, 13.38.

General Methods.

^{1}H NMR spectra were acquired on a JEOL JNM-ESA 600 spectrometer. ESI-TOF mass spectra were recorded on a JEOL JMS-T100CS spectrometer. UV-vis and UV-vis-NIR spectra were recorded on Shimadzu UV-2600 and UV-3600 spectrophotometer, respectively. Luminescence spectra were recorded on a Shimadzu RF-5300PC spectrofluorophotometer. Emission decays were recorded on a HORIBA FluoroCube 3000USKU using a HORIBA N-470L diode laser (472 nm) as an excitation source. Luminescence quantum yields were determined using a Hamamatsu C9920-02 absolute photoluminescence quantum yield measurement system equipped with a 150 W Xe lamp coupled to a monochromator for wavelength discrimination, an integrating sphere as a sample chamber, and a Hamamatsu C10027-01 multichannel detector for

signal detection. Nanosecond laser flash photolysis experiments were carried out using a Unisoku TSP-1000M-03R system equipped with a Nd:YAG laser (Minilite II-10, Continuum, CA, USA) as a pump source and a 150 W Xe lamp (L2195, Hamamatsu) as a probe source. Transient absorption spectra were recorded using multichannel detector with a gated image-intensifer (C954603, Hamamatsu), while single-wavelength transient absorption traces were monitored using an amplified photomultiplier tube (R2949, Hamamatsu). Molar conductivity measurements were carried out at 20 °C in water using a TOA CM-20S conductometer with a TOA CG-511B conductivity cell having a cell constant of 0.969 cm^{-1}. Analysis of multi-step ion-pair formation equilibria was carried out based on our published procedures.[2] Square wave voltammograms were recorded on a BAS ALS Model 6022D electrochemical analyser, using a three electrode system consisting of a platinum working electrode, a platinum wire counter electrode, and a Ag/Ag$^+$ reference electrode (0.249 V vs. SCE), where TBAH (tetra(n-butyl)ammonium hexafluorophosphate) was used as a supporting electrolyte and all potentials reported were standardized by simultaneously observing the Fc/Fc$^+$ couple (Fc/Fc$^+$ = 0.155 V vs. SCE).

In Situ ESR Studies. ESR spectra were acquired on a JEOL JES-FA200 ESR spectrometer equipped with a EFM 2000AX NMR field meter (ECHO Electronic Co. Ltd.) for field calibration, using a ES-LC12 quartz flat cell (60 mm x 10 mm x 0.3 mm) for aqueous sample measurements. The spectra of monoradical species (MV$^+$•), in situ generated by photolysis, were measured under Ar atmosphere at room temperature by careful exclusion of O$_2$ which immediately quenches radicals (MV$^+$• + O$_2$ → MV^{2+} + O$_2^-$•). Photolysis was performed using an Asahi Spectra MAX-303 300 W Xe lamp equipped with a visible mirror module (λ = 385-740 nm) with the light intensity diminished to 50% (ND filter). Radicals are also quite sensitive to the metallic impurities over the glassware surfaces since they can catalyze water reduction (2MV$^+$• + 2H$^+$ → 2MV^{2+} + H$_2$). Therefore, the quartz cell was sufficiently cleaned by soaking in aqua regia prior to the use. The spin density of the monoradical site generated over the charge-separators was calibrated by measuring the ESR intensity of MV$^+$• generated by photoirradiating the EDTA/[Ru(bpy)$_3$]$^{2+}$/MV^{2+} solution under the same experimental conditions, where calibration also relied on the concentrations of monoradical separately determined by in situ absorption spectroscopy performed under the same conditions (Fig. S9). The concentration of the monoradical site in the charge-separators were determined by spectral deconvolution as noted above.

Photochemical H$_2$ Evolution Experiments. Visible light irradiation (400 < λ < 800 nm) was carried out using an ILC Technology CERMAX LX-300 Xe lamp (300 W) equipped with a

CM-1 cold mirror which suppresses UV and NIR irradiation. Photolysis was carried out in a Pyrex glass vial (ca. 20 mL in inner volume), immersed in a water bath thermostatted at 20 °C, and each photolysis solution (10 mL) was continuously purged with Ar (10 mL/min; STEC SEC-E40/PAC-D2 digital mass flow controller) with stirring. The vent gas was introduced into our computer-controlled automated gas chromatographic analysis line (Shimadzu GC-8A gas chromatograph equipped with a molecular sieve 5A column (2 m x 3 mm i.d.; 30 ºC) with an Ar carrier), the details for which have been described elsewhere.[7]

Molecular-Mechanics and Quantum-Mechanical Calculations. Molecular modeling studies were carried out using SCIGRESS (version 2; Fujitsu Limited, 2009).[8] Energy-minimized structures were located using molecular mechanics calculations (MM3),[9–11] where electrostatic interactions were taken into consideration by approximating that two positive charges on each viologen cation are respectively located at the pyridinium nitrogen centres and a negative charge on each PF_6^- anion at the phosphorous centre.

Density functional theory (DFT) calculations were performed using the Gaussian 09 package of programs[12] in order to understand the structural and spin-state candidates for the π-dimers given by stacking of singly reduced viologen derivatives. Calculations were also performed to simulate the UV-Vis-NIR absorption spectra of the candidates computed. For this purpose, we adopted a model compound given by condensation of N-acetyl-aspartic acid (CH_3–CONH–CH(CH_2–COOH)–COOH) and two equivalents of one-electron-reduced N-methyl-N'-(2-aminoethyl)-4,4'-bipyridinium cations (abbreviated as H_2N–CH_2–MV^+); that is, CH_3–CONH–CH(CH_2–CONH–CH_2–MV^+)–CONH–CH_2–MV^+, noted as Asp-based $(MV^+)_2$. Calculations were also performed for the simplest model of a π-dimer given by stacking of one-electron-reduced N,N'-dimethyl-4,4'-bipyridinium cations, noted as non-derivatized $(MV^+)_2$. The structures were fully optimized using the M06 hybrid functional, developed by Truhlar *et al.*,[13–15] and the 6-31G** basis set with the effects of solvation in water taken into consideration using polarizable continuum model (PCM).[16–18] We experienced that calculations using M06 with PCM afford quite reasonable geometries involving this type of weak π-π stacking and/or bonding interactions. Spin-unrestricted UM06 theory was used for triplet states, while spin-restricted and -unrestricted methods (i.e., M06 and UM06) were respectively employed for closed- and open-shell singlet states. Particularly, UM06 calculations (Guess=Mix) in broken symmetry (BS) were performed for the open-shell singlet states. For such BS singlet-state calculations, spin contamination is exhibited by nonzero values for the spin-squared expectation value, defined with $\langle S^2 \rangle = S(S+1)$, where S is the molecular spin quantum number. Actually, the spin-squared expectation values after spin annihilation were in the range $\langle S^2 \rangle = 0.0026$–$0.0703$, confirming that spin contamination of the triplet state is

negligibly small. These support the validity of the BS approach for these open-shell singlet states without employing the spin-projected methods eliminating the redundant spin contaminations. For the non-derivatized $(MV^+)_2$, two types of stacking geometries, eclipsed and staggered ones, were realized for all three possible spin states with the triplet only 1–2 kcal/mol higher in energy. When the Asp-based $(MV^+)_2$ was optimized for an eclipsed conformation, only the closed-shell singlet preserved the eclipsed conformation at the end of optimization, while the other two spin states resulted in slipped conformations of two MV^+ moieties. When the Asp-based $(MV^+)_2$ was optimized for the staggered conformation, all spin states preserved the conformation with the triplet similarly higher than the others in energy. All stationary points were characterized by their harmonic vibrational frequencies as minima. The unscaled frequencies were used to compute the zero-point vibrational energy corrections to the energies. For all the candidates computed, electronic excited states were calculated by the TD-DFT method as implemented in Gaussian 09[19–21] with use of the functional and the basis set described above. For each candidate, a sufficient number of excited states were calculated so that spectral simulation covers the wavelength range down to around 200 nm. The calculated transitions were replaced by a Gaussian broadening function with a full width at half maximum height of 0.2 eV to simulate the electronic transition spectrum. Molecular orbital pictures were generated using GaussView 5.0.[22]

The choice of basis set (6-31G**) was confirmed to be valid within the scope of our study by testing the results computed using a larger basis set. For instance, the M06/6-311+G(2d,p)/PCM level of calculations afford optimized geometry consistent with that computed at the M06/6-31G**/PCM level (Fig. S19). Moreover, the spectral features simulated using the TD-DFT results given by these two different calculation levels are essentially same (Figs. S20a-c). Consequently, the 6-31G** basis set was adopted in all calculations in order to minimize the computational time and cost available.

Monte Carlo Simulation of CS Lifetimes. The simulation program has been coded in Pascal using Delphi ver. 5.0 and is available for any purposes at the authors' website:

http:// www.scc.kyushu-u.ac.jp/Sakutai/softwares//cs_lifetime_vs_migration.zip

This program supposes that several equivalent branches involving a few equivalent viologen acceptor sites are tethered to a single $Ru(bpy)_3^{2+}$-type photosensitizer, as depicted in Fig. 4a. The test case defined in Fig. 4a supposes that one branch has interaction with two equivalent branches. Even after conducting an inter-branch ET event, an exactly same situation is supposed to be recovered. Therefore, three branches, in this case, should be positioned in a trigonal

fashion. Our model also supposes that locations of two MV^{2+}/MV^+ sites within a branch are rapidly exchanged or moving around so that inter-branch ET toward every adjacent branch can take place with an equal probability. Under such conditions, ET events can be classified into three types, intra-branch ET, inter-branch ET, and BET, as illustrated in the above picture. Our model supposes that probabilities of conducting these three ET events are different. Here the frequency factors for intra-branch ET, inter-branch ET, and BET are defined by (n_intra) x (intra_ff), (n_inter) x (inter_ff), and 1, respectively, where n_intra defines the number of adjacent viologen units within the branch which has already accepted one electron from the photoexcited pigment, and n_inter is the number of equivalent adjacent branches available for ET, while intra_ff and inter_ff are used to further tune the probabilities of intra-branch and inter-branch ET processes, respectively. Note that the frequency factor of BET is not defined as a variable parameter and is fixed as unity in this model. In the model depicted above, n_intra and n_inter must be specified as 1 and 2, respectively. In the experiments in Fig. 4b, intra_ff = 4 and inter_ff = 10 are adopted as roughly optimized values to reproduce the experimentally observed CS decay profiles. When the CS decay profile of $[Ru(\mathbf{x,x'}\text{-}\mathbf{MV4})_3]^{26+}$ is examined, an appropriate model can be defined by supposing n_intra = 1, n_inter = 4, intra_ff = 4, and inter_ff = 10, by which the probabilities of conducting intra-branch ET, inter-branch ET, and BET are given as (n_intra x intra_ff)/{(n_intra x intra_ff) + (n_inter x inter_ff) + 1} = 4/45, (n_inter x inter_ff)/{(n_intra x intra_ff) + (n_inter x inter_ff) + 1} =40/45, and 1/45, respectively. In these experiments, three additional parameters are defined. One is a permeation coefficient (κ_{BET}) when conducting BET and is defined as κ_{BET} = 1/3. On the other hand, the permeation coefficient (κ_{EM}) for conducting all the remaining ET events leading to EM is also defined as unity (κ_{EM} = 1 for intra_branch and inter_branch ET events). These specify that the probability of having a BET event is (1/45)x(1/3) = 1/135 in each step, while that of having a migration event is 44/45. A set of parameters defined with n_intra = 1, n_inter = 0, intra_ff = 4, and inter_ff = 10 is appropriate to examine the behavior of $[Ru(bpy)_2(\mathbf{5,5'}\text{-}\mathbf{MV4})]^{10+}$ since the inter-branch ET among the 5,5'-positioned branches can be ruled out. The last parameter is the time spent to complete each ET step (t_{div}). This include the time spent for diffusion, and is postulated as t_{div} = 6 ns in these test cases. In summary, by using the values listed below, the lifetimes of a hundred thousand of CS states were generated by the Monte Carlo technique. As a result, the computed results somehow reflect the observed tendency, which strengthens the validity of such statistical approach in predicting electron migration within a multi-acceptor system.

Parameters employed for the calculations given Fig. 4b:

n_intra = 1   no. of other MV^{2+} units within the branch accepted one electron

n_inter = 0, 1, 2, 3, 4   no. of adjacent branches available for ET

intra_ff = 4***   frequency factor to conduct intra-branch ET

inter_ff = 10   frequency factor to conduct inter-branch ET

κ_{BET} = 1/3   permeation coefficient for conducting BET

κ_{EM} = 1   permeation coefficient for conducting self exchange among MV^+ and MV^{2+}

t_{div} = 6 ns   time spent for completing each step

*** The lower intra_ff value relative to inter_ff may be due to the fact that stronger association of a PF_6^- anion within each branch makes the intra-branch ET more difficult to proceed in compared with the inter-branch ET process.
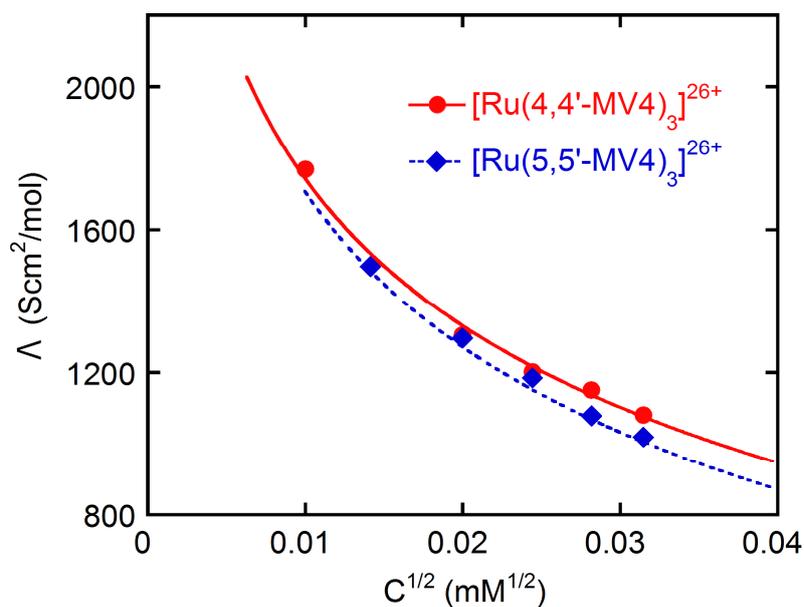
Figure S1. The observed and calculated molar conductivity vs. the square root of the total PCS concentration (C_t), measured for [Ru(**4,4'-MV4**)$_3$](PF$_6$)$_{26}$ and [Ru(**5,5'-MV4**)$_3$](PF$_6$)$_{26}$. The solid and dashed lines show the fitting based on our published methods.[2]

Table S1. The observed molar conductivity of PCSs in water vs. the square root of the total concentration (C_t), measured in air at 20 ^{o}C.

Complex	$C_t^{1/2}$ (mM$^{1/2}$)	Λ (Scm^{2}mol^{-1})
[Ru(**4,4'-MV4**)$_3$]$^{26+}$	0.03147	1081
	0.02817	1151
	0.02442	1202
	0.01996	1304
	0.009995	1769
[Ru(**5,5'-MV4**)$_3$]$^{26+}$	0.03147	1019
	0.02817	1079
	0.02442	1185
	0.01996	1296
	0.01413	1498

Table S2. The α values, the stepwise formation constants (K_n), and the total stability constants (β_n) used to simulate the ion-pair formation behaviours shown in Fig. S1, α is defined as $\alpha = K_n/K_{n-1}$ and is approximated to be constant; see ref. 2.

Params	$[Ru(\textbf{4,4'-MV4})_3]^{26+}$	$[Ru(\textbf{5,5'-MV4})_3]^{26+}$
α	0.67	0.69
K_1 (β_1)	2.000×10^5 (2.0×10^5)	1.500×10^5 (2.0×10^5)
K_2 (β_2)	1.340×10^5 (2.68×10^{10})	1.035×10^5 (1.553×10^{10})
K_3 (β_3)	89780 (2.406×10^{15})	71420 (1.109×10^{15})
K_4 (β_4)	60150 (1.447×10^{20})	49280 (5.463×10^{19})
K_5 (β_5)	40300 (7.416×10^{24})	34000 (1.858×10^{24})
K_6 (β_6)	27000 (1.575×10^{29})	23460 (4.358×10^{28})
K_7 (β_7)	18090 (2.85×10^{33})	16190 (7.055×10^{32})
K_8 (β_8)	12120 (3.454×10^{37})	11170 (7.880×10^{36})
K_9 (β_9)	8121 (2.805×10^{41})	7707 (6.073×10^{40})
K_{10} (β_{10})	5441 (1.526×10^{45})	5318 (3.229×10^{44})
K_{11} (β_{11})	3645 (5.565×10^{48})	3669 (1.185×10^{48})
K_{12} (β_{12})	2443 (1.359×10^{52})	2531 (3.000×10^{51})
K_{13} (β_{13})	1637 (2.224×10^{55})	1747 (5.251×10^{54})
K_{14} (β_{14})	1096 (2.439×10^{58})	1205 (6.317×10^{57})
K_{15} (β_{15})	734.6 (1.792×10^{61})	831.7 (5.254×10^{60})
K_{16} β_{16})	492.2 (8.820×10^{63})	573.9 (3.015×10^{63})
K_{17} (β_{17})	329.8 (2.909×10^{66})	396.0 (1.194×10^{66})
K_{18} (β_{18})	221.0 (6.427×10^{68})	273.2 (3.263×10^{68})
K_{19} (β_{19})	148.0 (9.514×10^{70})	188.5 (6.151×10^{70})
K_{20} (β_{20})	99.19 (9.437×10^{72})	130.0 (8.001×10^{72})
K_{21} (β_{21})	66.45 (6.271×10^{74})	89.76 (7.182×10^{74})
K_{22} (β_{22})	44.52 (2.792×10^{76})	61.93 (4.448×10^{76})
K_{23} (β_{23})	29.83 (8.329×10^{77})	42.73 (1.901×10^{78})
K_{24} (β_{24})	19.99 (1.665×10^{79})	29.49 (5.605×10^{79})
K_{25} (β_{25})	13.39 (2.229×10^{80})	20.35 (1.140×10^{81})
K_{26} (β_{26})	8.972 (2.000×10^{81})	14.04 (1.601×10^{82})

Table S3. The relative abundances of the chemical species derived from the PCSs under the conditions adopted in photochemical H_2 evolution studies, where the formation constants listed in Table S2 are used to estimate the values listed in this table.

Chemical species	$[Ru(\textbf{4,4'-MV4})_3]^{26+}$ $C_t = 0.04$ mM	$[Ru(\textbf{5,5'-MV4})_3]^{26+}$ $C_t = 0.04$ mM
A^{26+}	2.40×10^{-12}	1.15×10^{-11}
AX^{25+}	2.64×10^{-10}	9.44×10^{-10}
AX_2^{24+}	1.94×10^{-8}	5.32×10^{-8}
AX_3^{23+}	9.60×10^{-7}	2.07×10^{-6}
AX_4^{22+}	3.18×10^{-5}	5.56×10^{-5}
AX_5^{21+}	7.04×10^{-4}	1.03×10^{-4}
AX_6^{20+}	1.05×10^{-2}	1.32×10^{-2}
AX_7^{19+}	1.04×10^{-1}	1.16×10^{-1}
AX_8^{18+}	6.93×10^{-1}	7.06×10^{-1}
AX_9^{17+}	3.10	2.97
AX_{10}^{16+}	9.27	8.60
AX_{11}^{15+}	18.6	17.2
AX_{12}^{14+}	25.0	23.7
AX_{13}^{13+}	22.5	22.6
AX_{14}^{12+}	13.5	14.8
AX_{15}^{11+}	5.47	6.71
AX_{16}^{10+}	1.48	2.10
AX_{17}^{9+}	2.69×10^{-1}	4.53×10^{-1}
AX_{18}^{8+}	3.23×10^{-2}	6.74×10^{-2}
AX_{19}^{7+}	2.66×10^{-3}	6.93×10^{-3}
AX_{20}^{6+}	1.45×10^{-4}	4.91×10^{-4}
AX_{21}^{5+}	5.30×10^{-6}	2.40×10^{-5}
AX_{22}^{4+}	1.30×10^{-7}	8.10×10^{-7}
AX_{23}^{3+}	2.13×10^{-9}	1.89×10^{-8}
AX_{24}^{2+}	2.34×10^{-11}	3.03×10^{-10}
AX_{25}^{+}	1.72×10^{-13}	3.36×10^{-12}
AX_{26}	8.51×10^{-16}	2.57×10^{-14}
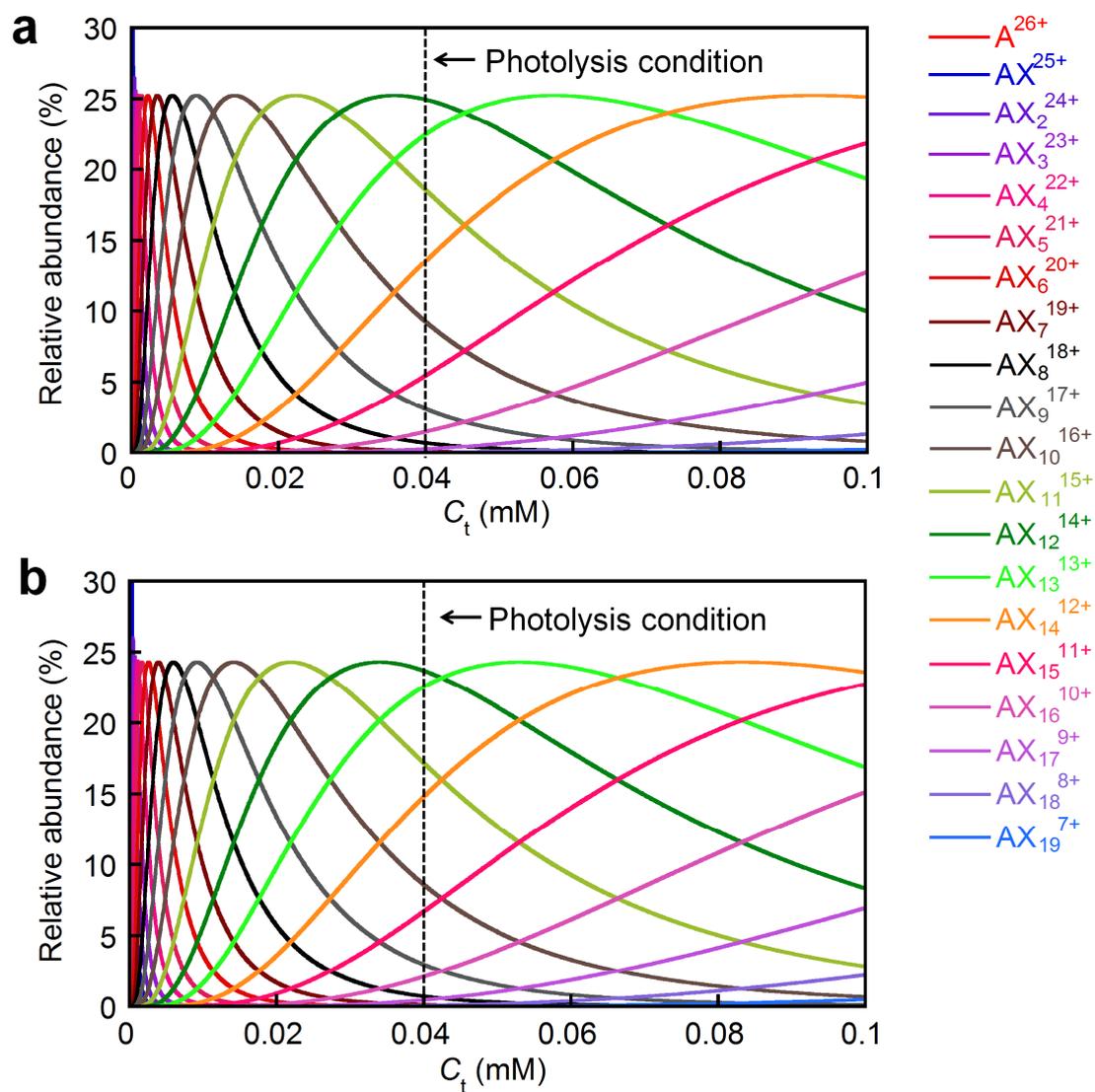
Figure S2. Relative abundances of the $AX_m^{(z-m)+}$ species ($X = PF_6^-$, m =1, 2, 3, ...) vs. C_t are calculated for (a) [Ru(**4,4'-MV4**)$_3$](PF$_6$)$_{26}$ and (b) [Ru(**5,5'-MV4**)$_3$](PF$_6$)$_{26}$ using the parameters determined for Fig. S1 (see Table S3 for details).
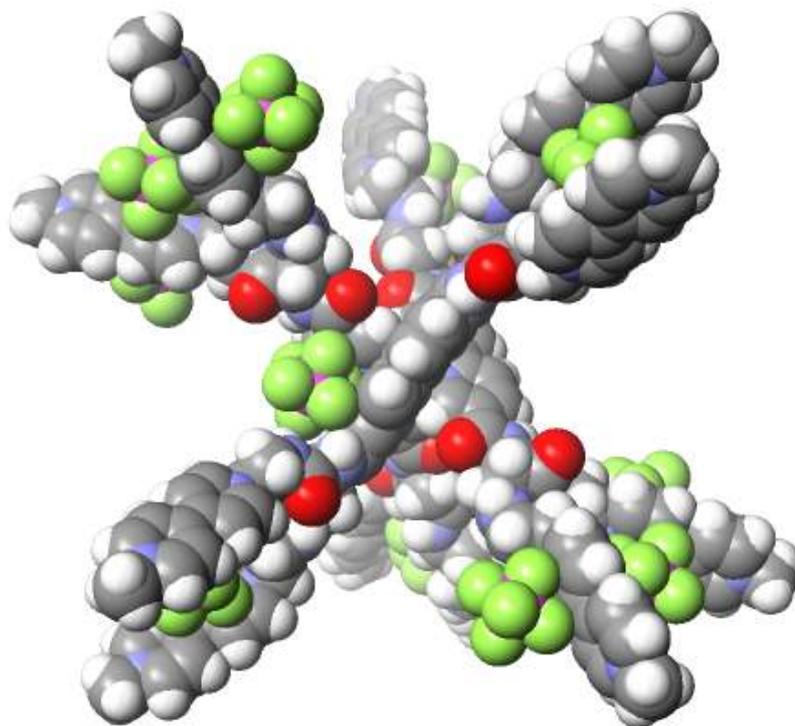
Figure S3. The space-filling model computed for one of the ion-pair adducts, {[Ru(**5,5'-MV4**)$_3$](PF$_6$)$_{12}$}$^{14+}$ (computed by MM3).
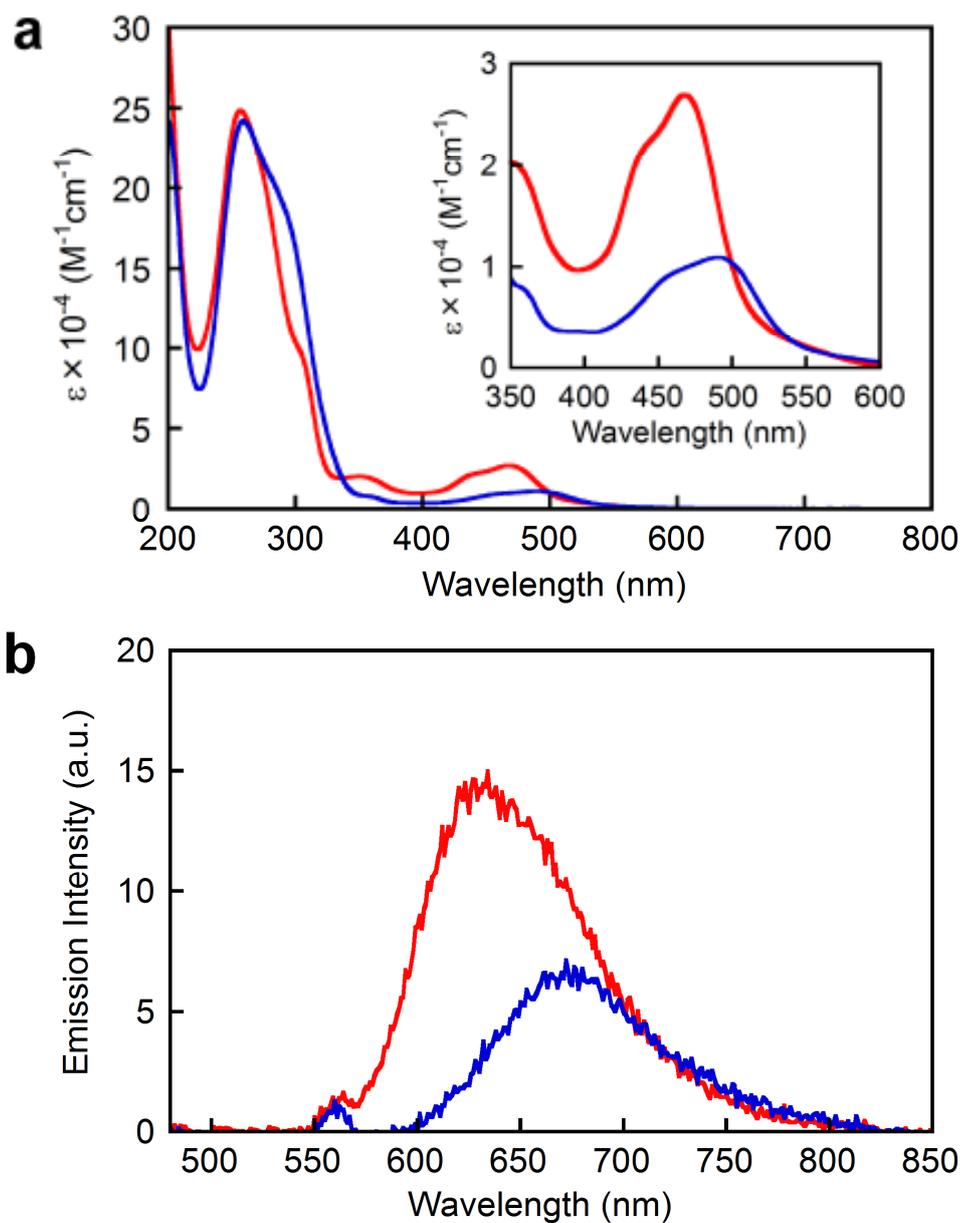
Figure S4. (a) Absorption spectra recorded for an aqueous solution of each complex at 20 ºC in air. The inset shows the magnification of the [1]MLCT bands. (b) Emission spectra recorded for an aqueous solution of each complex under Ar atmosphere at 20 °C. The excitation wavelength was 470 nm and both solutions had an equal absorbance at 470 nm (0.05). The red and blue lines correspond to the spectral data observed for [Ru(**4,4'-MV4**)₃](PF₆)₂₆ and [Ru(**5,5'-MV4**)₃](PF₆)₂₆, respectively.

Table S4. Absorption and emission properties of PCSs together with those of [Ru(bpy)$_3$]Cl$_2$·6H$_2$O.

Complex	λ_{abs} (nm)	ε (M^{-1}cm^{-1})	λ_{em} (nm)	Φ_{em}[a]
[Ru(**4,4'-MV4**)$_3$](PF$_6$)$_{26}$	468	27 100	633	0.002
	257	248 600		
[Ru(**5,5'-MV4**)$_3$](PF$_6$)$_{26}$	490	11 000	670	0.001
	259	242 300		
[Ru(bpy)$_3$]Cl$_2$·6H$_2$O[b]	452	14 000	628	0.042
	286	81 400		

[a]Emission quantum yields were determined using an absolute photoluminescence quantum yield measurement system equipped with an integrating sphere, as described in Experimental Section. [b]Values taken from ref. 23.
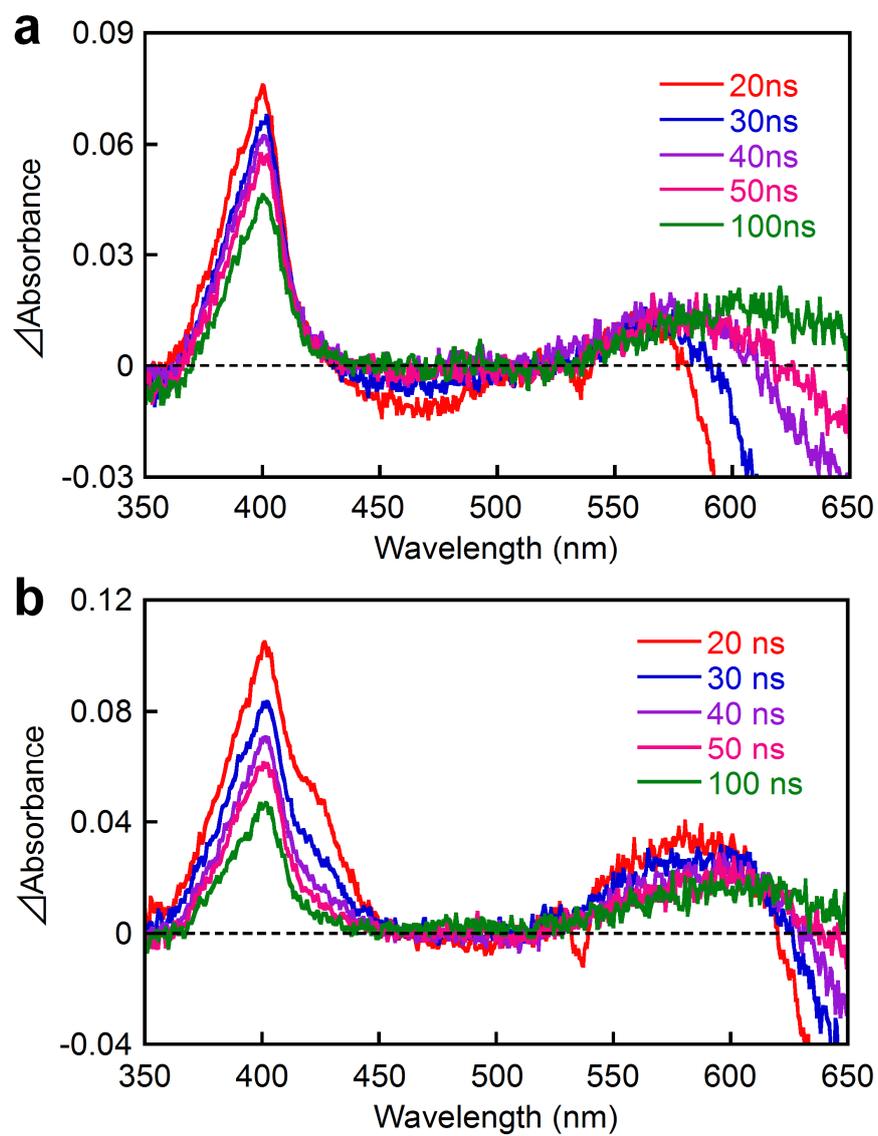
Figure S5. Transient absorption spectral changes observed after laser pulse excitation at 532 nm for an aqueous solution of (a) [Ru(**4,4'-MV4**)$_3$](PF$_6$)$_{26}$ and (b) [Ru(**5,5'-MV4**)$_3$](PF$_6$)$_{26}$ in the absence of EDTA under Ar atmosphere at room temperature.
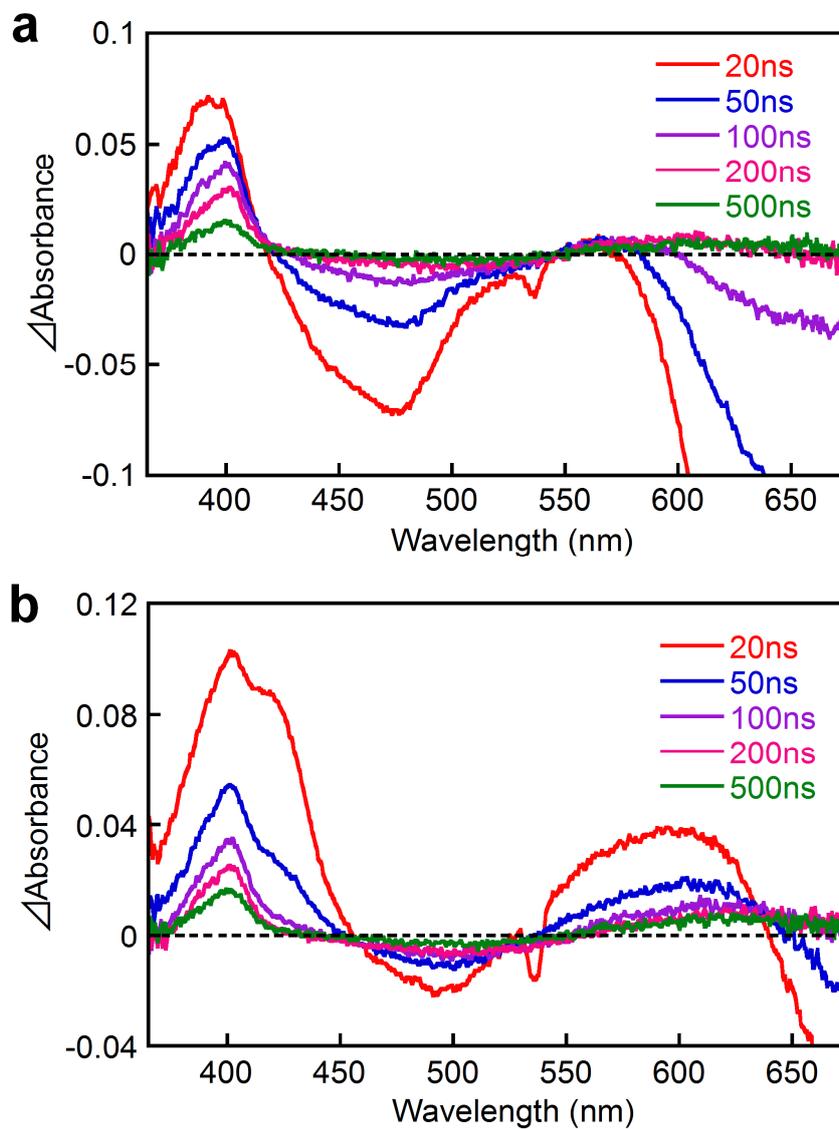
Figure S6. Transient absorption spectral changes observed after laser pulse excitation at 532 nm for an aqueous acetate buffer solution (0.1 M, pH 5.0) of (a) [Ru(**4,4'-MV4**)$_3$](PF$_6$)$_{26}$ and (b) [Ru(**5,5'-MV4**)$_3$](PF$_6$)$_{26}$ in the absence of EDTA under Ar atmosphere at room temperature.
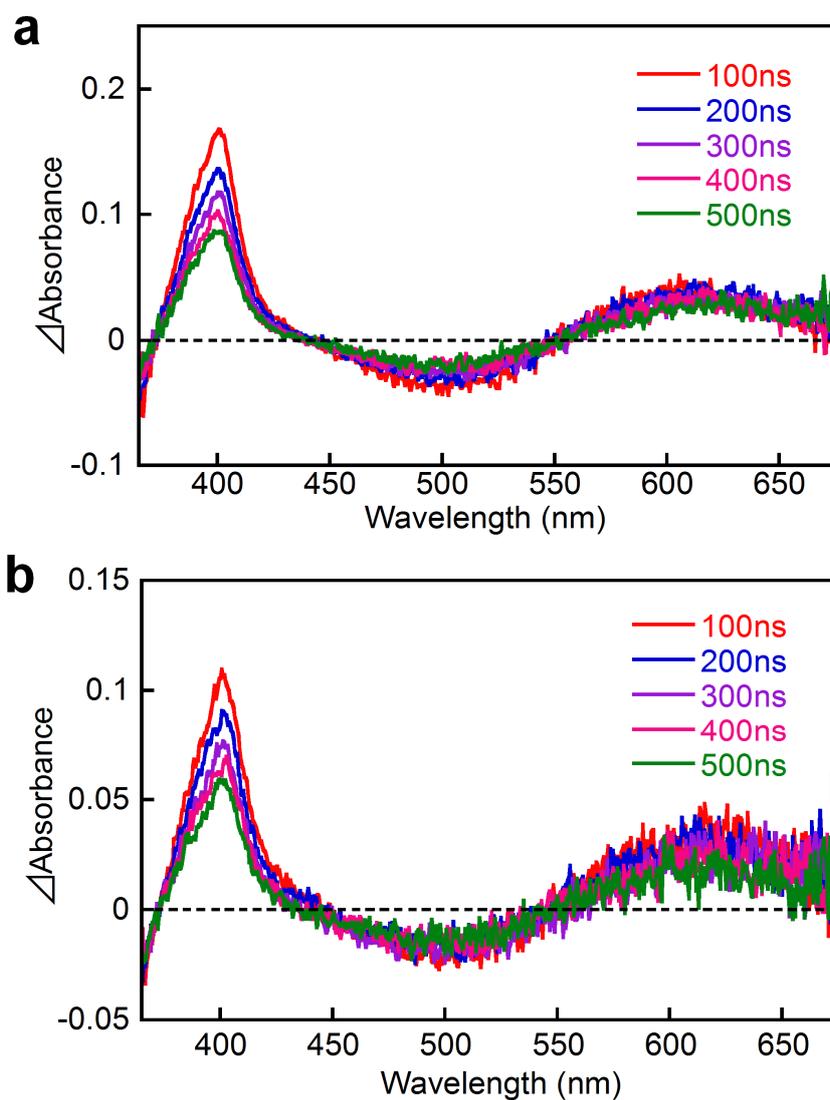
Figure S7. Transient absorption spectral changes observed after laser pulse excitation at 532 nm for an aqueous acetate buffer solution (0.1 M, pH 5.0) of (a) [Ru(**4,4'-MV4**)$_3$](PF$_6$)$_{26}$ and (b) [Ru(**5,5'-MV4**)$_3$](PF$_6$)$_{26}$ in the presence of EDTA (30 mM) under Ar atmosphere at room temperature. The emission bleach seen above 600 nm in Figs. S5,S6 are not observable here, revealing that the triplet component has a minor contribution under these conditions.
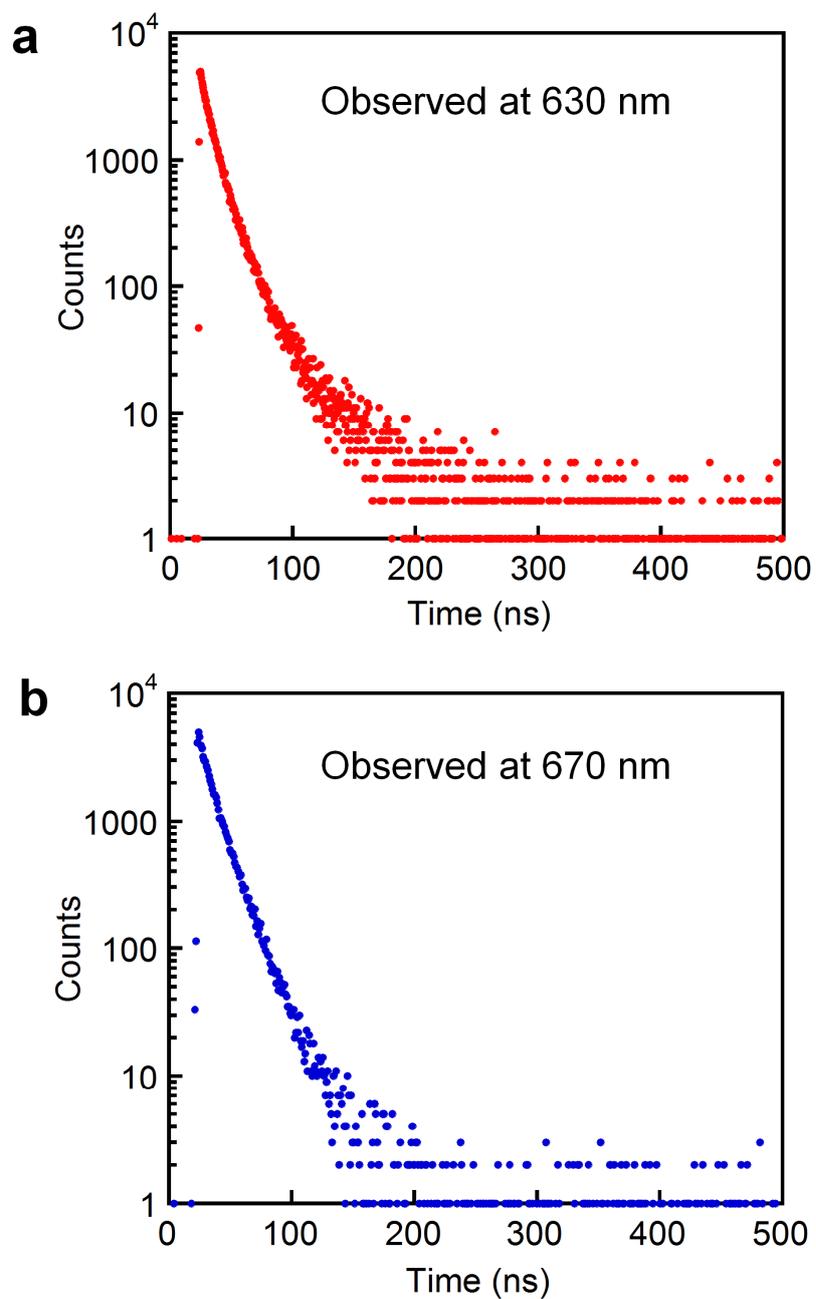
Figure S8. Emission decays after laser pulse excitation at 472 nm, observed for an aqueous solution of (a) [Ru(**4,4'-MV4**)$_3$](PF$_6$)$_{26}$ and (b) [Ru(**5,5'-MV4**)$_3$](PF$_6$)$_{26}$ under Ar atmosphere at 20 °C.
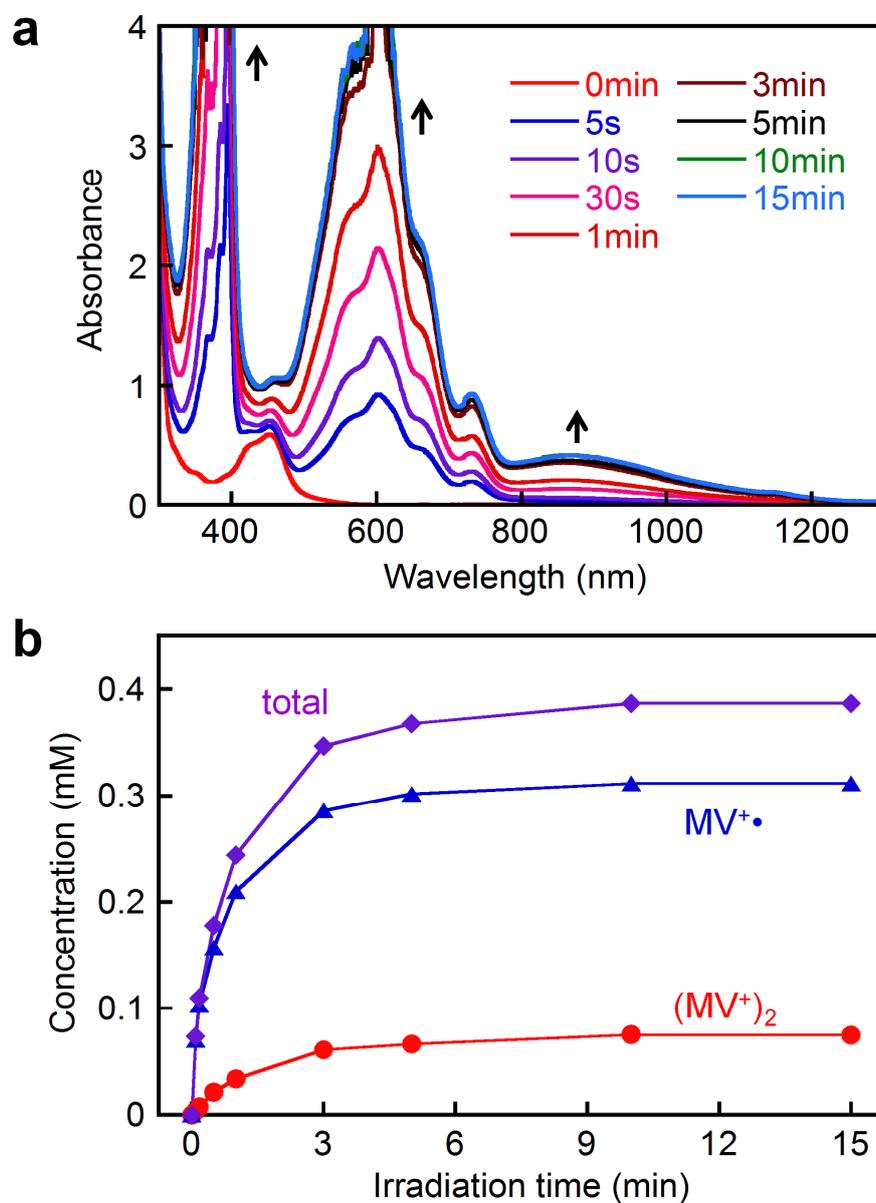
Figure S9. (a) Spectral changes during photolysis of an aqueous acetate buffer solution (0.1 M, pH = 5.0) containing 0.04 mM [Ru(bpy)$_3$](NO$_3$)$_2$, 2 mM MV(NO$_3$)$_2$, and 30 mM EDTA under Ar atmosphere at 20 °C. (b) The total concentration of MV$^+\bullet$ together with those divided into MV$^+\bullet$ and (MV$^+$)$_2$ components as a function of time.
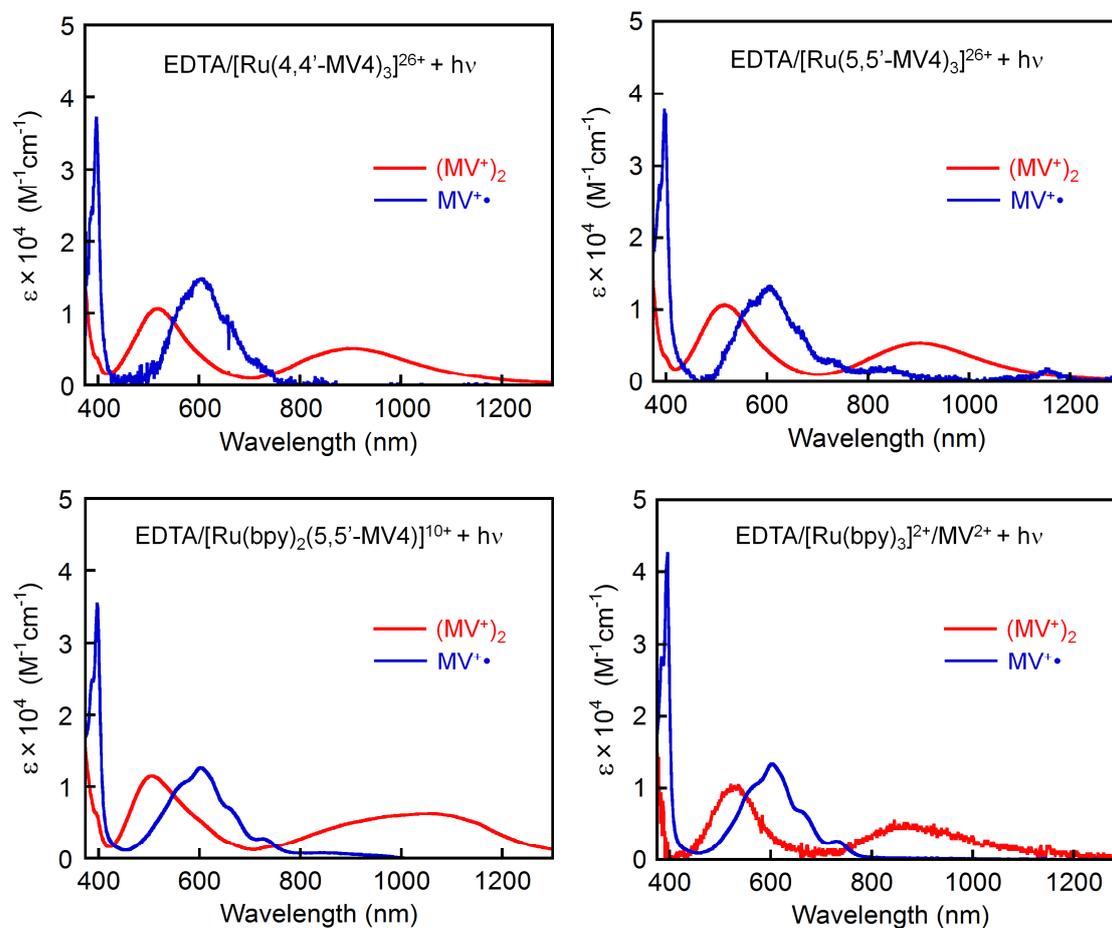
Figure S10. Two spectral components extracted in spectral deconvolution analysis. In each case, all spectra observed during multi-charge storage can be expressed as the sum of two spectral components arising from $MV^{+}\bullet$ and $(MV^{+})_2$, with a definition of $\mathrm{Abs}(w, t) = C_m(t)\varepsilon_m(w) + C_d(t)\varepsilon_d(w)$, where Abs is absorbance, C_m and C_d are molar concentrations of $MV^{+}\bullet$ and $(MV^{+})_2$, respectively, ε_m and ε_d are molar absorptivities of $MV^{+}\bullet$ and $(MV^{+})_2$, respectively, t is time, and w is wavelength. The original scans are those given in Figs. 5a-c and S9a.

Table S5. Absorption maxima and molar absorptivities for the $MV^{+}\bullet$ and $(MV^{+})_2$ sites generated in each system. The values are determined from the spectra shown in Fig. S10, which were obtained by spectral deconvolution in Figs. S11–14.

Complex	Species	λ_{abs} / nm	ε/ $M^{-1}cm^{-1}$
$[Ru(\mathbf{4,4'\text{-}MV4})_3]^{26+}$	$(MV^{+})_2$	358	27 800
		517	10 700
		894	5 200
	$MV^{+}\bullet$	397	37 100
		603	14 800
$[Ru(\mathbf{5,5'\text{-}MV4})_3]^{26+}$	$(MV^{+})_2$	359	26 700
		516	10 700
		896	5 400
	$MV^{+}\bullet$	397	37 700
		604	13 300
$[Ru(bpy)_2(\mathbf{5,5'\text{-}MV4})]^{10+}$	$(MV^{+})_2$	354	27 300
		508	11 500
		1060	6 300
	$MV^{+}\bullet$	397	35 400
		602	12 600
$[Ru(bpy)_3]^{2+}/MV^{2+}$ system	$(MV^{+})_2$	360	26 600
		521	10 400
		872	4 600
	$MV^{+}\bullet$	396	42 600
		603	13 300

Table S6. The net concentrations of the $MV^+\bullet$ and $(MV^+)_2$ sites generated over $[Ru(\textbf{4,4'-MV4})_3]^{26+}$ during the photolysis with EDTA (original spectral data in Fig. 5a). Some relevant parameters are also listed.

Irradiation time	$MV^+\bullet$ (M)	$(MV^+)_2$ (M)	$MV^+\bullet$ (%)	$(MV^+)_2$ (%)	Number of electrons stored (molecule^{-1})	K_d (M^{-1})
5 s	1.05×10^{-5}	2.98×10^{-5}	2.19	12.4	1.75	2.69×10^5
10 s	1.29×10^{-5}	4.25×10^{-5}	2.68	17.7	2.45	2.57×10^5
30 s	1.51×10^{-5}	6.49×10^{-5}	3.16	27.1	3.63	2.83×10^5
1 min	1.74×10^{-5}	8.31×10^{-5}	3.63	34.6	4.59	2.73×10^5
3 min	1.81×10^{-5}	1.04×10^{-4}	3.76	43.3	5.65	3.19×10^5
5 min	1.82×10^{-5}	1.12×10^{-4}	3.79	46.7	6.06	3.39×10^5
10 min	1.81×10^{-5}	1.20×10^{-4}	3.76	49.9	6.44	3.67×10^5
20 min	1.78×10^{-5}	1.23×10^{-4}	3.71	51.2	6.59	3.87×10^5
30 min	1.77×10^{-5}	1.25×10^{-4}	3.69	52.3	6.71	3.99×10^5
40 min	1.79×10^{-5}	1.26×10^{-4}	3.73	52.3	6.72	3.91×10^5
60 min	1.76×10^{-5}	1.27×10^{-4}	3.67	52.8	6.78	4.08×10^5

Table S7. The net concentrations of the $MV^+\bullet$ and $(MV^+)_2$ sites generated over $[Ru(\textbf{5,5'-MV4})_3]^{26+}$ during the photolysis with EDTA (original spectral data in Fig. 5b). Some relevant parameters are also listed.

Irradiation time	$MV^+\bullet$ (M)	$(MV^+)_2$ (M)	$MV^+\bullet$ (%)	$(MV^+)_2$ (%)	Number of electrons stored (molecule^{-1})	K_d (M^{-1})
5 s	7.26×10^{-6}	8.96×10^{-6}	1.51	3.73	0.63	1.70×10^5
10 s	9.28×10^{-6}	1.66×10^{-5}	1.93	6.91	1.06	1.92×10^5
30 s	1.31×10^{-5}	3.73×10^{-5}	2.73	15.5	2.19	2.17×10^5
1 min	1.51×10^{-5}	5.30×10^{-5}	3.15	22.1	3.03	2.31×10^5
3 min	1.72×10^{-5}	7.91×10^{-5}	3.58	33.0	4.39	2.68×10^5
5 min	1.79×10^{-5}	9.04×10^{-5}	3.72	37.7	4.97	2.83×10^5
10 min	1.87×10^{-5}	1.04×10^{-4}	3.89	43.2	5.65	2.97×10^5
20 min	1.93×10^{-5}	1.13×10^{-4}	4.03	47.2	6.14	3.03×10^5
30 min	1.96×10^{-5}	1.16×10^{-4}	4.08	48.5	6.31	3.04×10^5
40 min	1.86×10^{-5}	1.19×10^{-4}	3.88	49.5	6.41	3.42×10^5
60 min	2.02×10^{-5}	1.20×10^{-4}	4.21	50.1	6.52	2.95×10^5

Table S8. The net concentrations of the MV$^+\bullet$ and (MV$^+$)$_2$ sites generated over [Ru(bpy)$_2$(**5,5'-MV4**)]$^{10+}$ during the photolysis with EDTA (original spectral data in Fig. 5c). Some relevant parameters are also listed.

Irradiation time	MV$^+\bullet$ (M)	(MV$^+$)$_2$ (M)	MV$^+\bullet$ (%)	(MV$^+$)$_2$ (%)	Number of electrons stored (molecule^{-1})	K_d (M^{-1})
1 min	8.06×10^{-6}	2.11×10^{-7}	5.04	0.026	0.20	3.24×10^2
3 min	1.58×10^{-5}	2.00×10^{-7}	9.86	0.25	0.41	7.61×10^2
5 min	2.29×10^{-5}	6.75×10^{-7}	14.3	0.84	0.61	1.28×10^3
10 min	3.26×10^{-5}	2.82×10^{-6}	20.4	3.52	0.96	2.65×10^3
15 min	3.29×10^{-5}	6.01×10^{-6}	20.6	7.52	1.12	5.55×10^3
20 min	3.33×10^{-5}	8.44×10^{-6}	20.8	10.5	1.25	7.61×10^3
30 min	3.09×10^{-5}	1.31×10^{-5}	19.3	16.4	1.43	1.37×10^4
40 min	2.96×10^{-5}	1.56×10^{-5}	18.5	19.5	1.52	1.78×10^4
50 min	2.87×10^{-5}	1.66×10^{-5}	17.9	20.8	1.55	2.02×10^4
60 min	3.13×10^{-5}	1.58×10^{-5}	19.6	19.8	1.58	1.61×10^4

Table S9. The net concentrations of MV$^+\bullet$ and (MV$^+$)$_2$ generated in solution during the photolysis the EDTA/[Ru(bpy)$_3$]$^{2+}$/MV^{2+} system (original spectral data in Fig. S9a). Some relevant parameters are also listed.

Irradiation time	MV$^+\bullet$ (M)	(MV$^+$)$_2$ (M)	MV$^+\bullet$ (%)	(MV$^+$)$_2$ (%)	K_d (M^{-1})
5 s	6.99×10^{-5}	1.79×10^{-6}	3.50	0.179	3.66×10^2
10 s	1.03×10^{-6}	3.66×10^{-6}	5.14	0.366	3.46×10^2
30 s	1.57×10^{-4}	1.06×10^{-5}	7.83	1.06	4.33×10^2
1 min	2.10×10^{-4}	1.68×10^{-5}	10.5	1.68	3.81×10^2
3 min	2.86×10^{-4}	3.05×10^{-5}	14.3	3.05	3.73×10^2
5 min	3.02×10^{-4}	3.31×10^{-5}	15.1	3.31	3.64×10^2
10 min	3.12×10^{-4}	3.76×10^{-5}	15.6	3.76	3.86×10^2
15 min	3.12×10^{-4}	3.73×10^{-5}	15.6	3.73	3.82×10^2
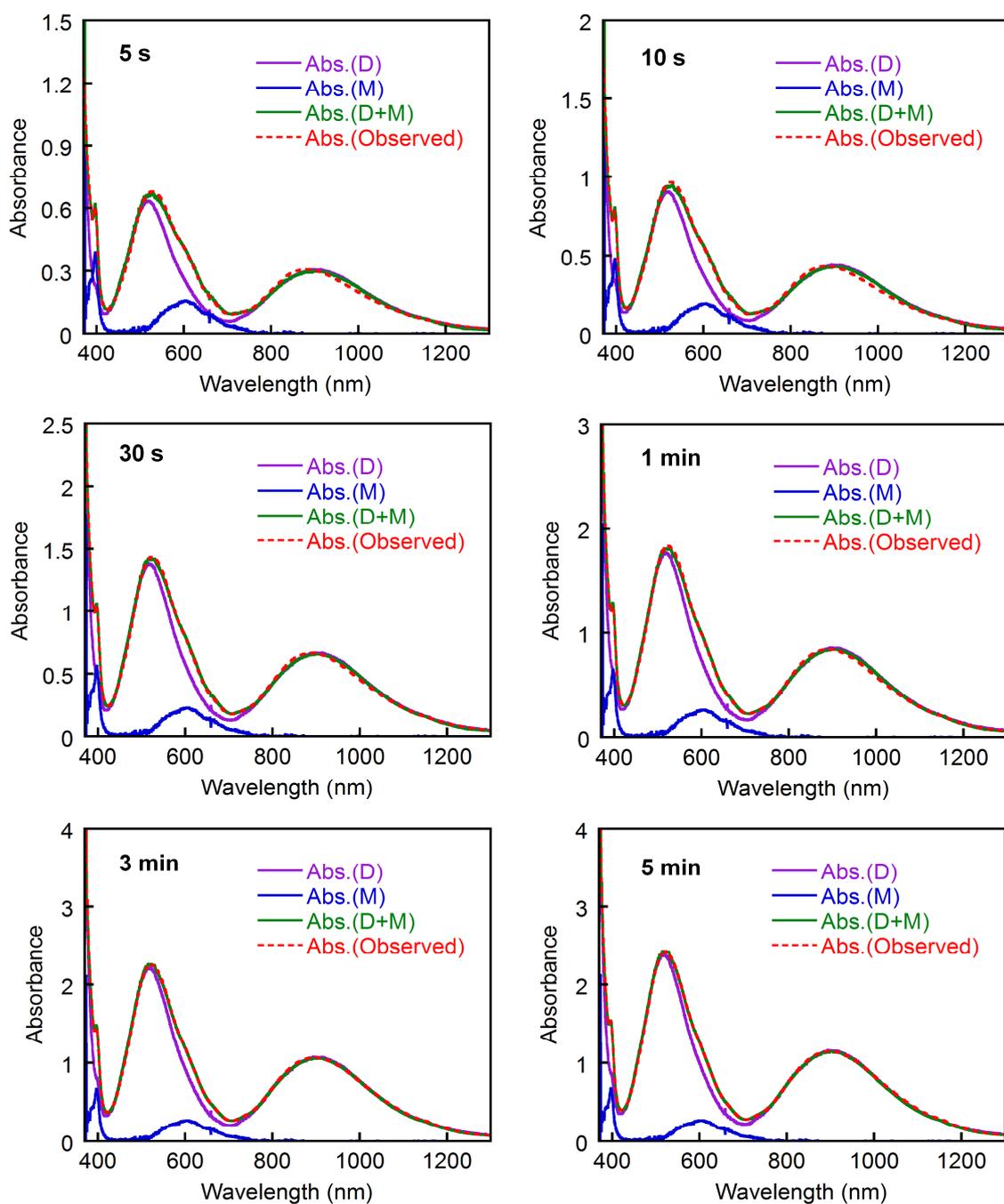
Figure S11. Deconvolution of spectral changes observed during the photolysis of [Ru(**4,4'-MV4**)$_3$](PF$_6$)$_{26}$. The raw data were taken from those in Fig. 5a, where the spectral component derived from the unphotolyzed charge separator was removed by substruction. Each spectrum was fitted to the sum of two spectral components shown in Fig. S10a, the concentrations of MV$^+\bullet$ and (MV$^+$)$_2$ were determined by the least-squares method implemented in our program.[24]
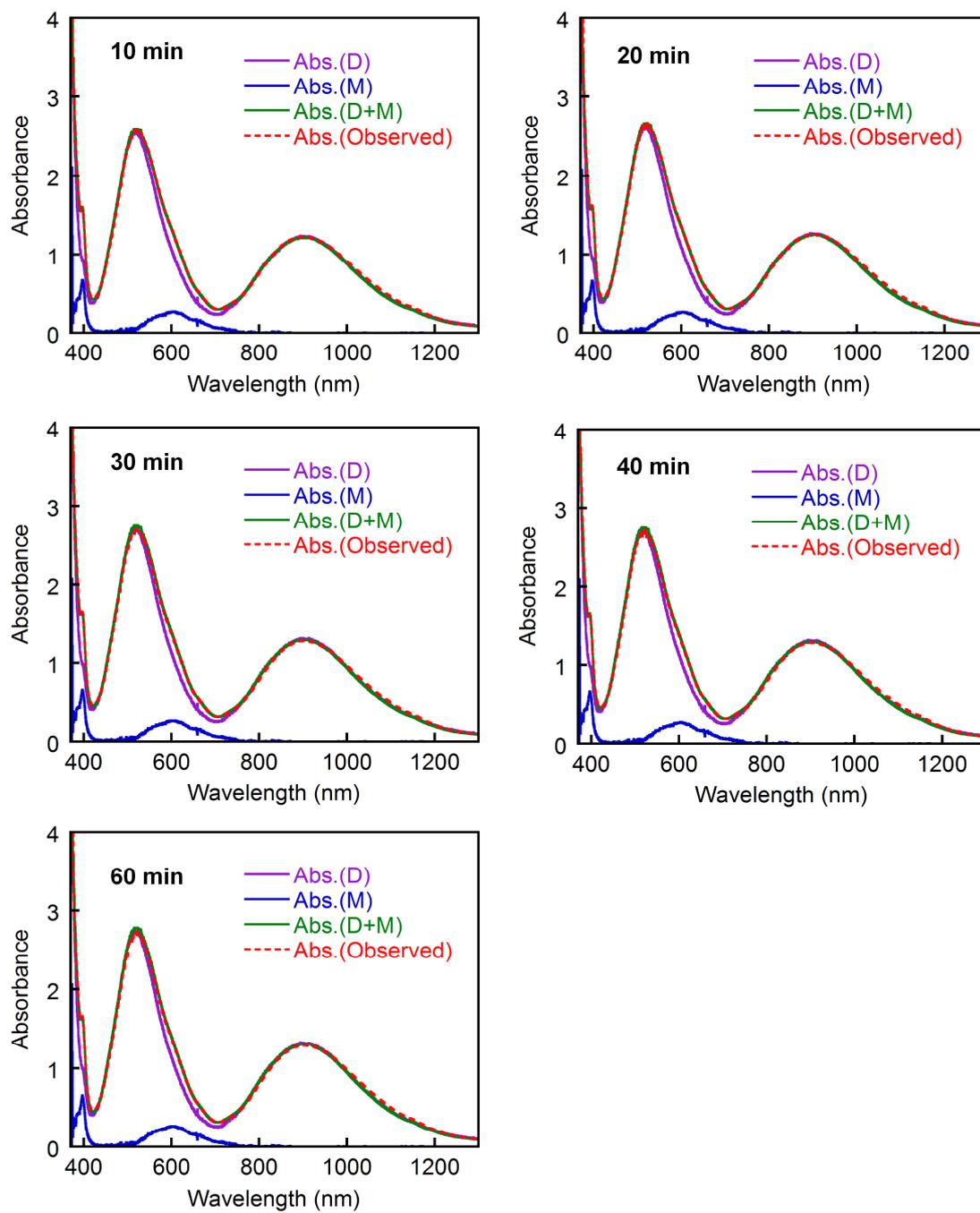
Figure S11 (Continued).
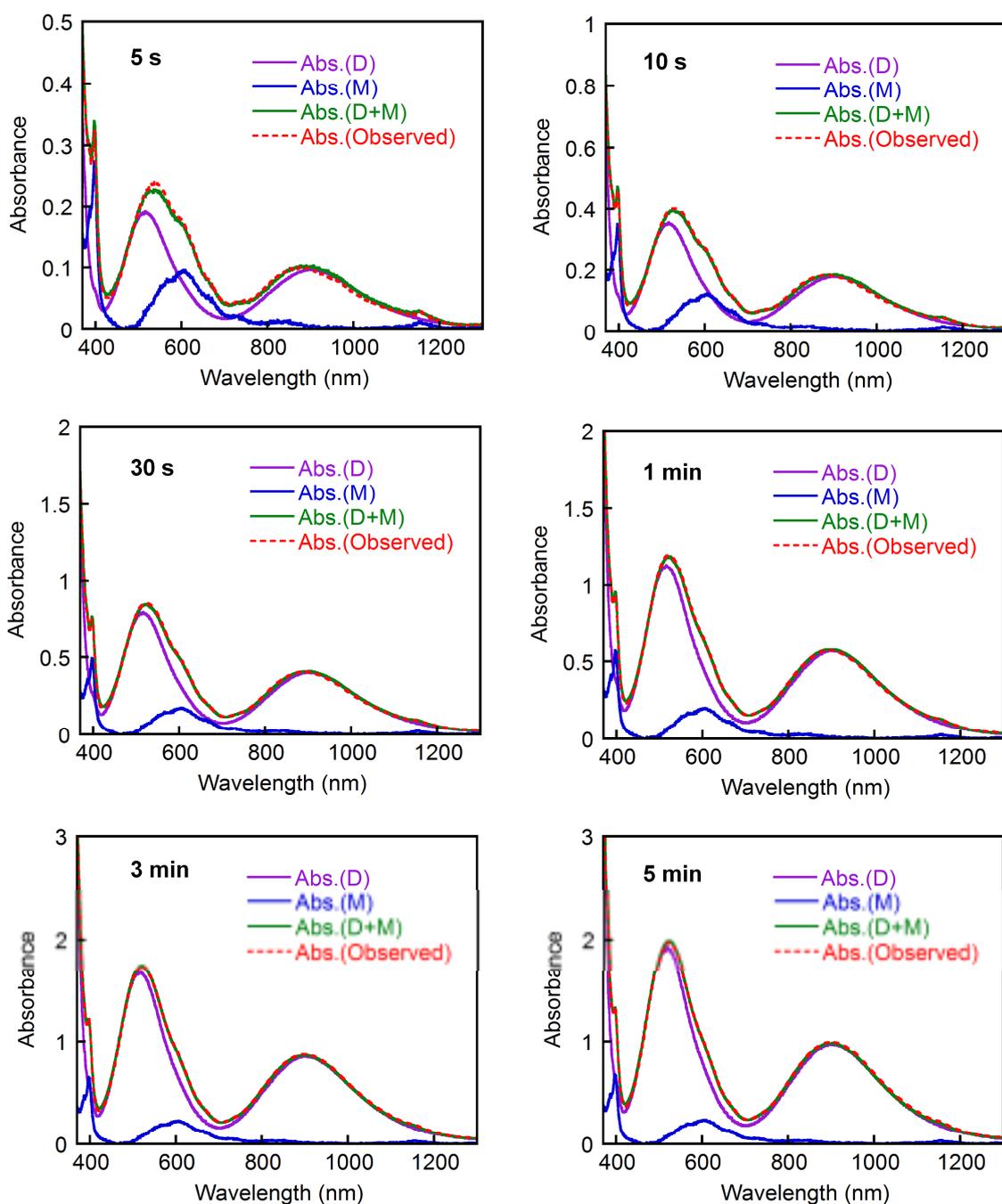
Figure S12. Deconvolution of spectral changes observed during the photolysis of [Ru(**5,5'-MV4**)$_3$](PF$_6$)$_{26}$. The raw data were taken from those in Fig. 5b, where the spectral component derived from the unphotolyzed charge separator was removed by substruction. Each spectrum was fitted to the sum of two spectral components shown in Fig. S10b, the concentrations of MV^{+}• and (MV^{+})$_2$ were determined by the least-squares method implemented in our program.[24]
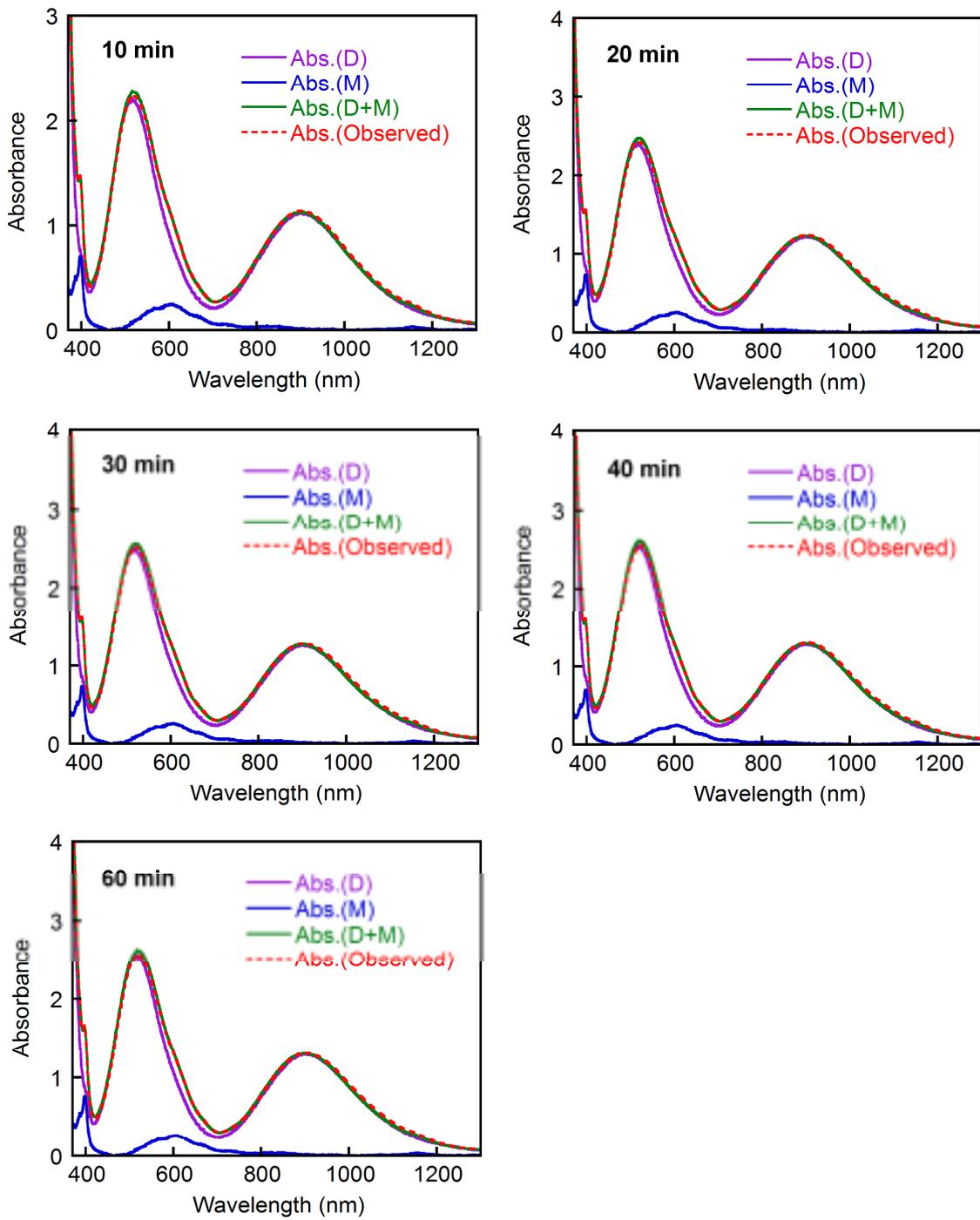
Figure S12 (Continued).
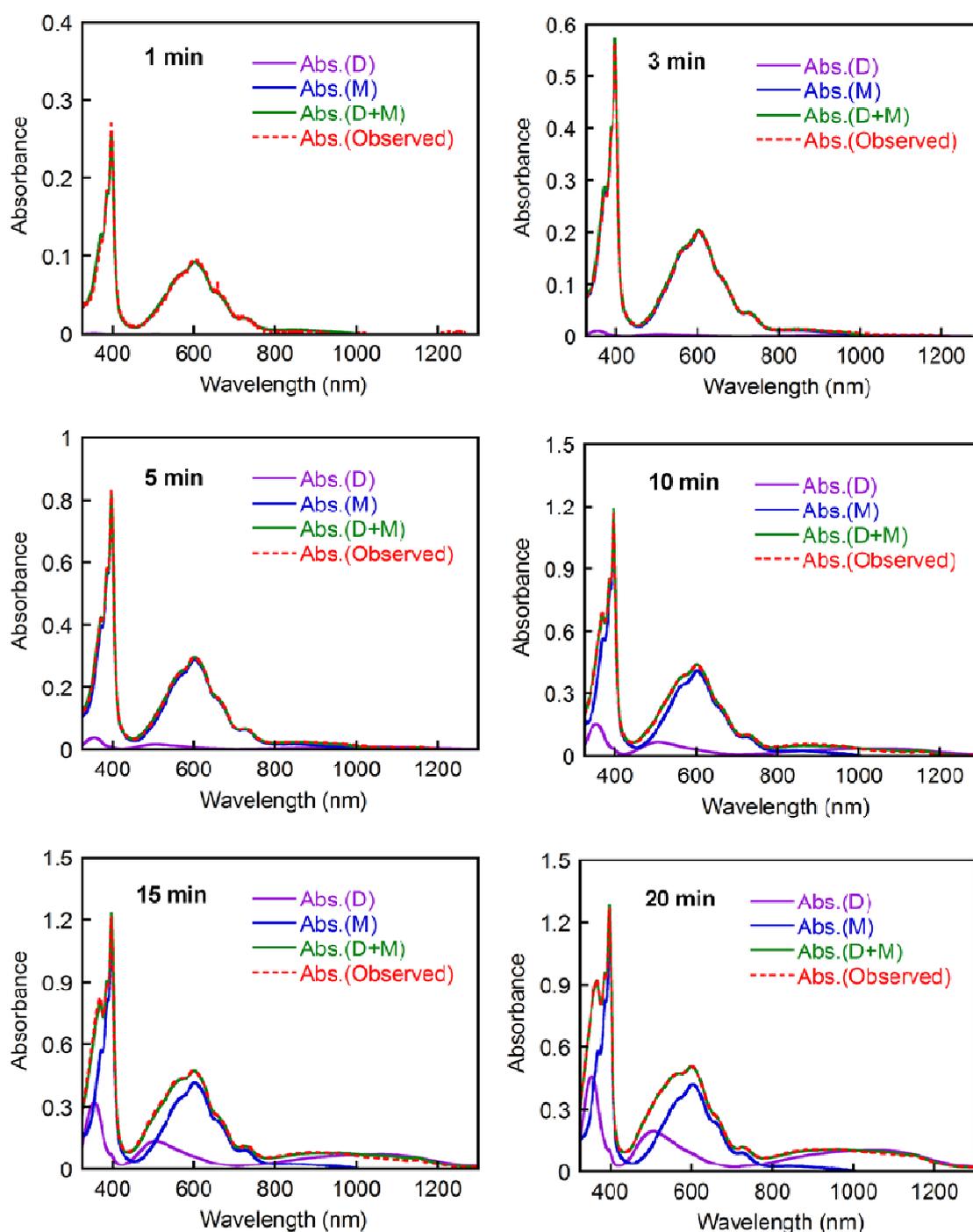
Figure S13. Deconvolution of spectral changes observed during the photolysis of [Ru(bpy)$_2$(**5,5'-MV4**)](PF$_6$)$_{10}$. The raw data were taken from those in Fig. 5c, where the spectral component derived from the unphotolyzed charge separator was removed by substruction. Each spectrum was fitted to the sum of two spectral components shown in Fig. S10c, the concentrations of MV$^+$• and (MV$^+$)$_2$ were determined by the least-squares method implemented in our program.[24]
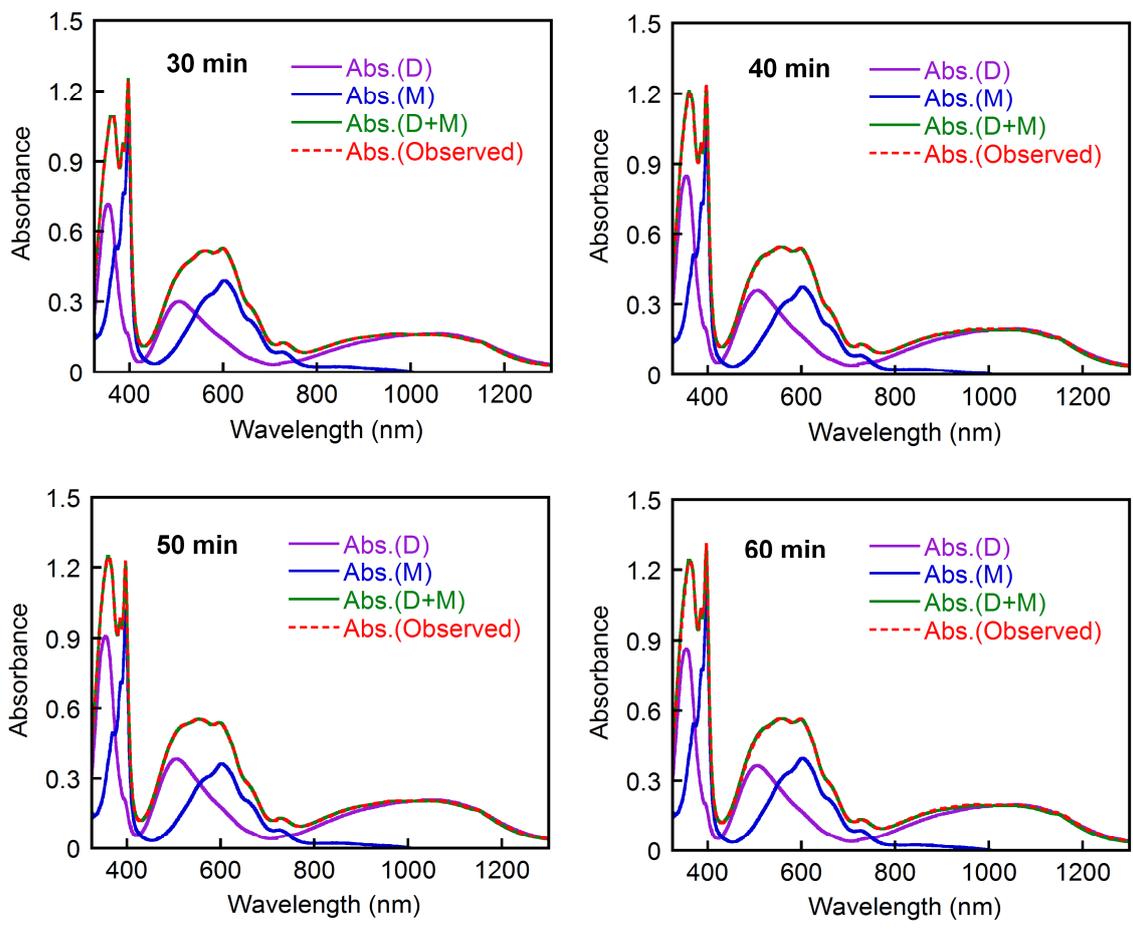
Figure S13 (Continued).
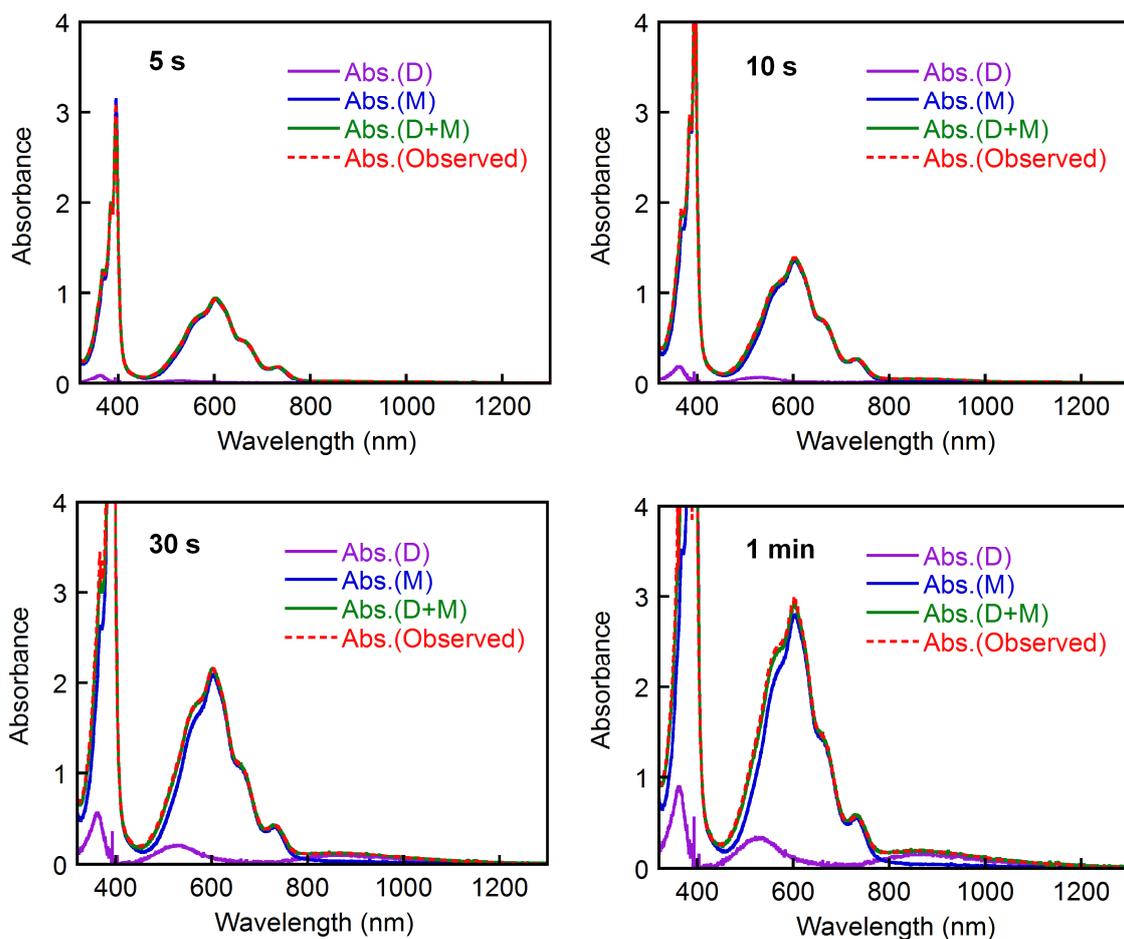
Figure S14. Deconvolution of spectral changes observed during the photolysis of $[Ru(bpy)_3]^{2+}/MV^{2+}$ system. The raw data were taken from those in Fig. S9a, where the spectral component derived from the unphotolyzed charge separator was removed by substruction. Each spectrum was fitted to the sum of two spectral components shown in Fig. S10d, the concentrations of $MV^+\bullet$ and $(MV^+)_2$ were determined by the least-squares method implemented in our program.[24]
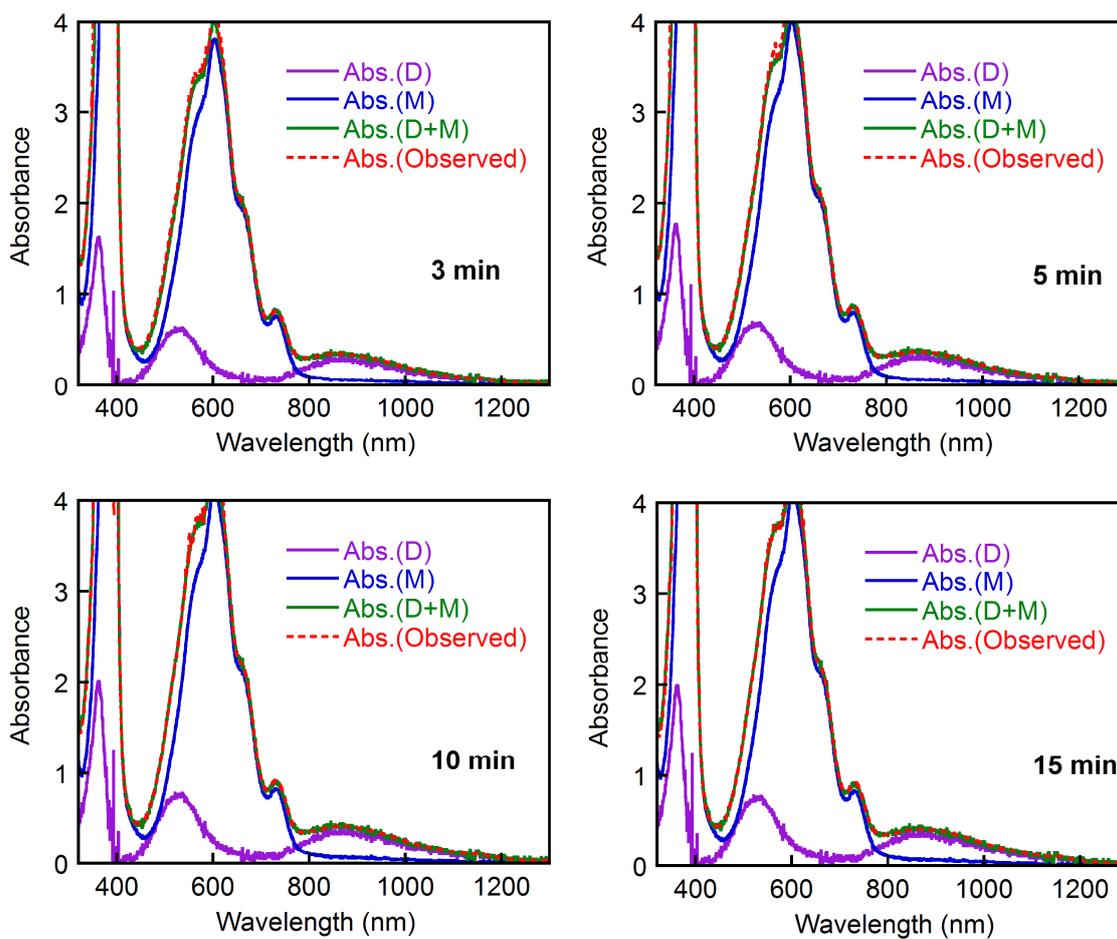
Figure S14 (Continued).
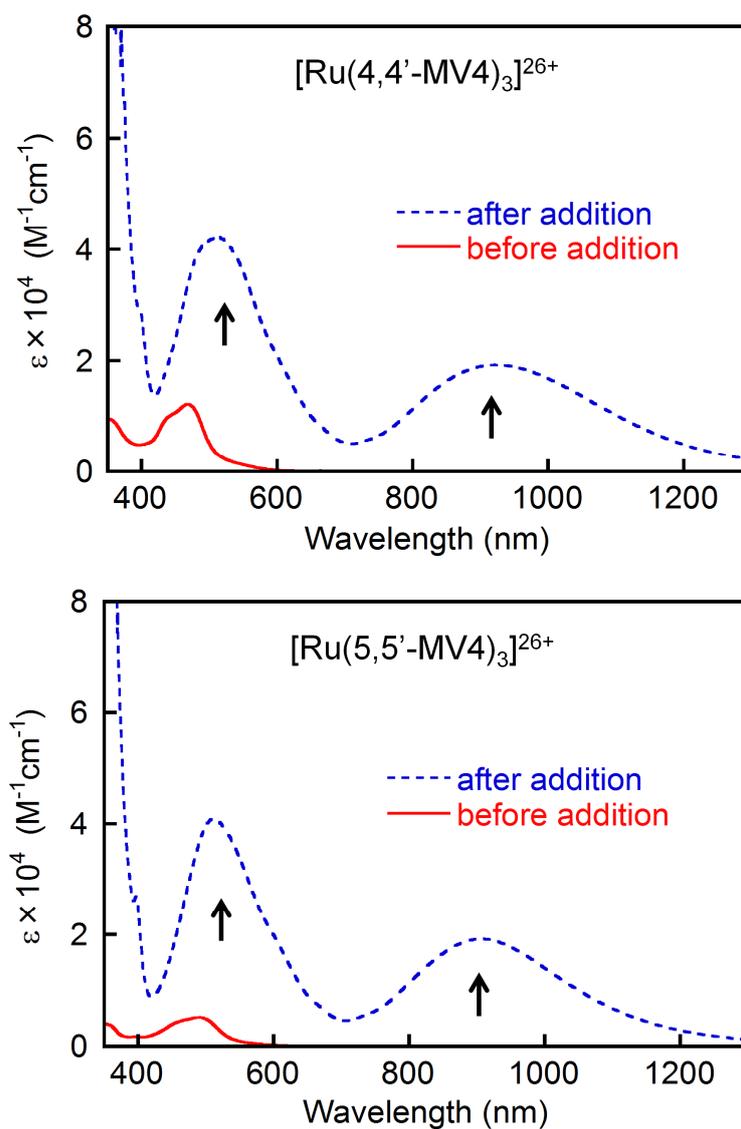
Figure S15. Molar absorptivities of 12-electron reduced species generated by adding $Na_2S_2O_4$. For each case, spectra before (—) and after (---) adding an excess of $Na_2S_2O_4$ (ca. 0.4 mg, 2.30 μmol) were observed for a 0.04 mM solution of each complex in an aqueous 0.1 M acetate buffer solution (pH = 5.0) under Ar atmosphere at 20 °C. Measurements were carried out using a quartz cell having a path length of 5 mm.

Table S10. The number of electrons stored over the PCSs at the saturation stage, determined by using the molar absorptivities of 12-electron-reduced species generated by adding a large excess of $Na_2S_2O_4$ (see Fig. S15).

	$[Ru(\textbf{4,4'-MV4})_3]^{26+}$		$[Ru(\textbf{5,5'-MV4})_3]^{26+}$	
Reduction Method	Photochemically (60-min irradiation)	Thermally	Photochemically (60-min irradiation)	Thermally
Reductant	EDTA	$Na_2S_2O_4$	EDTA	$Na_2S_2O_4$
△Abs at 530 nm	2.660	1.930[a]	2.510	1.850[a]
△Abs at 900 nm	1.290	0.948[a]	1.310	0.959[a]
Number of electron stored (molecule^{-1}) (calcd. from △Abs at 530 nm)	8.27	12	8.14	12
Number of electron stored (molecule^{-1}) (calcd. from △Abs at 900 nm)	8.16	12	8.20	12
Number of electron stored (molecule^{-1}) (average)	**8.2**	--	**8.2**	--

[a]Measurements were carried out using a quartz cell having an optical path length of 5 mm.
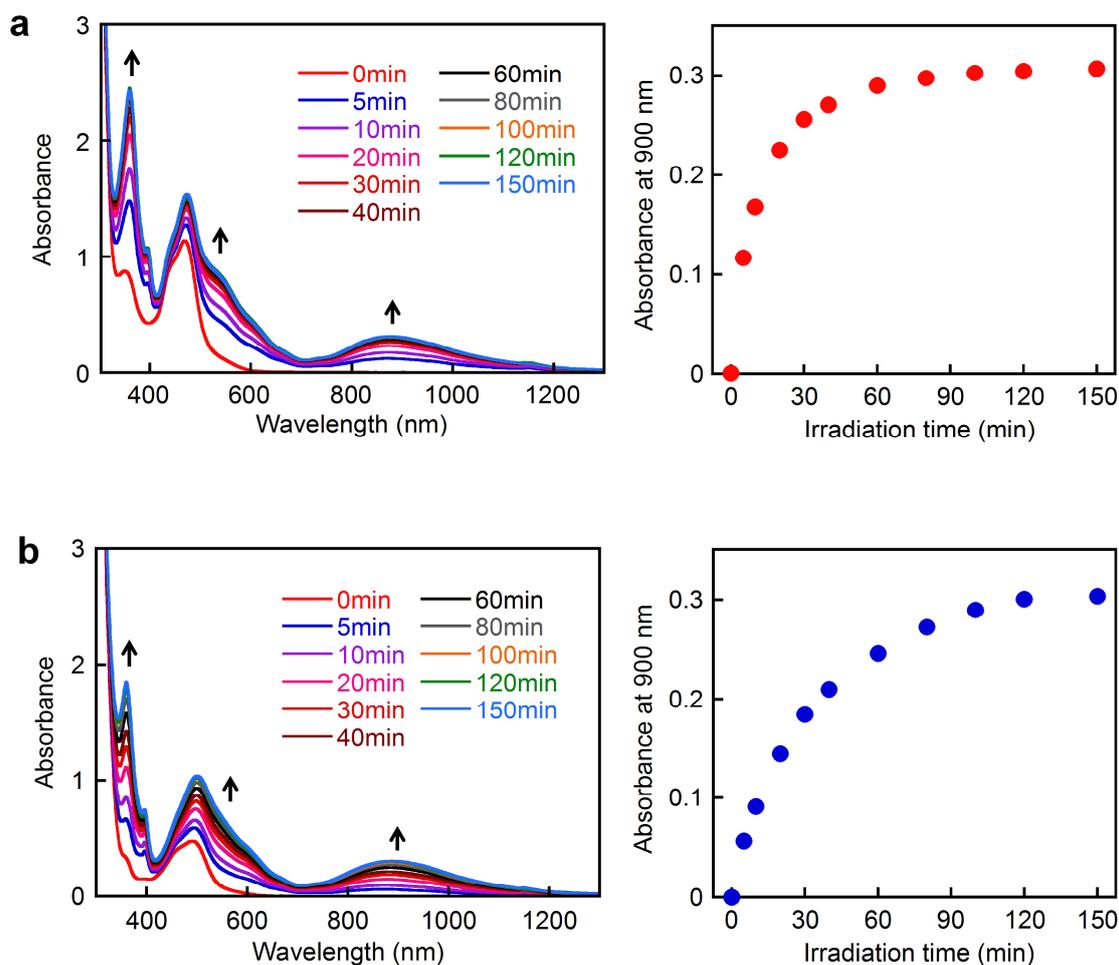
Figure S16. Reduced charge storage efficiency with a neutral donor. Spectral changes during photolysis of an aqueous solution (pH = 7.0) containing 30 mM triethanolamine (TEOA) in the presence of each PCS (0.04 mM) under Ar atmosphere at 20 ℃, where the pH was adjusted with HCl. The results in **a** and **b** were given for [Ru(**4,4'-MV4**)$_3$](PF$_6$)$_{26}$ and [Ru(**5,5'-MV4**)$_3$](PF$_6$)$_{26}$, respectively. The number of electrons stored at saturation was estimated to be 1.9 for [Ru(**4,4'-MV4**)$_3$](PF$_6$)$_{26}$ and 1.7 for [Ru(**5,5'-MV4**)$_3$](PF$_6$)$_{26}$ using the absorption coefficient per viologen unit at 548 nm where an isosbestic point is given for the monomer-dimer equilibrium, i.e., $\varepsilon_{548}(MV^+\bullet) = {}^1/_2\varepsilon_{548}((MV^+)_2) = 8920$ M^{-1}cm^{-1}, which was reported in the literature.[25]
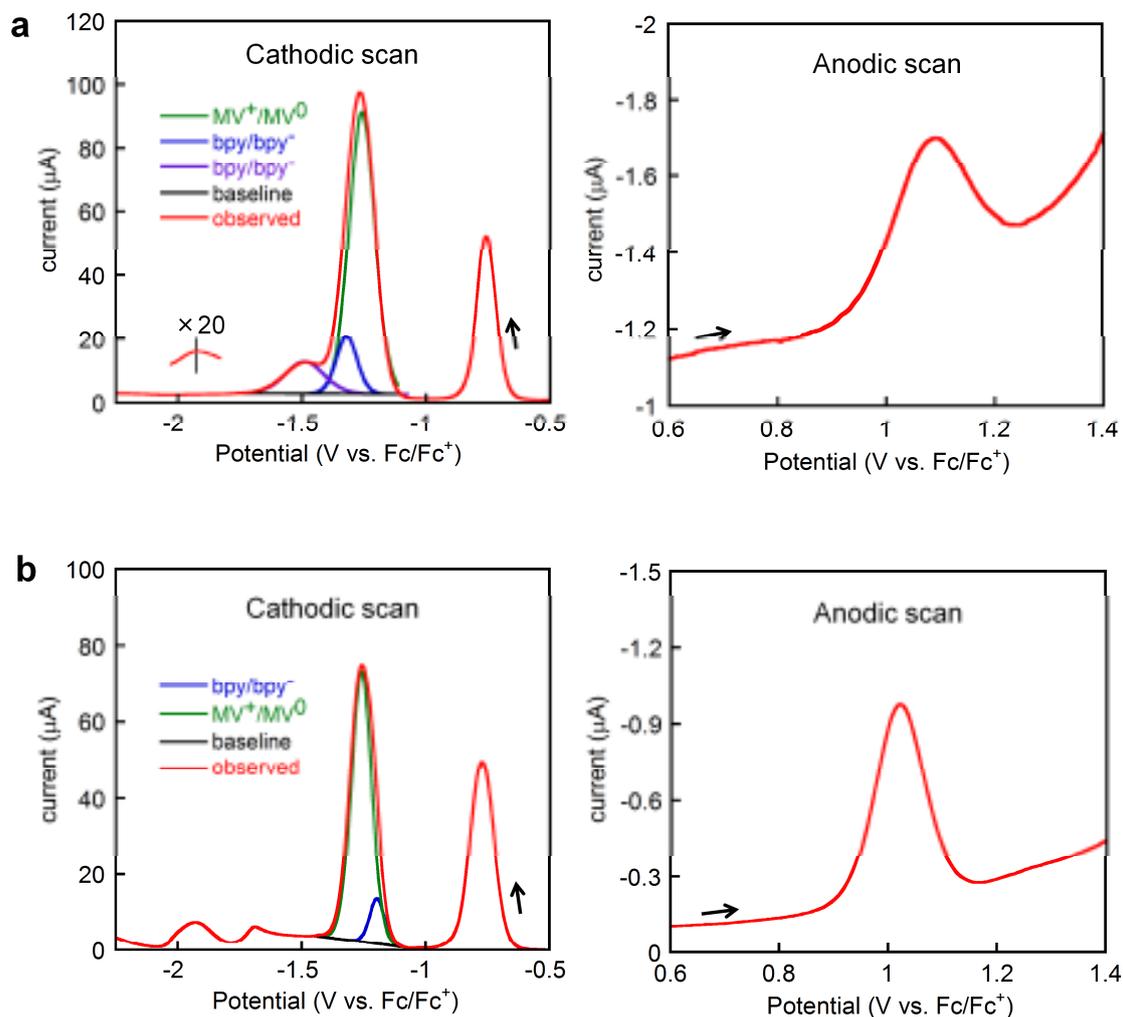
Figure S17. Oxidation and reduction waves for (a) [Ru(**4,4'-MV4**)$_3$](PF$_6$)$_{26}$ and (b) [Ru(**5,5'-MV4**)$_3$](PF$_6$)$_{26}$, observed using square wave voltammetry. Measurements were carried out for a 1 mM solution of each complex in acetonitrile containing 0.1 M tetra(n-butyl)ammonium hexafluorophosphate (TBAH) at room temperature under Ar. The validity of these deconvolution treatments was confirmed by observing the bpy/bpy⁻• redox couples of the controls free of viologen tethers [Ru(**4,4'-ME2**)$_3$](PF$_6$)$_2$ and [Ru(**5,5'-ME2**)$_3$](PF$_6$)$_2$.
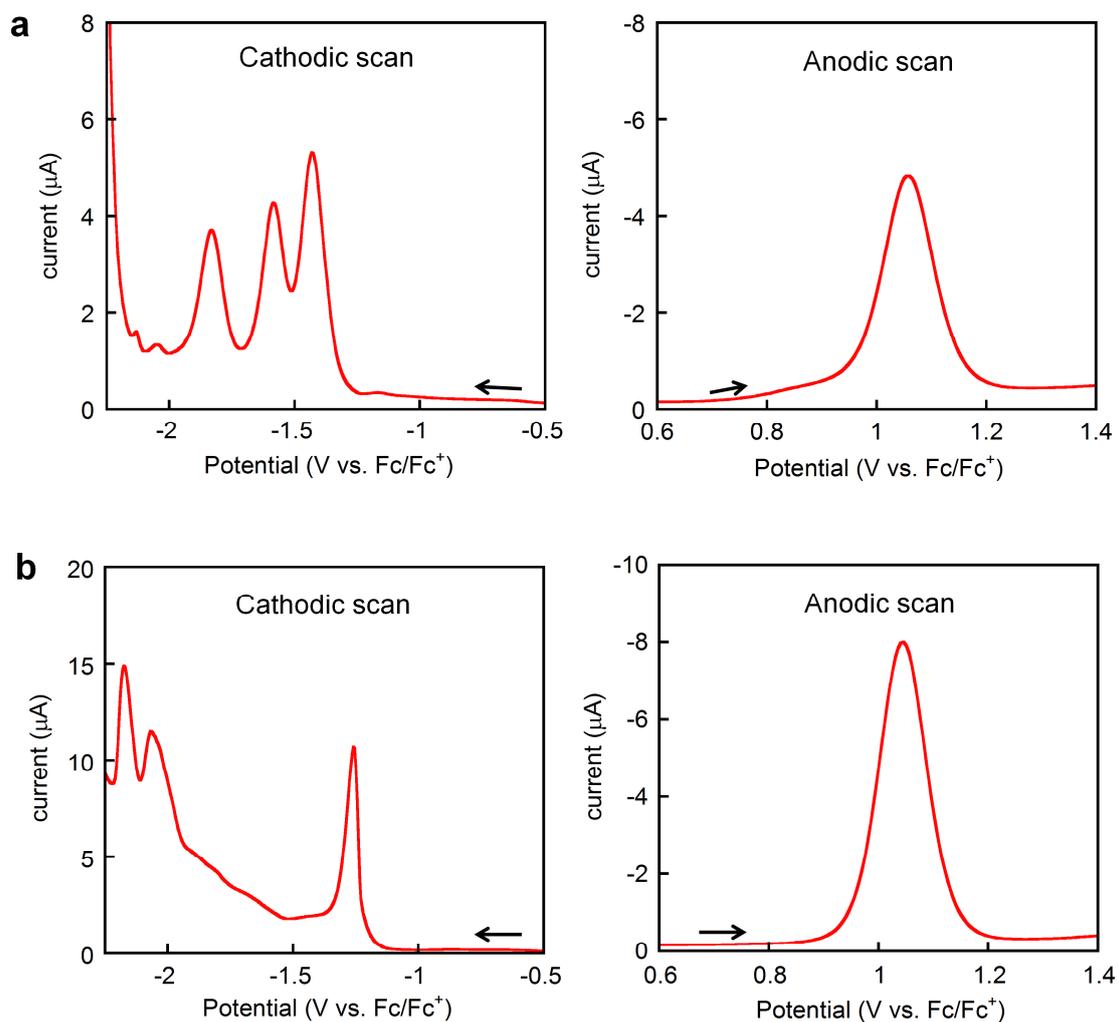
Figure S18. Oxidation and reduction waves for (a) [Ru(**4,4'-ME2**)$_3$](PF$_6$)$_2$ and (b) [Ru(**5,5'-ME2**)$_3$](PF$_6$)$_2$, observed using square wave voltammetry. Measurements were carried out for a 1 mM solution of each complex in acetonitrile containing 0.1 M tetra(n-butyl)ammonium hexafluorophosphate (TBAH) at room temperature under Ar.

Table S11. Redox potentials for the PCSs together with the corresponding controls. Measurements were carried out for a solution of each complex (1 mM) in an acetonitrile solution containing 0.1 M tetra(n-butyl)ammonium hexafluorophosphate (TBAH) at room temperature under Ar atmosphere. Potentials are given in volts vs. Fc/Fc^+.

Complex	Oxidation	Reduction				
	$E_{ox,1}$	$E_{red,1}{}^a$	$E_{red,2}{}^b$	$E_{red,3}{}^c$	$E_{red,4}{}^c$	$E_{red,5}{}^c$
Photo-charge-separators						
$[Ru(\mathbf{4,4'\text{-}MV4})_3]^{26+}$	1.10	−0.78	−1.25	−1.33	−1.49	−1.92
$[Ru(\mathbf{5,5'\text{-}MV4})_3]^{26+}$	1.02	−0.79	−1.27	−1.21	−1.70	−1.94
Controls						
$[Ru(\mathbf{4,4'\text{-}ME2})_3]^{2+}$	1.06	-	-	−1.40	−1.56	−1.84
$[Ru(\mathbf{5,5'\text{-}ME2})_3]^{2+}$	1.02	-	-	−1.25	−2.06	−2.17

[a]Reduction for the $MV^{2+}/MV^{+}\bullet$ couple. [b]Reduction for the $MV^{+}\bullet/MV^0$ couple. [c]Reductions at the 2,2'-bipyridine moieties, where these reduction peaks are overlapped with that of the $MV^{+}\bullet/MV^0$ couple (see Fig. S17).

Table S12. SCF energies given for the model systems optimized at the M06/6-31G** level of DFT in either restricted or unrestricted model under water solvated condition using polarizable continuum model (PCM) method implemented in the Gaussian 09 package. All the structures given were confirmed as a local minimum structure.[a]

Initial geometry	spin state	Uncorrected SCF Energy (hartree)	ZPE (hartree)	ZPE-Corrected SCF Energy (hartree)	ZPE-Corrected SCF Energy (kcal/mol)	Relative Energy (kcal/mol)	Coordinates
π-dimer of one-electron-reduced non-derivatized N,N-dimethyl-4,4'-bipyridinium, $(MV^+)_2$							
Eclipsed	closed-shell singlet	-1149.266	0.478646	-1148.787	-720875.5	0.5	Table S13
	open-shell singlet	-1149.266	0.478587	-1148.788	-720875.7	0.3	Table S14
	triplet	-1149.264	0.477917	-1148.786	-720874.7	1.4[b]	Table S15
Staggered	closed-shell singlet	-1149.265	0.477755	-1148.788	-720875.7	0.3	Table S16
	open-shell singlet	-1149.267	0.478704	-1148.788	-720876	0.0	Table S17
	triplet	-1149.263	0.478221	-1148.785	-720874	2.0	Table S18
π-dimer of Asp-based $(MV^+)_2$ model system							
Eclipsed	closed-shell singlet	-1850.349	0.683717	-1849.665	-1160683	8.4	Table S19
	open-shell singlet	-1850.36	0.684557	-1849.676	-1160690	1.6[b]	Table S20
	triplet	-1850.356	0.683761	-1849.672	-1160688	3.8[b]	Table S21
Staggered	closed-shell singlet	-1850.36	0.684653	-1849.676	-1160690	1.5	Table S22
	open-shell singlet	-1850.362	0.683778	-1849.678	-1160692	0.0	Table S23
	triplet	-1850.359	0.685284	-1849.674	-1160689	2.6	Table S24
one-electron-reduced N,N-dimethyl-4,4'-bipyridinium, $MV^+\bullet$ (monomer)							
NA	doublet	-574.6239	0.236928	-574.387	-360433.6	4.5	Table S25

[a]ZPE = zero point energy given in frequency calculations. All the structures, except for those with notification b, converged with structures satisfying the initial type of stacking manner. [b]The geometry optimization of these three systems rather converged with the structures converted into slipped geometries. Several attempts to preserve the initial eclipsed structures failed with some of them converted into staggered geometries.

Table S13. Geometry optimized for the eclipsed π-dimer of non-derivatized MV$^+$, i.e., (MV$^+$)$_2$, in its closed-shell singlet state (stereo view shown below). Optimized at the M06/6-31G** level under water solvated model (PCM, polarizable continuum model).[a]
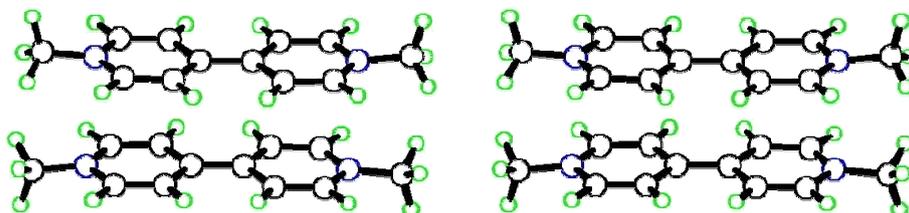
Atom	X	Y	Z
N1	-3.448225	-1.705794	-0.000135
N2	-3.617504	1.590656	0.000131
N3	3.617522	-1.590900	-0.000184
N4	3.448205	1.705686	0.000209
C5	-1.394671	-1.621856	1.202244
C6	-2.754735	-1.672647	-1.176631
C7	-0.630212	-1.593205	-0.000161
C8	-2.754638	-1.674060	1.176349
C9	-1.394777	-1.620338	-1.202529
C10	0.796786	-1.571969	-0.000195
C11	1.562432	-1.567728	1.201262
C12	1.562431	-1.567885	-1.201645
C13	2.924132	-1.581115	-1.176355
C14	2.924131	-1.580945	1.175984
C15	5.070484	-1.732203	-0.000181
C16	-4.898090	-1.863295	-0.000095
C17	-1.562423	1.567477	1.201582
C18	-2.924110	1.581544	-1.176043
C19	-0.796796	1.572163	0.000134
C20	-2.924130	1.580479	1.176298
C21	-1.562399	1.568611	-1.201334
C22	0.630242	1.593395	0.000152
C23	1.394736	1.621316	-1.202230
C24	1.394680	1.621378	1.202558
C25	2.754661	1.673439	1.176686
C26	2.754713	1.673380	-1.176301
C27	4.898105	1.862957	0.000243
C28	-5.070528	1.731607	0.000139
H29	-3.354590	-1.694586	2.080766
H30	-0.919839	-1.582216	-2.177272
H31	-3.354741	-1.691993	-2.081041
H32	1.087270	-1.545754	-2.176687
H33	3.524243	-1.582952	-2.080879
H34	3.524251	-1.582530	2.080505
H35	5.483696	-1.252746	-0.890378
H36	5.353375	-2.789227	0.000177
H37	-5.315480	-1.387334	-0.890548
H38	-5.315462	-1.387361	0.890389

H39	-5.172922	-2.922644	-0.000100
H40	-1.087279	1.544767	2.176624
H41	-3.524238	1.581710	2.080828
H42	-3.524211	1.583643	-2.080572
H43	0.919591	1.584876	2.177291
H44	3.354622	1.693529	2.081107
H45	3.354701	1.693329	-2.080705
H46	5.315383	1.386856	0.890673
H47	5.173084	2.922270	0.000428
H48	-5.483597	1.251814	-0.889950
H49	-5.353649	2.788559	0.000339
H50	-5.483685	1.251523	0.890032
H51	1.087258	-1.545162	2.176291
H52	-0.919597	-1.585834	2.177002
H53	-1.087198	1.547285	-2.176390
H54	0.919697	1.584650	-2.176982
H55	5.315384	1.387118	-0.890333
H56	5.483784	-1.252132	0.889651

[a]Part of the Gaussian output file:

SCF Done: E(RM06) =   -1149.26596594   A.U. after   1 cycles

	1	2	3
	A	A	A
Frequencies --	25.1103	35.3224	64.3741
Red. masses --	4.4862	6.2447	3.7135

Zero-point correction=   0.478646 (Hartree/Particle)
Thermal correction to Energy=   0.503873
Thermal correction to Enthalpy=   0.504817
Thermal correction to Gibbs Free Energy=   0.425881
Sum of electronic and zero-point Energies=   -1148.787320
Sum of electronic and thermal Energies=   -1148.762093
Sum of electronic and thermal Enthalpies=   -1148.761149
Sum of electronic and thermal Free Energies=   -1148.840085

Item	Value	Threshold	Converged?
Maximum Force	0.000022	0.000450	YES
RMS Force	0.000003	0.000300	YES

Table S14. Geometry optimized for the eclipsed π-dimer of non-derivatized MV$^+$, i.e., (MV$^+$)$_2$, in its open-shell singlet state based on a broken-symmetry DFT approach (stereo view shown below). Optimized at the UM06/6-31G** level using PCM.[a]
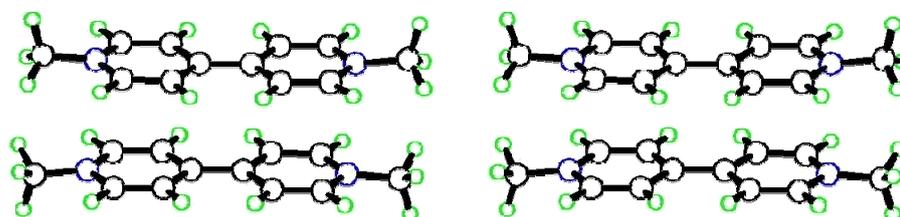
Atom	X	Y	Z	Spin Density
N1	-3.422494	1.730174	0.000090	-0.072261
N2	-3.642457	-1.582569	-0.000081	0.073625
N3	3.642453	1.582500	0.000301	-0.073624
N4	3.422498	-1.730198	-0.000297	0.072261
C5	-1.369378	1.639637	-1.202546	-0.019761
C6	-2.728920	1.695912	1.176672	-0.026791
C7	-0.604858	1.609284	0.000045	-0.079255
C8	-2.728938	1.696354	-1.176518	-0.026795
C9	-1.369364	1.639182	1.202655	-0.019765
C10	0.821730	1.582446	0.000086	-0.082308
C11	1.587600	1.573010	-1.201452	-0.018974
C12	1.587423	1.572303	1.201725	-0.018983
C13	2.949009	1.578046	1.176588	-0.027804
C14	2.949183	1.578719	-1.176101	-0.027805
C15	5.096711	1.710807	0.000456	0.005643
C16	-4.872433	1.887376	0.000140	0.005463
C17	-1.587505	-1.572404	-1.201640	0.018981
C18	-2.949110	-1.578626	1.176273	0.027802
C19	-0.821726	-1.582417	-0.000048	0.082305
C20	-2.949085	-1.578192	-1.176416	0.027802
C21	-1.587526	-1.572856	1.201538	0.018980
C22	0.604851	-1.609234	-0.000094	0.079255
C23	1.369448	-1.639639	1.202453	0.019762
C24	1.369304	-1.639041	-1.202748	0.019766
C25	2.728857	-1.695821	-1.176840	0.026790
C26	2.729003	-1.696392	1.176349	0.026795
C27	4.872429	-1.887430	-0.000462	-0.005463
C28	-5.096706	-1.710910	-0.000135	-0.005643
H29	-3.328995	1.717729	-2.080826	0.001648
H30	-0.894239	1.600327	2.177249	0.001588
H31	-3.328959	1.716922	2.080999	0.001648
H32	1.111942	1.552980	2.176646	0.001544
H33	3.549269	1.575573	2.080981	0.001666
H34	3.549589	1.576791	-2.080400	0.001666
H35	5.505162	1.226753	0.890295	-0.001163
H36	5.389005	2.765192	0.000479	-0.005326
H37	-5.289447	1.410916	0.890558	-0.001150
H38	-5.289477	1.411034	-0.890321	-0.001151

H39	-5.147670	2.946610	0.000225	-0.005151
H40	-1.112086	-1.553179	-2.176593	-0.001544
H41	-3.549409	-1.575830	-2.080768	-0.001666
H42	-3.549457	-1.576613	2.080611	-0.001666
H43	0.894138	-1.599981	-2.177316	-0.001588
H44	3.328849	-1.716773	-2.081200	-0.001648
H45	3.329108	-1.717813	2.080624	-0.001648
H46	5.289396	-1.410828	-0.890828	0.001150
H47	5.147655	-2.946665	-0.000719	0.005151
H48	-5.505296	-1.226974	0.889701	0.001165
H49	-5.388973	-2.765304	-0.000274	0.005327
H50	-5.505262	-1.226747	-0.889865	0.001164
H51	1.112273	1.554325	-2.176459	0.001544
H52	-0.894278	1.601019	-2.177164	0.001587
H53	-1.112137	-1.553950	2.176513	-0.001544
H54	0.894411	-1.601048	2.177102	-0.001587
H55	5.289552	-1.411204	0.890026	0.001150
H56	5.505354	1.226714	-0.889267	-0.001165

[a]Part of the Gaussian output file:

SCF Done: E(UM06) =   -1149.26617471   A.U. after   1 cycles

 Annihilation of the first spin contaminant:

 S**2 before annihilation   0.2387,   after   0.0026

	1	2	3
	A	A	A
Frequencies --	30.8328	37.6395	67.4139
Red. masses --	4.5266	6.3416	3.7880

Zero-point correction=   0.478587 (Hartree/Particle)

 Thermal correction to Energy=   0.503854

 Thermal correction to Enthalpy=   0.504799

 Thermal correction to Gibbs Free Energy=   0.425929

 Sum of electronic and zero-point Energies=   -1148.787588

 Sum of electronic and thermal Energies=   -1148.762320

 Sum of electronic and thermal Enthalpies=   -1148.761376

 Sum of electronic and thermal Free Energies=   -1148.840245

Item	Value	Threshold	Converged?
Maximum Force	0.000031	0.000450	YES
RMS Force	0.000008	0.000300	YES

Table S15. Geometry optimized for the *initially* eclipsed π-dimer of non-derivatized MV$^+$, i.e., (MV$^+$)$_2$, in its triplet state (stereo view shown below). Optimized at the UM06/6-31G** level using PCM.[a]
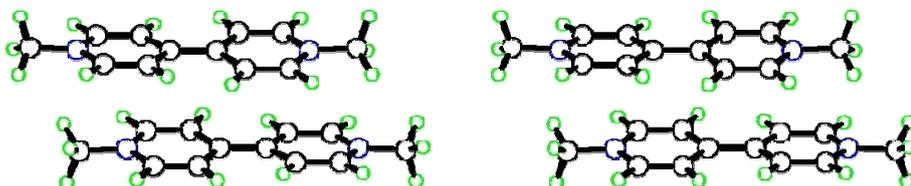
Atom	X	Y	Z	Spin Density
N1	-2.335340	-2.158700	0.087631	0.157926
N2	-4.612815	0.849699	-0.054047	0.151230
N3	4.612738	-0.852089	0.004658	0.153078
N4	2.335940	2.158959	-0.037744	0.154797
C5	-0.314818	-1.713871	1.267826	0.036817
C6	-1.659734	-2.064368	-1.095262	0.061852
C7	0.434357	-1.619315	0.057640	0.169516
C8	-1.649551	-1.980326	1.256164	0.060490
C9	-0.324096	-1.804856	-1.136333	0.040712
C10	1.835473	-1.358778	0.040766	0.146231
C11	2.578379	-1.071018	1.224320	0.050550
C12	2.602241	-1.368888	-1.162849	0.048404
C13	3.942030	-1.129295	-1.154163	0.046249
C14	3.917821	-0.831389	1.181507	0.045237
C15	6.058896	-0.655219	-0.009169	-0.011695
C16	-3.749464	-2.517534	0.110308	-0.011550
C17	-2.619618	1.371837	1.140416	0.033873
C18	-3.901467	0.827976	-1.220809	0.056064
C19	-1.835583	1.358860	-0.051931	0.167913
C20	-3.959021	1.131442	1.113403	0.059188
C21	-2.561541	1.068378	-1.245432	0.039910
C22	-0.434202	1.619242	-0.048316	0.160265
C23	0.330016	1.726823	-1.247846	0.040918
C24	0.309495	1.791904	1.156992	0.042281
C25	1.645661	2.050804	1.135335	0.053915
C26	1.664286	1.994949	-1.216614	0.057362
C27	3.749023	2.523054	-0.038867	-0.012298
C28	-6.058813	0.650795	-0.059080	-0.011739
H29	-2.235490	-2.061664	2.166115	-0.003451
H30	0.133768	-1.726803	-2.116761	-0.003254
H31	-2.252514	-2.207038	-1.993289	-0.003682
H32	2.143649	-1.575066	-2.123597	-0.003527
H33	4.543011	-1.141689	-2.057531	-0.002952
H34	4.497272	-0.605352	2.071186	-0.002946
H35	6.348623	-0.153440	-0.934901	0.002823
H36	6.578545	-1.615534	0.060515	0.010438
H37	-4.225463	-2.175576	-0.811874	0.002144
H38	-4.232999	-2.035198	0.963383	0.003861
H39	-3.871268	-3.601508	0.194902	0.012232

H40	-2.175599	1.583393	2.106794	-0.002884
H41	-4.572881	1.146380	2.008081	-0.003263
H42	-4.468090	0.599425	-2.118065	-0.003147
H43	-0.159859	1.699815	2.130794	-0.003205
H44	2.227571	2.179959	2.042462	-0.003247
H45	2.261247	2.088641	-2.118166	-0.003443
H46	4.210789	2.186838	0.892508	0.002752
H47	3.867716	3.607191	-0.125787	0.010600
H48	-6.336636	0.043078	-0.922334	0.003366
H49	-6.579157	1.611775	-0.111959	0.010615
H50	-6.357540	0.127292	0.851782	0.001639
H51	2.097239	-1.018812	2.195045	-0.003661
H52	0.155919	-1.587396	2.236949	-0.003049
H53	-2.066295	1.013320	-2.208904	-0.003146
H54	-0.129398	1.614210	-2.224097	-0.003214
H55	4.249297	2.039684	-0.881891	0.002169
H56	6.346272	-0.028252	0.837119	0.001939

[a]Part of the Gaussian output file:

SCF Done: E(UM06) =   -1149.26383418   A.U. after   1 cycles

Annihilation of the first spin contaminant:

S**2 before annihilation   2.0104,   after   2.0001

	1	2	3
	A	A	A
Frequencies --	16.7458	32.2392	57.9186
Red. masses --	4.6625	6.1281	3.6716

Zero-point correction=	0.477917 (Hartree/Particle)
Thermal correction to Energy=	0.503796
Thermal correction to Enthalpy=	0.504740
Thermal correction to Gibbs Free Energy=	0.421901
Sum of electronic and zero-point Energies=	-1148.785917
Sum of electronic and thermal Energies=	-1148.760038
Sum of electronic and thermal Enthalpies=	-1148.759094
Sum of electronic and thermal Free Energies=	-1148.841933

Item	Value	Threshold	Converged?
Maximum Force	0.000008	0.000450	YES
RMS Force	0.000002	0.000300	YES

Table S16. Geometry optimized for the staggered π-dimer of non-derivatized MV⁺, i.e., (MV⁺)₂, in its closed-shell singlet state (stereo view shown below). Optimized at the M06/6-31G** level using PCM.[a]

Atom	X	Y	Z
N1	3.042423	-1.794459	1.514777
N2	3.032392	1.793303	-1.529595
N3	-3.031467	1.827775	1.497494
N4	-3.041772	-1.828189	-1.486218
C5	0.660072	-1.778684	1.492015
C6	3.046155	-0.431160	1.543056
C7	0.617225	-0.350414	1.513550
C8	1.845626	-2.449747	1.476867
C9	1.887641	0.287933	1.557361
C10	-0.606433	0.384137	1.510289
C11	-1.876416	-0.253510	1.570222
C12	-0.649287	1.811976	1.465427
C13	-1.834938	2.482536	1.443742
C14	-3.035046	0.465178	1.549817
C15	-4.294453	2.546197	1.369678
C16	4.305652	-2.515007	1.401170
C17	1.876801	-0.288446	-1.572832
C18	1.835256	2.449162	-1.488604
C19	0.606854	0.350003	-1.522679
C20	3.035663	0.430447	-1.560795
C21	0.649799	1.778612	-1.502839
C22	-0.616842	-0.384244	-1.512111
C23	-1.887246	0.253176	-1.566435
C24	-0.659485	-1.812011	-1.463887
C25	-1.844998	-2.482666	-1.436062
C26	-3.045686	-0.465607	-1.539981
C27	-4.304403	-2.546585	-1.354411
C28	4.288797	2.519392	-1.383312
H29	1.897783	-3.533012	1.448294
H30	1.979165	1.367862	1.607305
H31	4.023991	0.041239	1.571727
H32	0.254626	2.410364	1.445711
H33	-1.887547	3.565135	1.396459
H34	-4.012663	-0.006511	1.592936
H35	-4.135011	3.602865	1.587100
H36	-5.020290	2.143155	2.079417
H37	4.704491	-2.418392	0.385650
H38	4.143340	-3.569816	1.625262
H39	5.027010	-2.107652	2.113106
H40	1.968124	-1.368194	-1.625523
H41	4.012677	-0.042760	-1.595453
H42	1.888919	3.532456	-1.458276
H43	0.244477	-2.410401	-1.445876
H44	-1.897241	-3.565178	-1.386379
H45	-4.023554	0.005915	-1.579044
H46	-4.695533	-2.437065	-0.337153

H47	-4.144463	-3.604207	-1.566720
H48	4.587859	2.547555	-0.329639
H49	4.166344	3.538459	-1.752944
H50	5.066671	2.022005	-1.965815
H51	-1.967546	-1.332577	1.636257
H52	-0.244251	-2.376773	1.486284
H53	-0.254762	2.376370	-1.496653
H54	-1.978951	1.332189	-1.632827
H55	-5.030724	-2.147419	-2.065864
H56	-4.685832	2.441373	0.351991

[a]Part of the Gaussian output file:

SCF Done: E(RM06) =   -1149.26537041   A.U. after   1 cycles

	1	2	3
	A	A	A
Frequencies --	30.5881	43.7482	64.4238
Red. masses --	4.2558	4.9255	3.9748

|	
Zero-point correction=	0.477755 (Hartree/Particle)
Thermal correction to Energy=	0.503922
Thermal correction to Enthalpy=	0.504866
Thermal correction to Gibbs Free Energy=	0.422917
Sum of electronic and zero-point Energies=	-1148.787616
Sum of electronic and thermal Energies=	-1148.761449
Sum of electronic and thermal Enthalpies=	-1148.760505
Sum of electronic and thermal Free Energies=	-1148.842454

Item	Value	Threshold	Converged?
Maximum Force	0.000007	0.000450	YES
RMS Force	0.000001	0.000300	YES

Table S17. Geometry optimized for the staggered π-dimer of non-derivatized MV$^+$, i.e., (MV$^+$)$_2$, in its open-shell singlet state based on a broken-symmetry DFT approach (stereo view shown below). Optimized at the UM06/6-31G** level using PCM.[a]
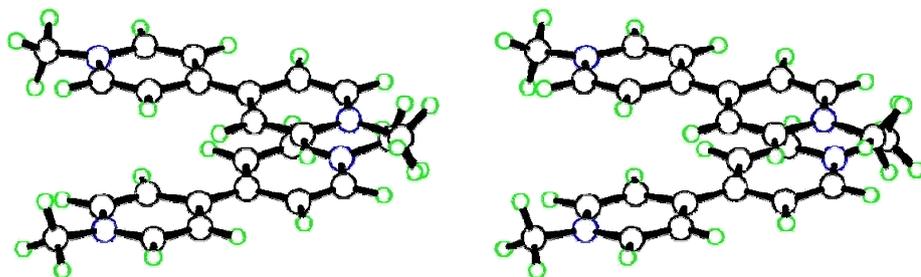
Atom	X	Y	Z	Spin Density
N1	-3.049958	-1.691405	-1.594336	-0.111228
N2	-3.049870	1.691400	1.594418	0.111226
N3	3.048308	1.882817	-1.422372	-0.111958
N4	3.048392	-1.882824	1.422322	0.111959
C5	-0.667774	-1.690841	-1.581450	-0.031845
C6	-3.044974	-0.327325	-1.598505	-0.041848
C7	-0.615011	-0.263714	-1.572718	-0.124397
C8	-1.856496	-2.355234	-1.576238	-0.035020
C9	-1.882945	0.384608	-1.598108	-0.031853
C10	0.614361	0.458904	-1.539110	-0.124710
C11	1.882257	-0.184722	-1.613417	-0.028867
C12	0.666514	1.881818	-1.425083	-0.034556
C13	1.855467	2.543210	-1.357686	-0.033328
C14	3.044027	0.523802	-1.547086	-0.043856
C15	4.311952	2.588927	-1.241088	0.008812
C16	-4.308080	-2.418289	-1.465997	0.008733
C17	-1.882843	-0.384612	1.598194	0.031861
C18	-1.856405	2.355233	1.576374	0.035026
C19	-0.614915	0.263718	1.572809	0.124397
C20	-3.044873	0.327316	1.598575	0.041846
C21	-0.667682	1.690845	1.581617	0.031834
C22	0.614457	-0.458893	1.539129	0.124709
C23	1.882363	0.184723	1.613394	0.028869
C24	0.666597	-1.881803	1.425094	0.034554
C25	1.855541	-2.543206	1.357674	0.033330
C26	3.044124	-0.523807	1.547026	0.043855
C27	4.312004	-2.588949	1.240860	-0.008812
C28	-4.307965	2.418296	1.465863	-0.008733
H29	-1.916482	-3.438551	-1.566018	0.002146
H30	-1.968092	1.465788	-1.624155	0.002570
H31	-4.019649	0.151451	-1.612740	0.002681
H32	-0.233745	2.484705	-1.381585	0.002936
H33	1.914247	3.621790	-1.256359	0.002091
H34	4.019750	0.049152	-1.598031	0.002813
H35	4.169792	3.648780	-1.455560	-0.000804
H36	5.058777	2.185144	-1.927936	-0.003196
H37	-4.588968	-2.507164	-0.410981	-0.007995

H38	-4.197971	-3.414926	-1.896308	-0.001467
H39	-5.093106	-1.884629	-2.004910	-0.002185
H40	-1.967989	-1.465792	1.624251	-0.002571
H41	-4.019551	-0.151458	1.612778	-0.002681
H42	-1.916403	3.438549	1.566204	-0.002146
H43	-0.233672	-2.484676	1.381617	-0.002936
H44	1.914313	-3.621785	1.256339	-0.002091
H45	4.019847	-0.049151	1.597933	-0.002813
H46	4.665181	-2.473116	0.210600	0.007744
H47	4.169869	-3.648785	1.455439	0.000804
H48	-4.588381	2.507672	0.410764	0.007996
H49	-4.198017	3.414742	1.896663	0.001470
H50	-5.093235	1.884421	2.004203	0.002181
H51	1.967194	-1.260518	-1.725164	0.002389
H52	0.234162	-2.293096	-1.579420	0.002824
H53	0.234251	2.293099	1.579672	-0.002823
H54	1.967312	1.260522	1.725099	-0.002389
H55	5.058944	-2.185121	1.927553	0.003194
H56	4.665314	2.473010	-0.210904	-0.007743

[a]Part of the Gaussian output file:

SCF Done: E(UM06) =   -1149.26682023   A.U. after   1 cycles

Annihilation of the first spin contaminant:
S**2 before annihilation   0.5574,   after   0.0165

	1	2	3
	A	A	A
Frequencies --	41.7060	41.7674	57.5305
Red. masses --	4.4950	5.6279	4.4980

Zero-point correction=	0.478704 (Hartree/Particle)
Thermal correction to Energy=	0.504599
Thermal correction to Enthalpy=	0.505544
Thermal correction to Gibbs Free Energy=	0.424677
Sum of electronic and zero-point Energies=	-1148.788117
Sum of electronic and thermal Energies=	-1148.762221
Sum of electronic and thermal Enthalpies=	-1148.761277
Sum of electronic and thermal Free Energies=	-1148.842143

Item	Value	Threshold	Converged?
Maximum Force	0.000007	0.000450	YES
RMS Force	0.000001	0.000300	YES

Table S18. Geometry optimized for the staggered π-dimer of non-derivatized MV⁺, i.e., $(MV^+)_2$, in its triplet state (stereo view shown below). Optimized at the UM06/6-31G** level using PCM.[a]

Atom	X	Y	Z	Spin Density
N1	3.603456	1.334508	1.332283	0.156519
N2	3.022191	-1.642972	-1.345125	0.155224
N3	-3.020395	1.884648	-1.072986	0.155761
N4	-3.607734	-1.557964	1.099455	0.157287
C5	1.258415	1.376910	1.742248	0.045623
C6	3.369127	1.529633	-0.000255	0.054831
C7	0.965935	1.594039	0.362611	0.165884
C8	2.539667	1.252503	2.185144	0.050061
C9	2.106119	1.655486	-0.492419	0.040390
C10	-0.367384	1.726726	-0.122260	0.153854
C11	-1.493097	1.794624	0.751669	0.044691
C12	-0.682592	1.772626	-1.512767	0.049395
C13	-1.972130	1.842879	-1.946368	0.048622
C14	-2.762434	1.877234	0.269110	0.052853
C15	-4.393421	2.006443	-1.551884	-0.011900
C16	4.963632	1.132434	1.820741	-0.011775
C17	1.497020	-1.947026	0.458373	0.045417
C18	1.973185	-1.418619	-2.189380	0.047335
C19	0.371299	-1.695708	-0.380455	0.152046
C20	2.766431	-1.922418	-0.032539	0.054750
C21	0.684981	-1.442432	-1.748822	0.048271
C22	-0.964423	-1.669055	0.115456	0.165996
C23	-2.095994	-1.519650	-0.740638	0.039906
C24	-1.270025	-1.764516	1.506090	0.045468
C25	-2.553416	-1.701133	1.956256	0.051972
C26	-3.361547	-1.474788	-0.242726	0.054361
C27	-4.966912	-1.413538	1.610262	-0.011843
C28	4.392925	-1.643298	-1.845497	-0.012187
H29	2.780031	1.077869	3.228782	-0.003178
H30	2.005751	1.822241	-1.559706	-0.003126
H31	4.249620	1.585002	-0.633129	-0.003607
H32	0.090778	1.722240	-2.272092	-0.003375
H33	-2.230106	1.861036	-3.000153	-0.003077
H34	-3.630335	1.941348	0.918293	-0.003591
H35	-4.457571	1.619197	-2.569843	0.001727
H36	-4.713724	3.052524	-1.541397	0.010950
H37	5.232805	0.071938	1.782478	0.010529
H38	5.035500	1.485267	2.850835	0.002608
H39	5.658425	1.703938	1.202849	0.002784
H40	1.377701	-2.177292	1.511614	-0.003454
H41	3.635210	-2.119714	0.587882	-0.003604
H42	2.230660	-1.211945	-3.223110	-0.002988
H43	-0.490135	-1.875260	2.251842	-0.003531
H44	-2.803529	-1.756940	3.010557	-0.003259
H45	-4.235043	-1.379972	-0.880358	-0.003611
H46	-5.204085	-0.358100	1.778772	0.010687

H47	-5.061077	-1.958163	2.551074	0.002430
H48	4.465772	-0.967141	-2.699227	0.002535
H49	4.691771	-2.649863	-2.153162	0.011078
H50	5.065670	-1.291773	-1.059773	0.002920
H51	-1.373586	1.799362	1.829390	-0.003449
H52	0.468981	1.284914	2.480631	-0.003451
H53	-0.089332	-1.238172	-2.480614	-0.003326
H54	-1.986762	-1.456611	-1.818023	-0.003025
H55	-5.672187	-1.829745	0.888661	0.002934
H56	-5.055985	1.420127	-0.910142	0.003656

[a]Part of the Gaussian output file:

SCF Done: E(UM06) =   -1149.26307483   A.U. after   1 cycles

Annihilation of the first spin contaminant:

S**2 before annihilation   2.0105,   after   2.0001

	1	2	3
	A	A	A
Frequencies --	25.1333	31.4966	38.4939
Red. masses --	5.1029	4.3719	3.9949

Zero-point correction=	0.478221 (Hartree/Particle)
Thermal correction to Energy=	0.504381
Thermal correction to Enthalpy=	0.505325
Thermal correction to Gibbs Free Energy=	0.421615
Sum of electronic and zero-point Energies=	-1148.784854
Sum of electronic and thermal Energies=	-1148.758694
Sum of electronic and thermal Enthalpies=	-1148.757750
Sum of electronic and thermal Free Energies=	-1148.841460

Item	Value	Threshold	Converged?
Maximum Force	0.000012	0.000450	YES
RMS Force	0.000003	0.000300	YES

Table S19. Geometry optimized for the eclipsed π-dimer of Asp-based $(MV^+)_2$ in its closed-shell singlet state (stereo view shown below). Optimized at the M06/6-31G** level using PCM.[a]
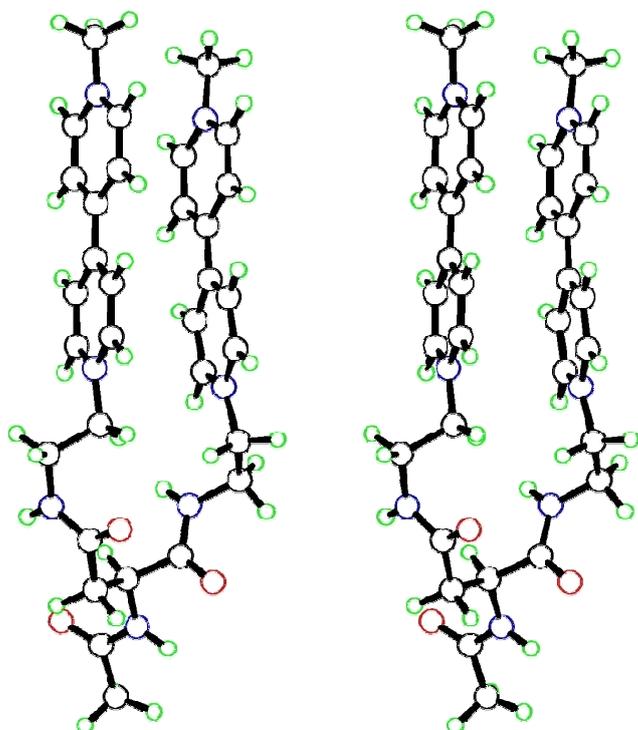
Atom	X	Y	Z
N1	0.381072	1.722839	-0.525541
N2	0.734344	-1.596734	-1.340183
N3	-6.580773	1.395853	0.604448
N4	-6.001083	-1.852822	0.792604
C5	-1.450766	1.523622	0.985835
C6	-0.494056	1.858090	-1.566368
C7	-2.396417	1.616522	-0.076983
C8	-0.114905	1.553728	0.741704
C9	-1.840779	1.822480	-1.373850
H10	0.624160	1.440234	1.529504
H11	-2.469931	1.951160	-2.247636
H12	-0.049126	1.999549	-2.546431
C13	-3.804174	1.545598	0.149814
C14	-4.362874	1.478162	1.459216
C15	-4.749502	1.519068	-0.912118
C16	-6.089063	1.445502	-0.667056
C17	-5.709880	1.418603	1.653333
H18	-4.436134	1.527107	-1.951031
H19	-6.826335	1.419873	-1.462976
H20	-6.155393	1.379304	2.642480
C21	-8.023368	1.437555	0.831847
H22	-8.532038	0.909321	0.022321
H23	-8.375099	2.472850	0.861050

S52

C24	1.815507	1.600675	-0.747086
H25	1.985408	1.408549	-1.808930
H26	2.169859	0.722869	-0.189146
C27	2.618031	2.818776	-0.288763
H28	2.611690	3.590517	-1.068241
H29	2.163216	3.252054	0.607113
N30	3.975079	2.436738	0.049025
H31	4.305494	2.599495	0.990489
C32	4.769003	1.786862	-0.837681
O33	4.421293	1.572267	-1.995709
H34	-1.014877	-1.777757	1.497416
C35	-0.861472	-1.656056	0.430794
C36	-0.285321	-1.371219	-2.225707
C37	-1.958372	-1.513282	-0.467933
C38	0.426389	-1.717354	-0.016833
C39	-1.587918	-1.325534	-1.830229
H40	1.247056	-1.880727	0.671479
H41	0.010181	-1.243233	-3.262589
C42	-3.318442	-1.583850	-0.042953
C43	-4.406640	-1.645210	-0.965266
C44	-3.686971	-1.672152	1.331217
C45	-4.988983	-1.789426	1.710045
C46	-5.691066	-1.778206	-0.535635
H47	-2.946469	-1.612987	2.122067
H48	-5.288652	-1.846301	2.751704
H49	-6.529725	-1.837810	-1.222597
C50	-7.370569	-2.107497	1.223765
H51	-7.538964	-1.640441	2.197593
H52	-7.556509	-3.182566	1.310242
C53	2.094289	-1.776110	-1.896918
H54	2.465738	-0.805132	-2.255660
H55	1.978474	-2.426993	-2.769139
C56	3.132910	-2.384224	-0.968496
H57	2.709759	-3.177414	-0.343379
H58	3.885090	-2.855140	-1.608351
N59	3.853414	-1.422411	-0.153226
H60	3.499486	-1.160202	0.757552
C61	5.131680	-1.077487	-0.463876
O62	5.731111	-1.500249	-1.442388
C63	6.056575	1.239673	-0.269943
H64	6.738517	1.043202	-1.103065
H65	6.531754	1.937669	0.428809
C66	5.803774	-0.084666	0.475590
H67	5.194930	0.107852	1.368029
N68	7.046585	-0.673813	0.915917
H69	7.554999	-1.230391	0.239897
C70	7.603598	-0.350547	2.115120
O71	7.054416	0.412433	2.902304
C72	8.928790	-0.996802	2.410709
H73	9.687011	-0.215269	2.517679
H74	9.253262	-1.704801	1.644312

H75	8.859373	-1.514635	3.371482
H76	-3.738395	1.491866	2.345655
H77	-1.764565	1.372607	2.013192
H78	-2.331018	-1.136834	-2.598233
H79	-4.245283	-1.600231	-2.036848
H80	-8.067273	-1.683894	0.496650
H81	-8.258736	0.951749	1.780807

[a]Part of the Gaussian output file:

SCF Done: E(RM06) =   -1850.34855691   A.U. after   1 cycles

	1	2	3
	A	A	A
Frequencies --	20.2820	24.4298	34.5737
Red. masses --	5.6289	5.4753	6.9115

Zero-point correction=	0.683717 (Hartree/Particle)
Thermal correction to Energy=	0.722627
Thermal correction to Enthalpy=	0.723572
Thermal correction to Gibbs Free Energy=	0.613296
Sum of electronic and zero-point Energies=	-1849.664840
Sum of electronic and thermal Energies=	-1849.625929
Sum of electronic and thermal Enthalpies=	-1849.624985
Sum of electronic and thermal Free Energies=	-1849.735261

Item	Value	Threshold	Converged?
Maximum Force	0.000040	0.000450	YES
RMS Force	0.000005	0.000300	YES

Table 20. Geometry optimized for the *initially* eclipsed π-dimer of Asp-based (MV⁺)₂ in its open-shell singlet state based on a broken-symmetry DFT approach (stereo view shown below). Optimized at the UM06/6-31G** level using PCM, where a slipped dimer was given even though the initial structure was taken to be an eclipsed one.[a]
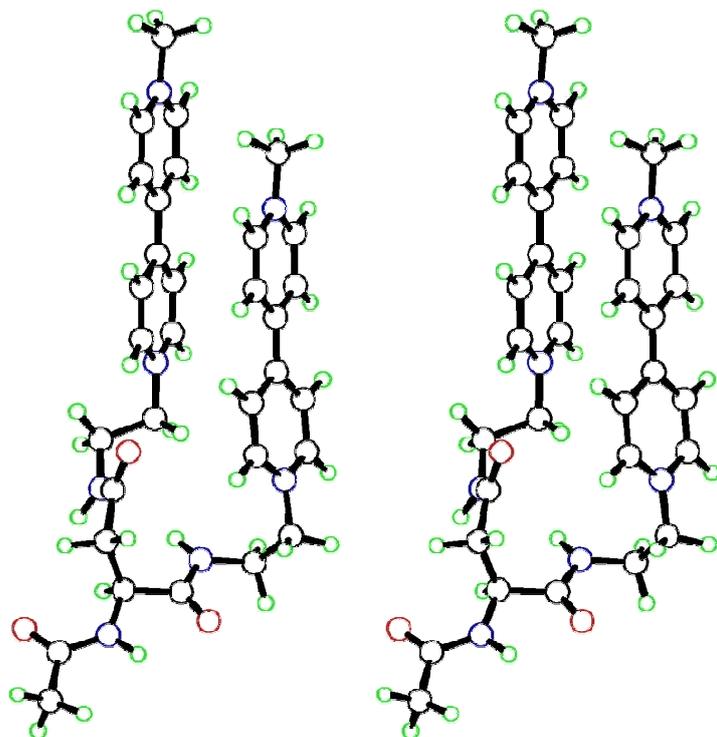
Atom	X	Y	Z	Spin Density
N1	-0.579215	0.799073	1.263225	0.143958
N2	2.107937	-2.901017	-0.012621	-0.148714
N3	-7.428932	1.835096	-0.143692	0.151134
N4	-4.750688	-1.553130	-1.025406	-0.147376
C5	-2.854936	0.663352	1.942194	0.048753
C6	-0.970899	1.312325	0.054634	0.063168
C7	-3.311760	1.211030	0.707293	0.154233
C8	-1.528359	0.476803	2.189161	0.050235
C9	-2.283770	1.523544	-0.231798	0.033504
H10	-1.162109	0.063774	3.123527	-0.002732
H11	-2.513536	1.922687	-1.213891	-0.003258
H12	-0.166538	1.515160	-0.648884	-0.003424
C13	-4.693055	1.415626	0.421918	0.170112
C14	-5.730113	1.060020	1.336899	0.038247
C15	-5.145305	1.993836	-0.802463	0.040300
C16	-6.470328	2.186142	-1.051349	0.051454
C17	-7.041749	1.270577	1.039138	0.051441
H18	-4.448528	2.310284	-1.570805	-0.003124
H19	-6.829854	2.625038	-1.976284	-0.003109
H20	-7.843315	1.003080	1.719995	-0.003096
C21	-8.846218	1.947628	-0.472456	-0.011668

H22	-9.222249	0.998546	-0.868564	0.010570
H23	-8.983838	2.729852	-1.220337	0.001668
C24	0.848116	0.600367	1.515735	-0.017335
H25	1.226827	-0.085474	0.747387	0.013018
H26	0.957009	0.111555	2.487961	0.000101
C27	1.618627	1.925484	1.460112	0.007507
H28	1.072250	2.642135	0.834063	-0.000703
H29	1.705131	2.363923	2.456483	-0.000355
N30	2.956696	1.735048	0.929323	-0.000235
H31	3.720927	2.171446	1.429217	0.000076
C32	3.116875	1.461413	-0.401256	-0.000636
O33	2.158521	1.238689	-1.132559	0.000799
H34	-0.836245	-3.538427	1.433859	0.002743
C35	-0.152336	-3.089991	0.721779	-0.031342
C36	1.712997	-2.043003	-0.999374	-0.055547
C37	-0.621800	-2.265131	-0.345219	-0.170081
C38	1.166814	-3.392255	0.852642	-0.058935
C39	0.400542	-1.724525	-1.183183	-0.042974
H40	1.537513	-4.052467	1.630747	0.003454
H41	2.503803	-1.632801	-1.620661	0.003763
C42	-2.007961	-2.018860	-0.566316	-0.152608
C43	-2.487030	-1.354472	-1.733889	-0.041881
C44	-3.017744	-2.422848	0.355805	-0.043307
C45	-4.336023	-2.184527	0.112390	-0.051799
C46	-3.817694	-1.151937	-1.939153	-0.052894
H47	-2.767488	-2.909736	1.292081	0.003293
H48	-5.118926	-2.471759	0.807024	0.002817
H49	-4.203977	-0.664883	-2.829243	0.003085
C50	-6.173261	-1.405793	-1.313683	0.013298
H51	-6.725441	-1.327172	-0.373792	-0.002664
H52	-6.542087	-2.265740	-1.880223	-0.009524
C53	3.510922	-3.287754	0.146743	0.010777
H54	4.015805	-3.145746	-0.813234	-0.001395
H55	3.542053	-4.356115	0.384254	-0.004590
C56	4.219584	-2.498971	1.234536	-0.008180
H57	3.663991	-2.558375	2.175945	0.000604
H58	5.202948	-2.954793	1.397789	-0.000975
N59	4.394533	-1.097818	0.901250	0.000019
H60	3.888507	-0.396432	1.429664	-0.000036
C61	5.414935	-0.708096	0.100750	-0.000097
O62	6.135569	-1.503969	-0.490315	-0.000135
C63	4.532835	1.446259	-0.921803	-0.000002
H64	4.514216	0.953048	-1.899909	0.000015
H65	4.839360	2.488629	-1.081043	-0.000040
C66	5.613169	0.800203	-0.038221	-0.000027
H67	5.605128	1.258345	0.961222	0.000000
N68	6.917077	1.008102	-0.615300	-0.000001
H69	7.354926	0.191377	-1.026965	0.000001
C70	7.544481	2.206904	-0.528345	-0.000004
O71	7.016230	3.176494	0.010309	-0.000009
C72	8.924707	2.269716	-1.121965	0.000001

H73	8.983844	3.136424	-1.785723	-0.000001
H74	9.203796	1.370582	-1.676768	0.000000
H75	9.648879	2.426609	-0.316486	0.000000
H76	-5.510164	0.612274	2.299938	-0.003008
H77	-3.547430	0.378954	2.726565	-0.003458
H78	0.169371	-1.028114	-1.982546	0.003732
H79	-1.807105	-1.010938	-2.506120	0.003346
H80	-6.329009	-0.493454	-1.895546	-0.003372
H81	-9.408438	2.213107	0.424834	0.003427

aPart of the Gaussian output file:

SCF Done: E(UM06) = -1850.36031410   A.U. after   1 cycles

 Annihilation of the first spin contaminant:

 S**2 before annihilation   0.9784,   after   0.0703

	1	2	3
	A	A	A
Frequencies --	12.4227	27.2485	33.0382
Red. masses --	5.4960	5.1177	5.8513

Zero-point correction=   0.684557 (Hartree/Particle)

 Thermal correction to Energy=   0.723256

 Thermal correction to Enthalpy=   0.724200

 Thermal correction to Gibbs Free Energy=   0.613813

 Sum of electronic and zero-point Energies=   -1849.675757

 Sum of electronic and thermal Energies=   -1849.637058

 Sum of electronic and thermal Enthalpies=   -1849.636114

 Sum of electronic and thermal Free Energies=   -1849.746501

Item	Value	Threshold	Converged?
Maximum Force	0.000073	0.000450	YES
RMS Force	0.000011	0.000300	YES

Table S21. Geometry optimized for the *initially* eclipsed π-dimer of Asp-based (MV$^+$)$_2$ in its triplet state (stereo view shown below). Optimized at the UM06/6-31G** level using PCM, where a slipped dimer was given even though the initial structure was taken to be an eclipsed one.[a]
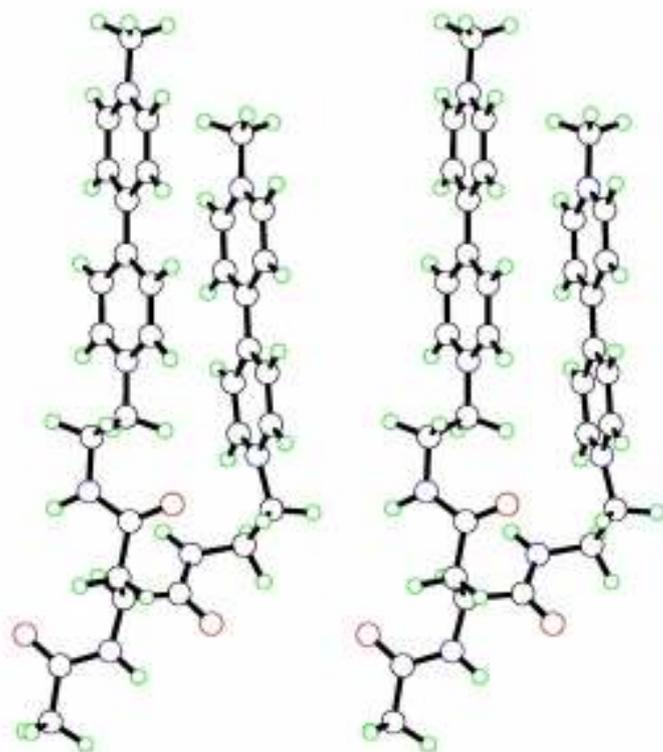
Atom	X	Y	Z	Spin Density
N1	-0.388639	1.148345	0.038265	0.155956
N2	1.750139	-2.587439	-0.247369	0.155715
N3	-7.419636	1.855048	-0.095039	0.154539
N4	-5.241323	-1.720993	0.478408	0.155526
C5	-2.425847	1.655935	1.159144	0.047102
C6	-1.081901	0.955056	-1.125932	0.053775
C7	-3.191323	1.454827	-0.027969	0.166059
C8	-1.072982	1.508077	1.164842	0.051732
C9	-2.432816	1.105261	-1.184883	0.035479
H10	-0.473520	1.664904	2.055643	-0.003342
H11	-2.910398	0.913114	-2.139823	-0.003079
H12	-0.489922	0.658207	-1.987006	-0.003319
C13	-4.610994	1.578993	-0.051123	0.164166
C14	-5.380990	1.779340	1.133732	0.042458
C15	-5.369413	1.509968	-1.257578	0.042578
C16	-6.724051	1.647485	-1.252757	0.053492
C17	-6.735568	1.909548	1.086253	0.048725
H18	-4.889533	1.367914	-2.219949	-0.003193
H19	-7.316554	1.606503	-2.160901	-0.003160
H20	-7.337604	2.058563	1.976754	-0.003043
C21	-8.878130	1.904179	-0.105671	-0.011802

H22	-9.220068	2.325586	-1.052359	0.002533
H23	-9.224891	2.539650	0.710874	0.002625
C24	1.066834	1.025046	0.045395	-0.009729
H25	1.350563	0.077896	-0.428039	0.003325
H26	1.404791	1.005467	1.086250	0.000787
C27	1.719646	2.176602	-0.709328	0.009051
H28	1.391186	2.162353	-1.757656	-0.000526
H29	1.408922	3.132521	-0.277830	-0.000492
N30	3.161223	2.092859	-0.650290	0.000800
H31	3.669251	2.841937	-0.200009	0.000051
C32	3.856694	1.115847	-1.286323	0.000164
O33	3.311442	0.189128	-1.880229	0.001030
H34	-0.504832	-2.114740	2.170876	-0.003065
C35	-0.148048	-2.223683	1.152519	0.037289
C36	0.933879	-2.498104	-1.344620	0.060341
C37	-1.040531	-2.175744	0.040491	0.182517
C38	1.186237	-2.445635	0.989228	0.060489
C39	-0.407640	-2.301769	-1.233453	0.031555
H40	1.848475	-2.515805	1.843568	-0.003610
H41	1.423286	-2.605865	-2.307442	-0.003474
C42	-2.449841	-2.020738	0.187345	0.147722
C43	-3.346211	-2.063403	-0.920836	0.054268
C44	-3.069490	-1.802655	1.452955	0.044864
C45	-4.418447	-1.657932	1.567290	0.046672
C46	-4.690743	-1.922766	-0.753191	0.040879
H47	-2.486787	-1.722431	2.363970	-0.003348
H48	-4.907523	-1.484949	2.521077	-0.003310
H49	-5.386375	-1.965271	-1.585050	-0.002942
C50	-6.688142	-1.648482	0.655122	-0.010371
H51	-6.926694	-0.855976	1.370426	0.004162
H52	-7.076208	-2.600374	1.029442	0.010888
C53	3.138550	-3.037440	-0.464702	-0.011406
H54	3.498670	-2.524411	-1.364939	0.003463
H55	3.113413	-4.115387	-0.666497	0.011150
C56	4.108257	-2.763377	0.666404	0.001199
H57	3.752485	-3.131727	1.632790	-0.000183
H58	5.018040	-3.326236	0.437574	-0.000296
N59	4.490313	-1.370804	0.775252	0.000220
H60	3.943937	-0.732231	1.338302	-0.000134
C61	5.571531	-0.916408	0.102636	0.000040
O62	6.298690	-1.635880	-0.573454	0.000049
C63	5.354947	1.223331	-1.136769	-0.000005
H64	5.827282	0.700604	-1.974916	-0.000006
H65	5.681883	2.268725	-1.136583	0.000012
C66	5.836431	0.577319	0.176454	0.000035
H67	5.319434	1.043102	1.025966	0.000000
N68	7.255165	0.766297	0.353559	0.000002
H69	7.860444	0.042856	-0.015724	0.000000
C70	7.752831	1.937511	0.830073	0.000000
O71	7.019738	2.859630	1.174667	0.000002
C72	9.251822	2.027216	0.905246	0.000000

H73	9.598635	2.773307	0.183467	0.000000
H74	9.756705	1.079330	0.703361	0.000000
H75	9.533728	2.381749	1.900276	0.000000
H76	-4.913972	1.824608	2.111689	-0.003318
H77	-2.894445	1.945778	2.093072	-0.003363
H78	-0.972963	-2.242606	-2.157302	-0.002701
H79	-2.989868	-2.221286	-1.932786	-0.003681
H80	-7.160088	-1.421216	-0.303076	0.000707
H81	-9.295844	0.899181	0.015156	0.010703

[a]Part of the Gaussian output file:

SCF Done: E(UM06) =   -1850.35591956   A.U. after   1 cycles

Annihilation of the first spin contaminant:

S**2 before annihilation   2.0103,   after   2.0001

	1	2	3
	A	A	A
Frequencies --	17.3525	26.5547	28.6000
Red. masses --	5.3934	5.8990	5.5435

|	
Zero-point correction=	0.683761 (Hartree/Particle)
Thermal correction to Energy=	0.722847
Thermal correction to Enthalpy=	0.723792
Thermal correction to Gibbs Free Energy=	0.611390
Sum of electronic and zero-point Energies=	-1849.672158
Sum of electronic and thermal Energies=	-1849.633072
Sum of electronic and thermal Enthalpies=	-1849.632128
Sum of electronic and thermal Free Energies=	-1849.744530

Item	Value	Threshold	Converged?
Maximum Force	0.000050	0.000450	YES
RMS Force	0.000008	0.000300	YES

Table S22. Geometry optimized for the staggered π-dimer of Asp-based $(MV^+)_2$ in its closed-shell singlet state (stereo view shown below). Optimized at the M06/6-31G** level using PCM.[a]
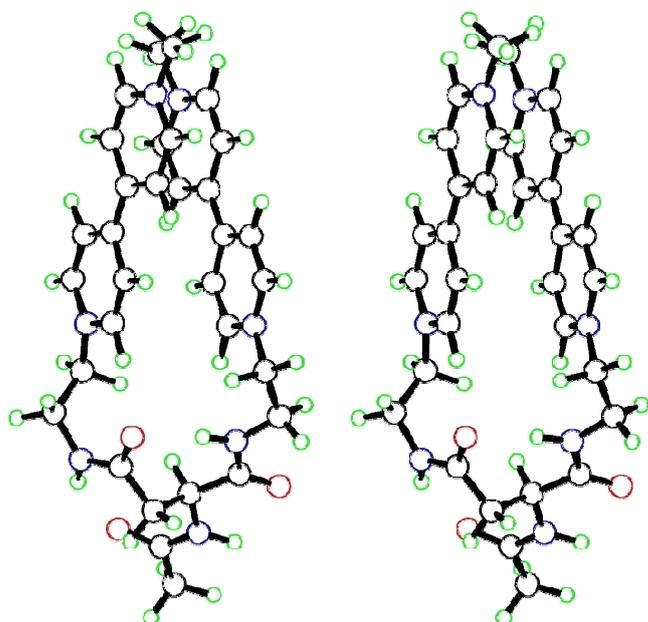
Atom	X	Y	Z
N1	-0.499509	-1.852438	-1.272666
N2	-0.352933	2.528756	0.458734
N3	6.036085	0.839645	-1.487463
N4	5.074862	-1.578092	2.418002
C5	1.848313	-2.130268	-0.971236
C6	-0.287505	-0.574398	-1.714330
C7	2.112987	-0.792553	-1.402975
C8	0.575725	-2.609714	-0.903068
C9	0.969121	-0.054423	-1.808966
H10	0.354436	-3.614886	-0.558927
H11	1.050316	0.959418	-2.187755
H12	-1.181508	-0.014078	-1.985726
C13	3.430153	-0.241487	-1.434726
C14	4.582181	-1.007424	-1.107406
C15	3.690174	1.115879	-1.794075
C16	4.957365	1.616574	-1.795747
C17	5.831086	-0.458928	-1.130518
H18	2.889269	1.793952	-2.066627
H19	5.172953	2.648527	-2.052864
H20	6.720403	-1.030453	-0.881190
C21	7.375268	1.412975	-1.397167
H22	7.420961	2.323033	-1.996400
H23	8.105444	0.698021	-1.781807
C24	-1.865909	-2.284637	-0.970792
H25	-2.261608	-1.608187	-0.199721
H26	-1.801773	-3.277290	-0.519267

C27	-2.815770	-2.282708	-2.182725
H28	-2.351122	-1.762550	-3.026304
H29	-3.028302	-3.302868	-2.508405
N30	-4.071524	-1.624353	-1.880298
H31	-4.807779	-2.137798	-1.398905
C32	-4.137898	-0.278542	-1.838406
O33	-3.212656	0.450082	-2.218191
H34	0.205219	-0.534707	1.663547
C35	0.468444	0.452711	1.298014
C36	0.935556	2.982421	0.374509
C37	1.820888	0.886197	1.236072
C38	-0.563339	1.255958	0.905544
C39	1.997070	2.221350	0.757346
H40	-1.596600	0.926277	0.949313
H41	1.058431	3.992283	-0.003242
C42	2.912224	0.056289	1.630295
C43	4.252945	0.531642	1.677147
C44	2.740129	-1.305479	2.030025
C45	3.803829	-2.075702	2.389564
C46	5.282889	-0.282791	2.046238
H47	1.762573	-1.774028	2.055341
H48	3.695070	-3.114986	2.682026
H49	6.312049	0.062712	2.081835
C50	6.213863	-2.448978	2.685029
H51	6.630216	-2.826061	1.744108
H52	5.893064	-3.290420	3.300822
C53	-1.437963	3.354786	-0.095604
H54	-1.555857	3.101825	-1.160384
H55	-1.096236	4.391684	-0.048100
C56	-2.771342	3.245514	0.620165
H57	-2.632724	3.212453	1.707710
H58	-3.344219	4.156187	0.401122
N59	-3.505251	2.067026	0.196390
H60	-3.304273	1.680521	-0.729235
C61	-4.558781	1.592260	0.897469
O62	-4.985232	2.107055	1.923702
C63	-5.365763	0.285791	-1.175261
C64	-5.138947	0.286697	0.355712
H65	-4.389152	-0.491098	0.585659
N66	-6.337272	-0.034440	1.082290
H67	-6.630003	0.631812	1.788802
C68	-6.828964	-1.296550	1.031512
O69	-6.336648	-2.152432	0.293458
C70	-8.014832	-1.587267	1.904437
H71	-8.856247	-1.883788	1.271207
H72	-8.316841	-0.739856	2.524157
H73	-7.777283	-2.438852	2.548249
H74	4.511742	-2.053370	-0.826678
H75	2.647071	-2.803036	-0.680837
H76	2.979633	2.673355	0.679104
H77	4.501850	1.556745	1.422207

H78	6.982949	-1.890042	3.221677
H79	7.613329	1.651432	-0.354974
H80	-5.554035	1.293634	-1.557203
H81	-6.235506	-0.337076	-1.395476

[a]Part of the Gaussian output file:

SCF Done: E(RM06) =   -1850.36048938   A.U. after   1 cycles

	1	2	3
	A	A	A
Frequencies --	22.9914	29.4012	37.7741
Red. masses --	5.3724	5.0956	6.0167

Zero-point correction=   0.684653 (Hartree/Particle)
Thermal correction to Energy=   0.722976
Thermal correction to Enthalpy=   0.723921
Thermal correction to Gibbs Free Energy=   0.616090
Sum of electronic and zero-point Energies=   -1849.675836
Sum of electronic and thermal Energies=   -1849.637513
Sum of electronic and thermal Enthalpies=   -1849.636569
Sum of electronic and thermal Free Energies=   -1849.744399

Item	Value	Threshold	Converged?
Maximum Force	0.000037	0.000450	YES
RMS Force	0.000005	0.000300	YES

Table S23. Geometry optimized for the staggered π-dimer of Asp-based $(MV^+)_2$ in its open-shell singlet state based on a broken-symmetry DFT approach (stereo view shown below). Optimized at the UM06/6-31G** level using PCM.[a]
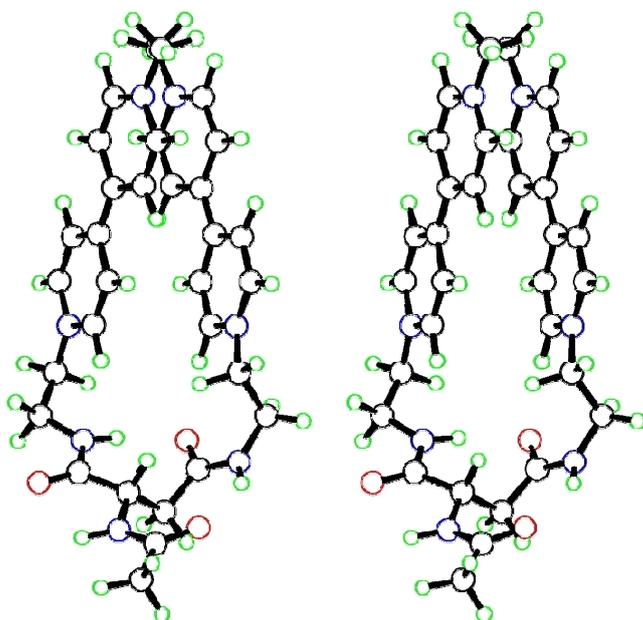
Atom	X	Y	Z	Spin Density
N1	-0.516901	-1.956060	-1.143114	0.110678
N2	-0.367372	2.561898	0.210663	-0.116615
N3	6.061896	0.599914	-1.538480	0.114695
N4	5.113146	-1.242465	2.582226	-0.112583
C5	1.826281	-2.249343	-0.830095	0.030973
C6	-0.282945	-0.731949	-1.711733	0.054233
C7	2.115770	-0.967290	-1.390813	0.134449
C8	0.546466	-2.696739	-0.710865	0.038465
C9	0.981219	-0.246243	-1.858438	0.023463
H10	0.309591	-3.659114	-0.268824	-0.002310
H11	1.079615	0.729290	-2.323900	-0.002169
H12	-1.169930	-0.181917	-2.023527	-0.003339
C13	3.441378	-0.444787	-1.460206	0.123878
C14	4.576901	-1.191309	-1.034509	0.035564
C15	3.730313	0.865135	-1.948861	0.033700
C16	5.002816	1.350331	-1.962722	0.035516
C17	5.831315	-0.660405	-1.072214	0.040082
H18	2.946466	1.521719	-2.310527	-0.002851
H19	5.240067	2.348583	-2.316079	-0.002175
H20	6.706810	-1.215027	-0.748421	-0.002570
C21	7.397065	1.181801	-1.454240	-0.009016
H22	7.518338	1.931066	-2.238184	0.001726
H23	8.144172	0.398663	-1.594440	0.002021
C24	-1.888304	-2.338024	-0.800104	-0.009123
H25	-2.274761	-1.586604	-0.097661	0.008233
H26	-1.837389	-3.283198	-0.254714	0.000067

C27	-2.838952	-2.441380	-2.006276	0.004650
H28	-2.381024	-1.984369	-2.889133	-0.000585
H29	-3.044232	-3.485818	-2.249499	-0.000117
N30	-4.097711	-1.769079	-1.751442	-0.000080
H31	-4.831083	-2.248675	-1.233220	-0.000019
C32	-4.164545	-0.423582	-1.803781	0.000086
O33	-3.238632	0.275083	-2.234981	0.000320
H34	0.225860	-0.363209	1.710499	0.002260
C35	0.474817	0.588796	1.252219	-0.026436
C36	0.915963	3.017435	0.074133	-0.041213
C37	1.823145	1.031237	1.145395	-0.137150
C38	-0.565073	1.338988	0.788089	-0.049868
C39	1.985464	2.307626	0.526152	-0.028534
H40	-1.595135	1.006066	0.864328	0.002749
H41	1.027839	3.983541	-0.407154	0.002469
C42	2.927157	0.266188	1.625466	-0.120881
C43	4.258397	0.773092	1.643998	-0.035455
C44	2.780287	-1.058684	2.136849	-0.034970
C45	3.853934	-1.769968	2.579539	-0.033350
C46	5.298262	0.021401	2.103723	-0.039947
H47	1.813180	-1.547862	2.177266	0.002895
H48	3.762422	-2.782192	2.959814	0.002095
H49	6.318304	0.393331	2.125361	0.002576
C50	6.261791	-2.057191	2.963751	0.008865
H51	6.680458	-2.559747	2.085419	-0.008032
H52	5.949831	-2.805272	3.693959	-0.001516
C53	-1.465693	3.338362	-0.388427	0.008802
H54	-1.598364	3.008641	-1.429699	-0.007859
H55	-1.129853	4.377814	-0.422458	-0.001404
C56	-2.786488	3.277220	0.355383	-0.001998
H57	-2.628935	3.331394	1.439499	0.000300
H58	-3.369436	4.164883	0.076178	0.000149
N59	-3.518208	2.065218	0.036635	-0.000006
H60	-3.322855	1.606861	-0.856842	-0.000086
C61	-4.565168	1.647013	0.781233	0.000025
O62	-4.985163	2.242407	1.765835	-0.000030
C63	-5.390079	0.184757	-1.175829	0.000063
C64	-5.150363	0.303241	0.348616	0.000189
H65	-4.400805	-0.457217	0.632152	-0.000021
N66	-6.342782	0.047378	1.110282	0.000015
H67	-6.619655	0.769924	1.766347	0.000004
C68	-6.837994	-1.212791	1.174249	-0.000002
O69	-6.360877	-2.129518	0.502720	0.000015
C70	-8.010993	-1.421794	2.087669	0.000000
H71	-8.875252	-1.727682	1.490414	0.000000
H72	-8.276219	-0.533517	2.665900	0.000000
H73	-7.782051	-2.243335	2.772100	0.000000
H74	4.484795	-2.209356	-0.672308	-0.002822
H75	2.612186	-2.905038	-0.472628	-0.002720
H76	2.965470	2.751265	0.388332	0.002764
H77	4.488392	1.781037	1.314755	0.002800

H78	7.025027	-1.419800	3.413554	-0.002216
H79	7.543798	1.652658	-0.476299	0.008241
H80	-5.586841	1.160457	-1.629932	-0.000004
H81	-6.258738	-0.456499	-1.340505	-0.000005

[a]Part of the Gaussian output file:

SCF Done: E(UM06) =   -1850.36205086   A.U. after   1 cycles

Annihilation of the first spin contaminant:
S**2 before annihilation   0.5925,   after   0.0189

	1	2	3
	A	A	A
Frequencies --	19.8549	26.5627	33.5035
Red. masses --	5.2190	5.2368	6.1737

Zero-point correction=	0.683778 (Hartree/Particle)
Thermal correction to Energy=	0.722623
Thermal correction to Enthalpy=	0.723567
Thermal correction to Gibbs Free Energy=	0.613354
Sum of electronic and zero-point Energies=	-1849.678273
Sum of electronic and thermal Energies=	-1849.639428
Sum of electronic and thermal Enthalpies=	-1849.638484
Sum of electronic and thermal Free Energies=	-1849.748697

Item	Value	Threshold	Converged?
Maximum Force	0.000012	0.000450	YES
RMS Force	0.000002	0.000300	YES

Table S24. Geometry optimized for the staggered π-dimer of Asp-based $(MV^+)_2$ in its triplet state. Optimized at the UM06/6-31G** level using PCM.[a]
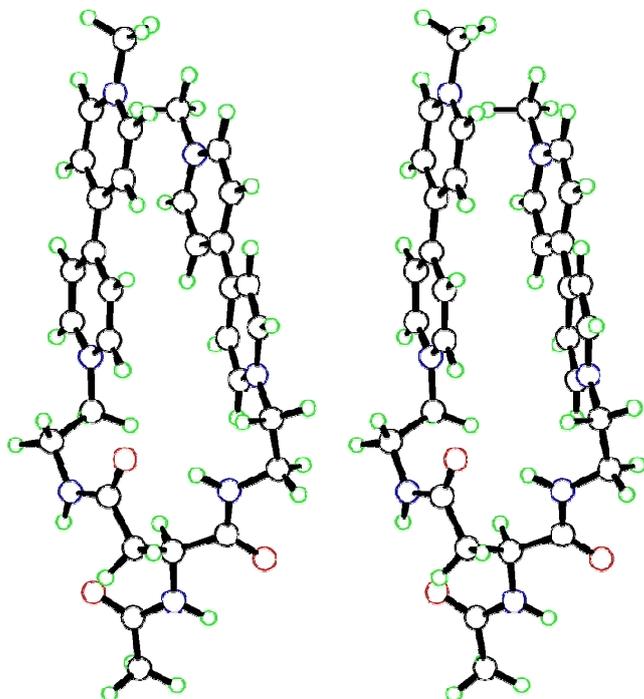
Atom	X	Y	Z	Spin Density
N1	-0.200701	-1.906104	-0.131274	0.148368
N2	-0.908868	2.783396	-0.539057	0.157431
N3	6.617846	-0.563608	-1.329726	0.156339
N4	5.061197	0.318801	2.341366	0.154206
C5	2.084624	-2.442850	0.247888	0.046290
C6	0.166611	-1.038074	-1.124767	0.062701
C7	2.520501	-1.510828	-0.740490	0.159017
C8	0.763403	-2.610820	0.529250	0.052718
C9	1.474662	-0.838780	-1.441061	0.035223
H10	0.412455	-3.299382	1.290903	-0.003165
H11	1.686158	-0.129988	-2.234397	-0.003227
H12	-0.654451	-0.524994	-1.623471	-0.003891
C13	3.897678	-1.225267	-0.969939	0.170992
C14	4.946744	-1.878711	-0.255182	0.031858
C15	4.330193	-0.229696	-1.895888	0.050012
C16	5.648832	0.073933	-2.048541	0.050337
C17	6.250867	-1.541028	-0.446415	0.057122
H18	3.623421	0.332406	-2.496656	-0.003650
H19	5.992785	0.836935	-2.738809	-0.003169
H20	7.065236	-2.027168	0.082793	-0.003867
C21	8.026488	-0.204204	-1.456078	-0.012029
H22	8.139895	0.542728	-2.241972	0.000186
H23	8.615241	-1.087942	-1.715325	0.007283
C24	-1.617548	-2.041402	0.197225	-0.009017
H25	-2.024241	-1.027082	0.301648	0.005211

H26	-1.698501	-2.529183	1.171839	0.000661
C27	-2.395503	-2.804422	-0.886217	0.008956
H28	-1.886789	-2.686636	-1.849456	-0.000896
H29	-2.438323	-3.872768	-0.664219	-0.000163
N30	-3.743342	-2.294543	-1.018590	0.000271
H31	-4.505615	-2.695134	-0.473261	-0.000009
C32	-3.928873	-1.064488	-1.540243	0.000326
O33	-3.007732	-0.409208	-2.043666	0.001264
H34	0.040765	0.822145	1.993588	-0.003728
C35	0.170947	1.464159	1.128006	0.038661
C36	0.317608	3.087948	-1.069549	0.066574
C37	1.467581	1.799915	0.638668	0.181005
C38	-0.961640	1.956390	0.548509	0.056922
C39	1.473656	2.633523	-0.518673	0.026972
H40	-1.947636	1.714058	0.929902	-0.003822
H41	0.305067	3.717988	-1.953395	-0.003798
C42	2.671407	1.330884	1.241061	0.138156
C43	3.956283	1.811426	0.854752	0.055886
C44	2.681039	0.328334	2.254960	0.042281
C45	3.849116	-0.154769	2.760381	0.047515
C46	5.096970	1.306322	1.401882	0.049630
H47	1.759339	-0.111912	2.621060	-0.003210
H48	3.883961	-0.939544	3.509721	-0.002977
H49	6.082966	1.665452	1.123330	-0.003475
C50	6.284360	-0.266309	2.880137	-0.012432
H51	6.312572	-1.336945	2.653693	0.008204
H52	6.325709	-0.123188	3.962929	0.008405
C53	-2.089957	3.377470	-1.193671	-0.012494
H54	-2.190655	2.923686	-2.189550	0.009347
H55	-1.870545	4.439354	-1.341973	0.006348
C56	-3.390721	3.258242	-0.437798	0.001095
H57	-3.278964	3.589872	0.602884	-0.000313
H58	-4.106443	3.947104	-0.904883	-0.000328
N59	-3.897468	1.900038	-0.471217	0.000249
H60	-3.476521	1.238692	-1.127848	-0.000577
C61	-5.018022	1.555671	0.200108	0.000014
O62	-5.671462	2.338871	0.878247	0.000007
C63	-5.303068	-0.486546	-1.332151	0.000047
C64	-5.376175	0.076090	0.107972	0.000088
H65	-4.623559	-0.456667	0.715713	0.000080
N66	-6.661233	-0.138737	0.715171	0.000017
H67	-7.139157	0.682986	1.069057	0.000004
C68	-7.028810	-1.395597	1.062708	-0.000002
O69	-6.333888	-2.373111	0.776293	0.000005
C70	-8.332405	-1.532571	1.793705	0.000001
H71	-9.000408	-2.170549	1.207729	0.000000
H72	-8.826468	-0.576693	1.983068	0.000000
H73	-8.151846	-2.039134	2.746167	0.000000
H74	4.740531	-2.661151	0.468088	-0.003171
H75	2.790081	-3.028393	0.826958	-0.003386
H76	2.399254	2.907747	-1.013922	-0.002693

H77	4.067399	2.602451	0.121201	-0.004008
H78	7.148449	0.216642	2.420883	0.000469
H79	8.393111	0.210671	-0.511907	0.008746
H80	-5.491603	0.288638	-2.080445	-0.000003
H81	-6.061121	-1.265869	-1.438673	0.000000

*a*Part of the Gaussian output file:

SCF Done: E(UM06) =   -1850.35941522   A.U. after   1 cycles

  Annihilation of the first spin contaminant:

  S**2 before annihilation   2.0104,   after   2.0001

	1	2	3
	A	A	A
Frequencies --	24.0821	24.5110	34.6882
Red. masses --	5.5299	5.7750	5.5969

Zero-point correction=	0.685284 (Hartree/Particle)
Thermal correction to Energy=	0.723522
Thermal correction to Enthalpy=	0.724466
Thermal correction to Gibbs Free Energy=	0.615389
Sum of electronic and zero-point Energies=	-1849.674131
Sum of electronic and thermal Energies=	-1849.635893
Sum of electronic and thermal Enthalpies=	-1849.634949
Sum of electronic and thermal Free Energies=	-1849.744027

Item	Value	Threshold	Converged?
Maximum Force	0.000062	0.000450	YES
RMS Force	0.000008	0.000300	YES

Table S25. Geometry optimized for the one-electron-reduced N,N'-dimethyl-4,4'-bipypridinium MV$^+$• (doublet). Optimized at the UM06/6-31G** level using PCM.[a]

Atom	X	Y	Z	Spin Density
N1	-3.535206	-0.001708	-0.025953	0.155170
N2	3.535208	-0.001671	0.025968	0.155170
C3	-1.480407	1.201345	0.010664	0.043079
C4	-2.840522	-1.177444	-0.038911	0.050615
C5	-0.712582	-0.001034	-0.004397	0.160178
C6	-2.840665	1.174805	0.002401	0.052738
C7	-1.479833	-1.203362	-0.031526	0.047263
C8	0.712581	-0.001026	0.004416	0.160181
C9	1.480396	1.201359	-0.010645	0.043093
C10	1.479843	-1.203349	0.031544	0.047246
C11	2.840529	-1.177417	0.038929	0.050621
C12	2.840658	1.174832	-0.002388	0.052734
C13	4.993231	0.005230	-0.033445	-0.012318
C14	-4.993230	0.005269	0.033373	-0.012318
H15	-3.441316	2.078407	0.016188	-0.003253
H16	-1.004889	-2.177809	-0.057868	-0.003433
H17	-3.439137	-2.082064	-0.059835	-0.003154
H18	1.004908	-2.177801	0.057886	-0.003432
H19	3.439162	-2.082025	0.059848	-0.003155
H20	3.441291	2.078446	-0.016182	-0.003253
H21	5.335276	0.082141	-1.069970	0.010885
H22	5.378054	-0.916758	0.405061	0.001922
H23	-5.378048	-0.917114	-0.404297	0.001915
H24	-5.375276	0.853536	-0.537735	0.003558
H25	-5.335329	0.083136	1.069807	0.010883
H26	1.005900	2.176156	-0.032644	-0.003242
H27	-1.005919	2.176147	0.032666	-0.003242
H28	5.375315	0.854013	0.536869	0.003549

[a]Part of the Gaussian output file:

SCF Done: E(UM06) =   -574.623888018   A.U. after   1 cycles

Annihilation of the first spin contaminant:

  S**2 before annihilation   0.7549,   after   0.7500

	1	2	3
	A	A	A
Frequencies --	35.9018	41.8198	56.6065
Red. masses --	1.0969	1.1182	2.8076

 Zero-point correction=   0.236928 (Hartree/Particle)

Thermal correction to Energy=   0.249931
Thermal correction to Enthalpy=   0.250875
Thermal correction to Gibbs Free Energy=   0.195163
Sum of electronic and zero-point Energies=   -574.386960
Sum of electronic and thermal Energies=   -574.373958
Sum of electronic and thermal Enthalpies=   -574.373013
Sum of electronic and thermal Free Energies=   -574.428725

Item	Value	Threshold	Converged?
Maximum Force	0.000006	0.000450	YES
RMS Force	0.000001	0.000300	YES

Table S26. Electronic transitions computed by TD-DFT for the closed-shell singlet state of the non-derivatized $(MV^+)_2$ in an eclipsed fashion, for which part of the Gaussian output is shown. Relevant MO's are shown below:
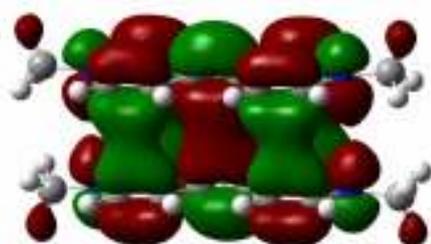
MO99 (HOMO)
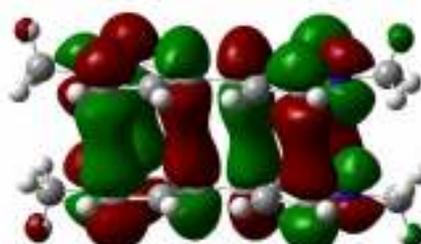
MO102 (LUMO+2)
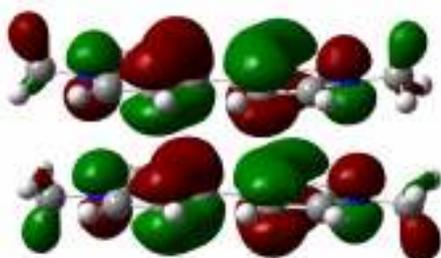
MO98 (HOMO-1)
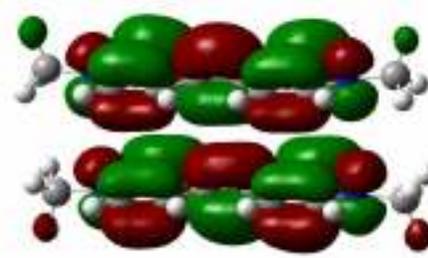
MO100 (LUMO)

Excitation energies and oscillator strengths (λ > 200 nm, f > 0.02 only):

Excited State	1:	Singlet-A	1.6799 eV	738.03 nm	f=0.3120	<S**2>=0.000
99 ->100		0.73701				
99 <-100		-0.21325				
Excited State	4:	Singlet-A	2.7443 eV	451.79 nm	f=0.4753	<S**2>=0.000
98 ->100		0.23317				
99 ->102		0.66898				
Excited State	8:	Singlet-A	3.9923 eV	310.56 nm	f=1.2227	<S**2>=0.000
98 ->100		0.66435				
99 ->102		-0.23418				
Excited State	10:	Singlet-A	4.2195 eV	293.83 nm	f=0.0883	<S**2>=0.000
96 ->100		0.69579				

**Table S27.** Electronic transitions computed by TD-DFT for the open-shell singlet state of the non-derivatized $(MV^+)_2$ in an eclipsed fashion, for which part of the Gaussian output is shown. Relevant MO's are shown below:


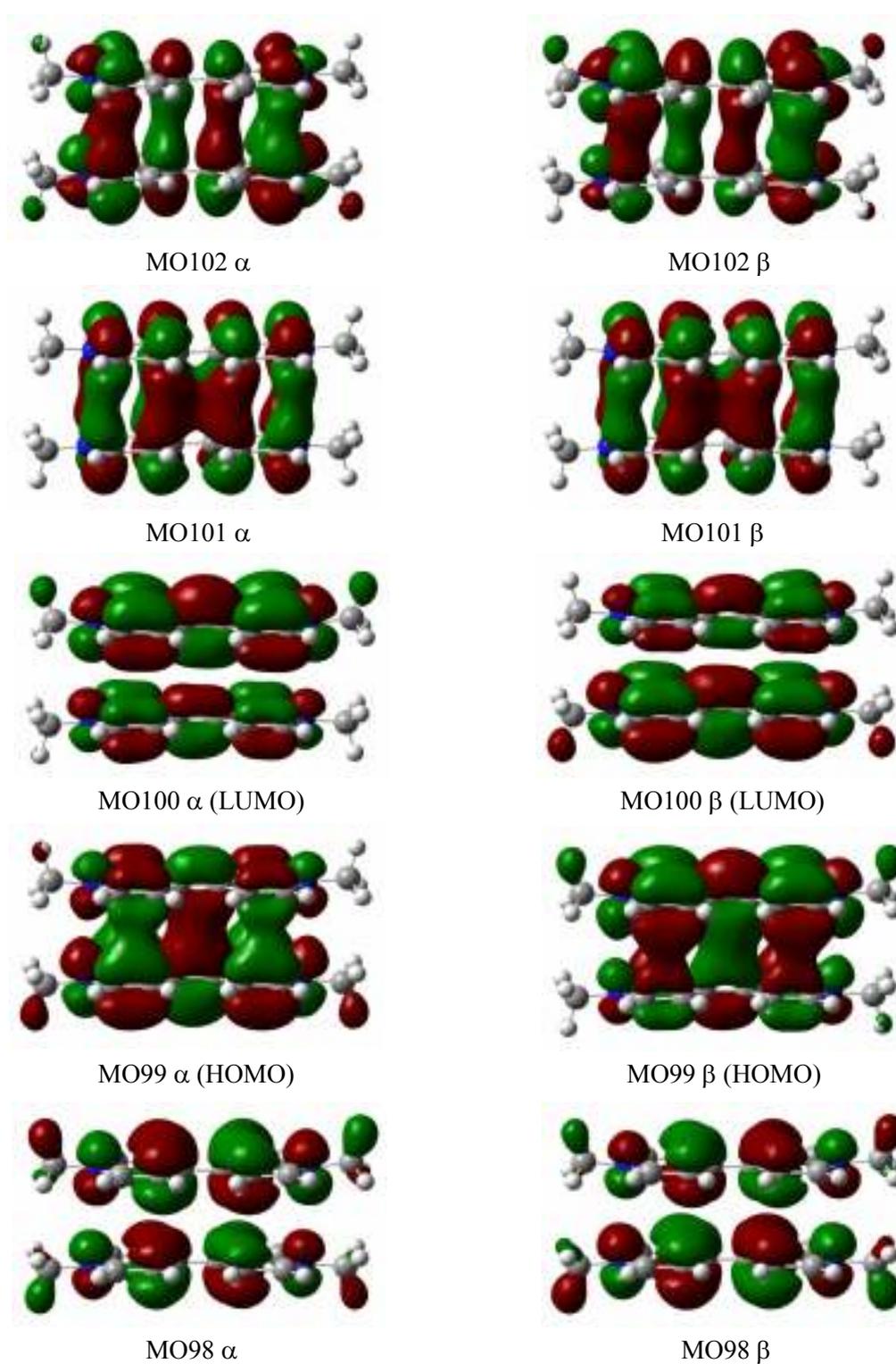MO102 α
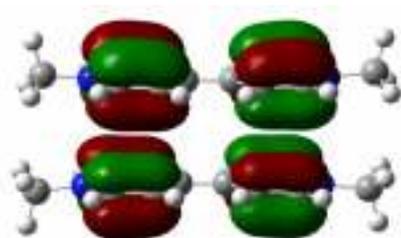

MO102 β

MO101 α

MO101 β

MO100 α (LUMO)

MO100 β (LUMO)

MO99 α (HOMO)

MO99 β (HOMO)

MO98 α

MO98 β

MO97 α   MO97 β

Excitation energies and oscillator strengths ($\lambda > 200$ nm, $f > 0.02$ only):

```
Excited State     2:  0.742-A    1.6413 eV   755.42 nm   f=0.2663   <S**2>=-0.112
     99A ->100A          0.72586
     99B ->100B         -0.72584
     99A <-100A         -0.17043
     99B <-100B          0.17043

Excited State     8:  2.122-A    2.6012 eV   476.64 nm   f=0.3999   <S**2>=0.876
     98A ->100A         -0.19097
     99A ->102A          0.57701
     99A ->105A         -0.34636
     98B ->100B          0.19100
     99B ->102B         -0.57700
     99B ->105B          0.34636

Excited State    10:  2.382-A    2.9757 eV   416.65 nm   f=0.0589   <S**2>=1.168
     98A ->100A         -0.14707
     99A ->102A          0.32958
     99A ->105A          0.59280
     98B ->100B          0.14706
     99B ->102B         -0.32955
     99B ->105B         -0.59279

Excited State    17:  2.694-A    3.7092 eV   334.26 nm   f=0.4538   <S**2>=1.565
     93A ->106A          0.11653
     94A ->104A          0.13372
     95A ->100A          0.33937
     96A ->103A         -0.23791
     97A ->101A          0.33293
     98A ->100A         -0.36276
     99A ->102A         -0.14749
     99A ->105A         -0.12408
     93B ->106B         -0.11653
     94B ->104B         -0.13372
     95B ->100B         -0.33936
     96B ->103B         -0.23790
     97B ->101B         -0.33293
     98B ->100B          0.36277
     99B ->102B          0.14748
     99B ->105B          0.12419
```

Excited State   20:   2.162-A   4.0578 eV   305.54 nm   f=0.7752   <S**2>=0.918
        94A ->104A   0.11446
        96A ->103A   -0.21479
        97A ->101A   0.32284
        98A ->100A   0.52239
        99A ->102A   0.19305
        94B ->104B   -0.11446
        96B ->103B   -0.21479
        97B ->101B   -0.32283
        98B ->100B   -0.52236
        99B ->102B   -0.19305

Excited State   22:   1.629-A   4.1760 eV   296.90 nm   f=0.0826   <S**2>=0.414
        93A ->100A   0.16280
        96A ->100A   0.65559
        97A ->102A   0.14673
        93B ->100B   -0.16280
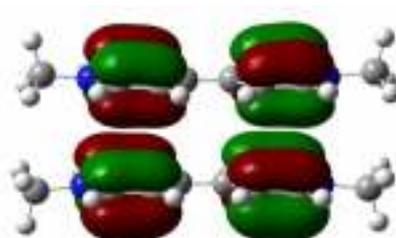   96B ->100B   -0.65557
        97B ->102B   -0.14672

Table S28. Electronic transitions computed by TD-DFT for the triplet state of the non-derivatized $(MV^+)_2$ in an *slipped* fashion, for which part of the Gaussian output is shown. Relevant MO's are shown below, where MO97β-MO100β are identical to the corresponding α MO's:

MO99 α (SOMO)

MO102 α (LUMO+1)

MO98 α

MO101 α (LUMO)

MO97 α

MO100 α (SOMO)
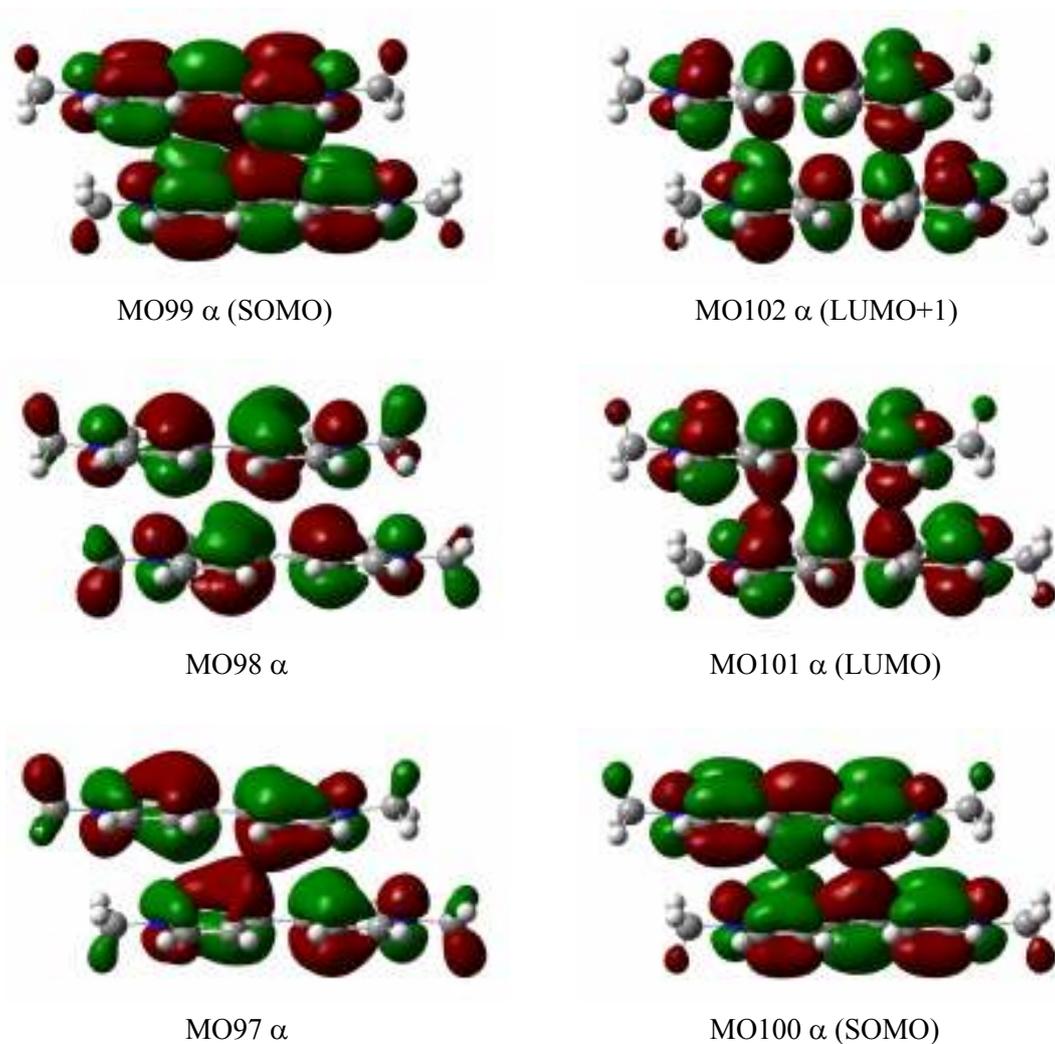
Excitation energies and oscillator strengths (λ > 200 nm, f > 0.02 only):

```
Excited State   4:  3.015-A     2.3723 eV  522.64 nm  f=0.4087  <S**2>=2.023
     99A ->102A        -0.34789
    100A ->101A         0.87362
     97B ->100B        -0.18650
     98B -> 99B         0.23950


Excited State   8:  3.010-A     2.5857 eV  479.49 nm  f=0.0419  <S**2>=2.014
     99A ->102A         0.87667
     99A ->105A        -0.11567
    100A ->101A         0.41804
```

```
    100A ->104A        0.11470
    98B -> 99B        -0.10201


Excited State   14:  3.174-A      3.5117 eV  353.06 nm  f=0.9354  <S**2>=2.269
     99A ->102A        0.19386
    100A ->101A       -0.18720
     93B ->106B        0.10785
     94B ->101B        0.14994
     95B ->102B       -0.17170
     96B ->104B       -0.13039
     97B ->100B       -0.40316
     98B -> 99B        0.78198


Excited State   18:  3.083-A      3.9906 eV  310.69 nm  f=0.0596  <S**2>=2.126
     96A ->101A        0.11504
     93B -> 99B        0.25223
     95B ->103B       -0.10791
     96B ->100B        0.70132
     97B ->100B       -0.51935
     98B -> 99B       -0.27644


Excited State   19:  3.088-A      4.0209 eV  308.35 nm  f=0.0592  <S**2>=2.134
     92B -> 99B        0.10082
     93B -> 99B        0.17787
     96B ->100B        0.53366
     97B -> 99B       -0.25861
     97B ->100B        0.57231
     98B -> 99B        0.38644
     98B ->100B       -0.21180


Excited State   23:  3.951-A      4.4538 eV  278.38 nm  f=0.2318  <S**2>=3.652
     93A ->106A       -0.19897
     94A ->103A        0.28117
     94A ->105A        0.13692
     95A ->105A       -0.26918
     96A ->104A       -0.37021
     97A ->105A        0.10490
     99A ->102A        0.13323
    100A ->101A       -0.13598
     93B ->106B       -0.20111
     94B ->101B       -0.27552
     94B ->104B       -0.14116
     95B ->102B        0.39435
     96B ->104B        0.28601
     96B ->105B       -0.10813
     97B ->100B       -0.26804
     98B -> 99B        0.16722
```

Table S29. Electronic transitions computed by TD-DFT for the closed-shell singlet state of the non-derivatized $(MV^+)_2$ in a staggered fashion, for which part of the Gaussian output is shown. Relevant MO's are shown below:
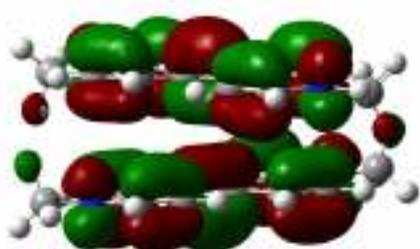
MO100 (LUMO)
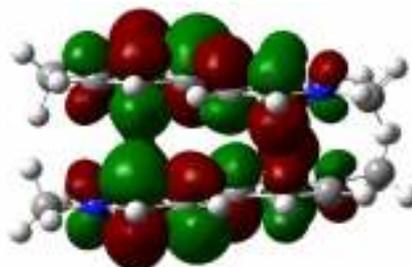
MO104 (LUMO+4)
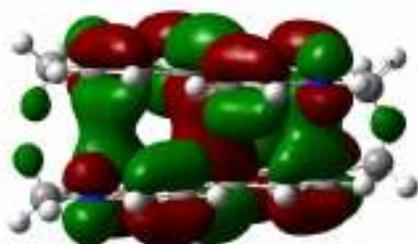
MO99 (HOMO)
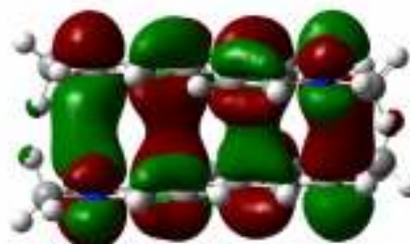
MO101 (LUMO+1)

Excitation energies and oscillator strengths ($\lambda > 200$ nm, $f > 0.02$ only):

Excited State   1:   Singlet-A   1.4640 eV   846.88 nm   f=0.1953   <S**2>=0.000
  99 ->100   0.74196
  99 <-100   -0.23040

Excited State   3:   Singlet-A   2.4325 eV   509.71 nm   f=0.1081   <S**2>=0.000
  99 ->101   0.59400
  99 ->104   -0.36905

Excited State   5:   Singlet-A   2.9353 eV   422.39 nm   f=0.2864   <S**2>=0.000
  98 ->100   -0.17435
  99 ->101   0.35250
  99 ->104   0.57964

Excited State   7:   Singlet-A   3.3217 eV   373.26 nm   f=0.1724   <S**2>=0.000
  97 ->100   0.12901
  99 ->102   0.10157
  99 ->105   0.68559

Excited State   8:   Singlet-A   4.0460 eV   306.44 nm   f=0.7514   <S**2>=0.000
  98 ->100   0.67448
  99 ->101   0.14835
  99 ->104   0.10819

Excited State   9:   Singlet-A   4.2205 eV   293.76 nm   f=0.2729   <S**2>=0.000

```
97 ->100          0.68961
99 ->105         -0.12360


Excited State   11:      Singlet-A      4.6795 eV   264.95 nm   f=0.0243   <S**2>=0.000
  95 ->100          0.69593


Excited State   26:      Singlet-A      5.9605 eV   208.01 nm   f=0.2897   <S**2>=0.000
  93 ->101          0.11917
  94 ->101         -0.11394
  96 ->102          0.64461
  97 ->103         -0.14925


Excited State   28:      Singlet-A      6.0344 eV   205.46 nm   f=0.0609   <S**2>=0.000
  95 ->102         -0.13384
  96 ->101         -0.19099
  97 ->104         -0.20762
  98 ->103          0.43061
  98 ->105         -0.31712
  99 ->112          0.24493


Excited State   29:      Singlet-A      6.0425 eV   205.19 nm   f=0.0460   <S**2>=0.000
  94 ->101         -0.10877
  95 ->102          0.16340
  96 ->101         -0.15655
  97 ->101          0.10820
  97 ->104          0.25685
  98 ->103          0.35964
  98 ->105          0.39632
  99 ->112          0.14818
```

**Table S30.** Electronic transitions computed by TD-DFT for the open-shell singlet state of the non-derivatized $(MV^+)_2$ in an staggered fashion, for which part of the Gaussian output is shown. Relevant MO's are shown below:


MO105 α (LUMO+5)	MO105 β (LUMO+5)
MO101 α (LUMO+1)	MO101 β (LUMO+1)
MO100 α (LUMO)	MO100 β (LUMO)
MO99α (SOMO)	MO99 β (SOMO)
MO98 α	MO98 β
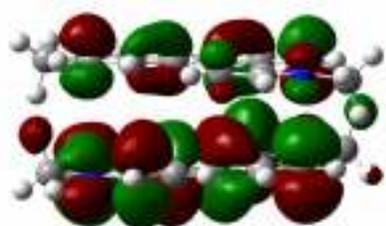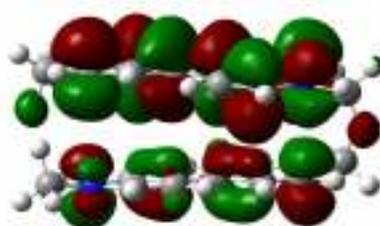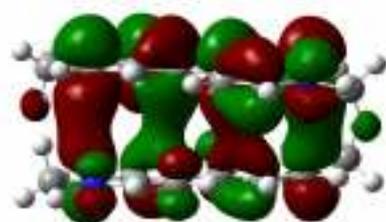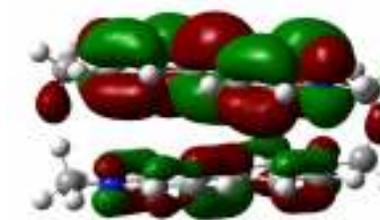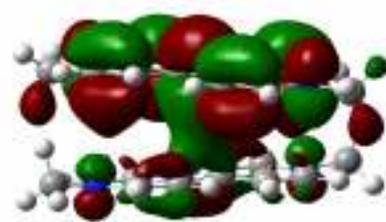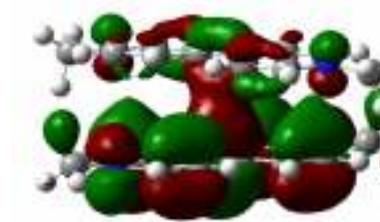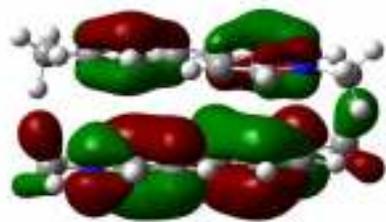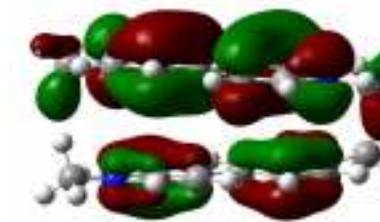
Excitation energies and oscillator strengths (λ > 200 nm, f > 0.02 only):

Excited State   2:   0.559-A   1.3991 eV   886.16 nm   f=0.1209   <S**2>=-0.172
    99A ->100A   0.71517
    99B ->100B   -0.71514
    99A <-100A   -0.11498
    99B <-100B   0.11499

Excited State   3:   2.681-A   1.9982 eV   620.49 nm   f=0.0329   <S**2>=1.547
    99A ->101A   -0.62177
    99A ->102A   -0.31879
    99B ->101B   0.62188
    99B ->102B   0.31903

Excited State   5:   2.199-A   2.1969 eV   564.35 nm   f=0.0306   <S**2>=0.959
    99A ->101A   0.29763
    99A ->102A   -0.54765
    99A ->103A   0.28440
    99A ->105A   0.13912
    99B ->101B   -0.29740
    99B ->102B   0.54773
    99B ->103B   -0.28447
    99B ->105B   -0.13913

Excited State   6:   2.173-A   2.4071 eV   515.07 nm   f=0.2876   <S**2>=0.930
    98A ->100A   0.14914
    99A ->101A   0.63940
    99A ->105A   -0.24384
    98B ->100B   0.14914
    99B ->101B   0.63943
    99B ->105B   -0.24381

Excited State   10:   2.172-A   2.8243 eV   438.99 nm   f=0.0253   <S**2>=0.929
    99A ->103A   0.64547
    99A ->105A   -0.24379
    99B ->103B   0.64552
    99B ->105B   -0.24384

Excited State   11:   2.116-A   3.1366 eV   395.28 nm   f=0.0338   <S**2>=0.869
    98A ->100A   0.16801
    99A ->101A   0.20819
    99A ->103A   0.23251
    99A ->105A   0.59560
    98B ->100B   0.16807
    99B ->101B   0.20819
    99B ->103B   0.23250
    99B ->105B   0.59566

Excited State   15:   2.153-A   3.4846 eV   355.80 nm   f=0.1681   <S**2>=0.909
    98A ->100A   -0.39261
    99A ->105A   0.53916
    98B ->100B   0.39262
    99B ->105B   -0.53914

Excited State   16:   2.582-A   3.5840 eV   345.94 nm   f=0.4461   <S**2>=1.416
    96A ->101A   0.10548

```
96A ->103A        -0.11065
97A ->100A        -0.39825
98A ->100A         0.47138
99A ->101A        -0.14740
99A ->105A        -0.11272
96B ->101B         0.10550
96B ->103B        -0.11066
97B ->100B        -0.39832
98B ->100B         0.47139
99B ->101B        -0.14739
99B ->105B        -0.11273

Excited State   18:   2.226-A      4.0654 eV   304.98 nm   f=0.2483   <S**2>=0.988
93A ->100A        -0.15966
95A ->100A         0.20920
97A ->100A         0.49248
98A ->100A         0.35229
93B ->100B        -0.15964
95B ->100B         0.20957
97B ->100B         0.49315
98B ->100B         0.35227

Excited State   19:   2.388-A      4.0766 eV   304.14 nm   f=0.1424   <S**2>=1.176
94A ->101A        -0.10433
95A ->100A         0.35581
96A ->100A         0.13967
96A ->105A        -0.12198
97A ->100A         0.54371
94B ->101B         0.10436
95B ->100B        -0.35561
96B ->100B        -0.13954
96B ->105B         0.12197
97B ->100B        -0.54326

Excited State   23:   2.996-A      4.3887 eV   282.51 nm   f=0.1232   <S**2>=1.994
93A ->100A         0.18272
93A ->102A         0.15911
93A ->106A        -0.13267
94A ->100A        -0.11733
94A ->102A         0.22809
95A ->100A        -0.18747
95A ->104A        -0.18332
96A ->101A        -0.13486
96A ->103A         0.28294
98A ->100A         0.26845
98A ->104A        -0.16577
93B ->100B         0.18272
93B ->102B         0.15910
93B ->106B        -0.13267
94B ->100B        -0.11733
94B ->102B         0.22814
95B ->100B        -0.18748
95B ->104B        -0.18331
96B ->101B        -0.13491
96B ->103B         0.28298
98B ->100B         0.26842
98B ->104B        -0.16579
```

Excited State   24:   3.227-A   4.4109 eV   281.09 nm   f=0.0381   <S**2>=2.354
      93A ->103A   -0.11428
      93A ->104A   -0.19829
      94A ->102A   0.12910
      94A ->103A   -0.18490
      94A ->104A   0.12972
      95A ->106A   -0.19810
      96A ->101A   0.11503
      96A ->102A   -0.36514
      96A ->103A   -0.16616
      97A ->100A   0.10433
      97A ->104A   0.15513
      97A ->106A   -0.11462
      98A ->100A   -0.17266
      93B ->103B   0.11438
      93B ->104B   0.19823
      94B ->102B   -0.12907
      94B ->103B   0.18486
      94B ->104B   -0.12980
      95B ->106B   0.19810
      96B ->101B   -0.11498
      96B ->102B   0.36524
      96B ->103B   0.16616
      97B ->100B   -0.10429
      97B ->104B   -0.15515
      97B ->106B   0.11466
      98B ->100B   0.17271

Excited State   62:   2.068-A   5.9834 eV   207.21 nm   f=0.2315   <S**2>=0.819
      96A ->102A   0.64568
      97A ->104A   -0.11802
      96B ->102B   0.64571
      97B ->104B   -0.11803

Excited State   64:   2.131-A   6.0380 eV   205.34 nm   f=0.1020   <S**2>=0.885
      94A ->102A   -0.10597
      96A ->101A   0.22198
      97A ->104A   -0.18197
      98A ->104A   -0.58006
      98A ->106A   -0.14204
      94B ->102B   0.10596
      96B ->101B   -0.22206
      97B ->104B   0.18197
      98B ->104B   0.58008
      98B ->106B   0.14205

Table S31. Electronic transitions computed by TD-DFT for the triplet state of the non-derivatized $(MV^+)_2$ in an staggered fashion, for whic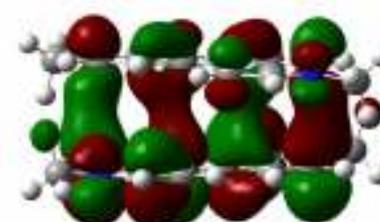h part of the Gaussian output. Relevant MO's are shown below, where MO97β-MO100β are identical to the corresponding α MO's:
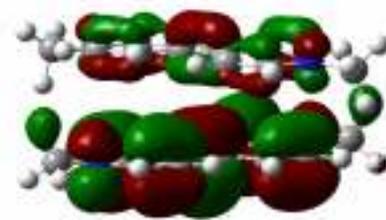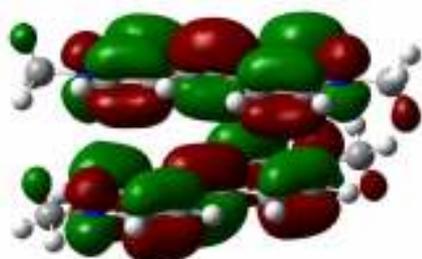

MO100 α (SOMO)

MO99 α (SOMO)

MO105 α

MO98 α

MO102 α

MO97 α
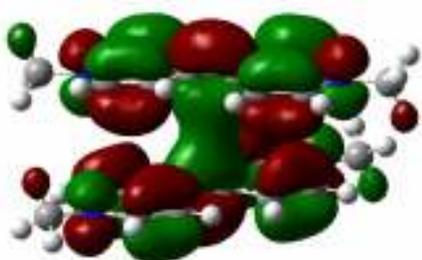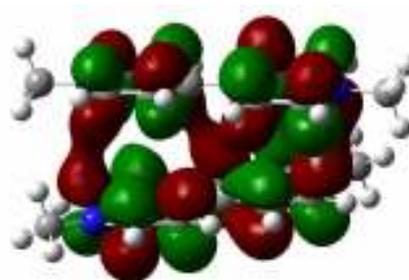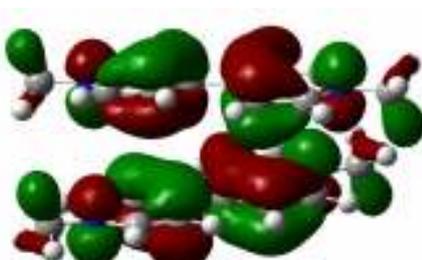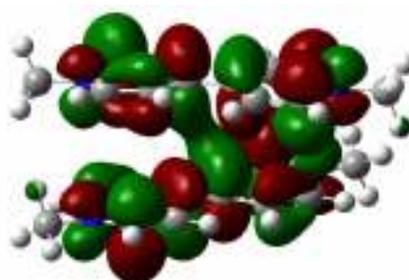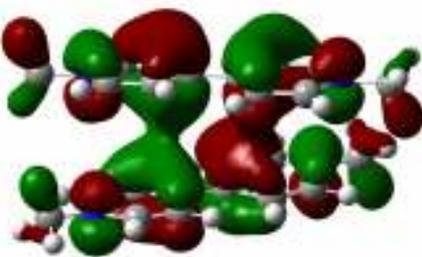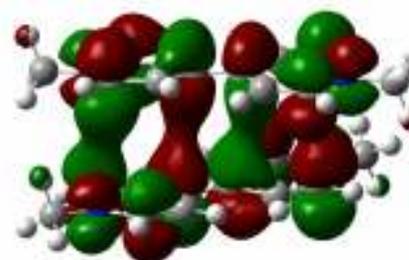
MO101 α

Excitation energies and oscillator strengths (λ > 200 nm, f > 0.02 only):

Excited State   3:   3.019-A   2.1254 eV   583.33 nm   f=0.0389   <S**2>=2.029
      99A ->102A   -0.36471
      99A ->103A   0.14728
     100A ->101A   0.77764
     100A ->104A   -0.44575
      98B -> 99B   0.12795

Excited State   4:   3.022-A   2.3611 eV   525.10 nm   f=0.2685   <S**2>=2.033
      99A ->101A   -0.24797
      99A ->106A   -0.18382
     100A ->102A   0.75994
     100A ->103A   0.39560
     100A ->105A   -0.30246
      97B -> 99B   -0.16827
      98B ->100B   -0.16809

Excited State   5:   3.035-A   2.4415 eV   507.82 nm   f=0.1222   <S**2>=2.053
      99A ->101A   -0.57325
      99A ->106A   0.32424
     100A ->102A   0.10707
     100A ->105A   0.68686
      97B -> 99B   -0.13504
      98B ->100B   -0.12996

Excited State   12:   3.058-A   3.3179 eV   373.69 nm   f=0.0332   <S**2>=2.087
      99A ->102A   -0.10219
      99A ->106A   0.64788
     100A ->105A   -0.32779
      97B ->100B   -0.24475
      98B -> 99B   -0.57686

Excited State   13:   3.068-A   3.3354 eV   371.73 nm   f=0.0458   <S**2>=2.104
      99A ->102A   0.10691
      99A ->105A   0.10770
      99A ->106A   0.60143
     100A ->105A   -0.30747
      97B ->100B   0.26118
      98B -> 99B   0.61690

Excited State   14:   3.178-A   3.5617 eV   348.11 nm   f=0.8337   <S**2>=2.276
      99A ->101A   -0.20662
     100A ->102A   0.14111
      93B ->106B   -0.11365
      94B ->101B   -0.11936
      95B ->101B   0.11231
      95B ->102B   0.10135
      96B ->102B   -0.11428
      97B -> 99B   0.66008
      98B ->100B   0.57984

Excited State   19:   3.116-A   4.1075 eV   301.85 nm   f=0.0674   <S**2>=2.177
        93B -> 99B   0.55394
        94B ->100B   0.33119
        95B -> 99B   -0.28032
        96B -> 99B   0.13523
        96B ->100B   0.41186
        97B -> 99B   -0.12051
        97B ->100B   -0.36832
        98B -> 99B   0.17591
        98B ->100B   0.15449

Excited State   25:   3.945-A   4.4969 eV   275.71 nm   f=0.1909   <S**2>=3.641
        93A ->106A   0.23414
        94A ->103A   0.16996
        94A ->104A   0.14975
        94A ->105A   -0.22840
        95A ->102A   0.13236
        95A ->103A   -0.22963
        96A ->104A   0.27217
        96A ->105A   0.13856
        97A ->103A   0.12561
        99A ->101A   0.12497
       100A ->102A   -0.11421
        93B ->100B   -0.11277
        93B ->106B   -0.23672
        94B -> 99B   0.10156
        94B ->101B   -0.26123
        94B ->102B   0.11869
        94B ->104B   0.19135
        95B ->100B   0.10958
        95B ->101B   0.18113
        95B ->102B   0.18192
        95B ->104B   0.12311
        96B ->101B   0.13013
        96B ->102B   -0.25076
        96B ->103B   -0.10801
        96B ->104B   0.12888
        97B -> 99B   -0.22013
        97B ->101B   -0.10624
        98B ->100B   -0.17223

Excited State   67:   3.419-A   6.1773 eV   200.71 nm   f=0.0329   <S**2>=2.673
        97A ->102A   -0.16440
        97A ->103A   0.57339
        98A ->104A   -0.50187
        99A ->111A   0.30062
       100A ->113A   0.21509
       100A ->114A   -0.29140
        91B ->100B   0.12203
        96B ->103B   0.12117

Table S32. Electronic transitions computed by TD-DFT for the closed-shell singlet state of the Asp-based $(MV^+)_2$ in an eclipsed fashion, for which part of the Gaussian output is shown.

Excitation energies and oscillator strengths ($\lambda > 200$ nm, f > 0.02 only):

```
Excited State    1:       Singlet-A      1.5167 eV  817.46 nm  f=0.2421   <S**2>=0.000
      151 ->152            0.73628
      151 <-152           -0.21955

Excited State    3:       Singlet-A      2.5721 eV  482.03 nm  f=0.0405   <S**2>=0.000
      151 ->154            0.24144
      151 ->155            0.66049

Excited State    4:       Singlet-A      2.7512 eV  450.65 nm  f=0.4915   <S**2>=0.000
      149 ->152           -0.17199
      150 ->152           -0.10718
      151 ->154            0.62296
      151 ->155           -0.24232

Excited State    8:       Singlet-A      3.9611 eV  313.00 nm  f=1.3062   <S**2>=0.000
      149 ->152            0.54340
      150 ->152            0.38060
      151 ->154            0.21646

Excited State    9:       Singlet-A      4.0590 eV  305.45 nm  f=0.0243   <S**2>=0.000
      146 ->152            0.68215
      147 ->152            0.12085

Excited State   11:       Singlet-A      4.1638 eV  297.76 nm  f=0.0633   <S**2>=0.000
      144 ->152            0.59955
      145 ->152            0.33481

Excited State   14:       Singlet-A      4.2901 eV  289.00 nm  f=0.0253   <S**2>=0.000
      141 ->152            0.11939
      144 ->152            0.16337
      145 ->152           -0.38915
      147 ->152            0.52461
      150 ->152            0.10204
```

Table S33. Electronic transitions computed by TD-DFT for the open-shell singlet state of the Asp-based $(MV^+)_2$ given in a ***slipped*** fashion, for which part of the Gaussian output is shown.

Excitation energies and oscillator strengths ($\lambda > 200$ nm, f > 0.02 only):

```
Excited State    6:  2.251-A       2.3654 eV  524.15 nm  f=0.5724   <S**2>=1.017
      148A ->152A         -0.15443
      151A ->153A          0.64891
      151A ->154A         -0.31065
      148B ->152B         -0.18951
      151B ->153B          0.59837
      151B ->154B         -0.11326

Excited State   14:  2.416-A       3.4814 eV  356.13 nm  f=0.7517   <S**2>=1.210
      148A ->152A          0.47209
```

```
149A ->152A        -0.29029
151A ->153A         0.11148
151A ->154A        -0.10509
151A ->155A         0.13859
151A ->156A         0.20085
151A ->158A        -0.43646
148B ->152B         0.49162
149B ->152B         0.19191
151B ->153B         0.13503

Excited State   15:   2.326-A      3.5034 eV   353.90 nm   f=0.1876   <S**2>=1.103
148A ->152A         0.31135
149A ->152A        -0.19102
151A ->155A        -0.19881
151A ->156A        -0.30939
151A ->158A         0.65594
148B ->152B         0.15717
151B ->155B        -0.11857
151B ->156B         0.14989
151B ->158B         0.40311

Excited State   16:   2.221-A      3.5304 eV   351.19 nm   f=0.0786   <S**2>=0.983
148A ->152A        -0.13184
151A ->156A         0.13376
151A ->158A        -0.35071
148B ->152B        -0.16483
151B ->155B        -0.19506
151B ->156B         0.27009
151B ->158B         0.80546

Excited State   20:   2.355-A      4.0356 eV   307.23 nm   f=0.0294   <S**2>=1.137
139A ->152A        -0.12124
140A ->152A        -0.11400
141A ->152A         0.18760
143A ->152A         0.62350
143A ->157A        -0.11328
144A ->152A        -0.25811
145A ->152A        -0.33598
146A ->152A         0.33980
147A ->152A         0.27925
149A ->152A        -0.16608
140B ->153B        -0.15492
143B ->152B         0.17523
146B ->152B         0.11147

Excited State   21:   2.350-A      4.0777 eV   304.05 nm   f=0.0404   <S**2>=1.130
140A ->153A        -0.15434
146A ->152A        -0.15684
139B ->152B         0.10461
143B ->152B         0.86768
143B ->157B        -0.15566
144B ->152B         0.26402
146B ->152B        -0.14558


Excited State   31:   3.087-A      4.4550 eV   278.30 nm   f=0.0267   <S**2>=2.133
139A ->156A        -0.19163
```

```
140A ->153A          0.10829
140A ->154A          0.25539
140A ->155A          0.15404
141A ->155A          0.10494
143A ->155A          0.11307
144A ->152A         -0.19527
145A ->152A          0.24119
146A ->154A          0.12625
146A ->158A         -0.12908
147A ->152A          0.19876
148A ->152A          0.12697
139B ->156B         -0.14569
140B ->154B          0.13960
141B ->152B         -0.17776
143B ->154B          0.18126
143B ->155B          0.27680
143B ->158B         -0.15032
145B ->152B          0.17825
146B ->152B         -0.16421
146B ->154B          0.14908
146B ->158B          0.14320
147B ->152B          0.25323
148B ->152B          0.25161
150B ->152B         -0.12385

Excited State   34:   2.601-A      4.5029 eV   275.34 nm   f=0.0240   <S**2>=1.441
    138A ->152A          0.19455
    141A ->152A          0.10397
    144A ->152A         -0.39649
    145A ->152A          0.53149
    146A ->152A         -0.10045
    146A ->156A         -0.10388
    147A ->152A          0.13785
    148A ->157A          0.12586
    140B ->154B         -0.12855
    141B ->152B          0.15840
    141B ->153B         -0.10617
    145B ->152B         -0.17745
    146B ->152B          0.16247
    146B ->156B          0.10065
    147B ->152B         -0.31615

Excited State   35:   2.806-A      4.5258 eV   273.95 nm   f=0.1071   <S**2>=1.719
    139A ->156A          0.14931
    140A ->154A         -0.17910
    140A ->155A         -0.10432
    144A ->152A         -0.10086
    145A ->152A          0.17559
    145A ->153A         -0.10508
    146A ->154A         -0.12273
    146A ->158A          0.11195
    147A ->152A          0.21815
    151A ->164A          0.11440
    138B ->152B         -0.18276
    139B ->156B          0.12755
    140B ->154B         -0.12331
    141B ->152B         -0.16715
```

```
142B ->152B          -0.11105
143B ->154B          -0.10046
143B ->155B          -0.17412
144B ->152B           0.10623
145B ->152B           0.13920
146B ->152B          -0.23839
146B ->154B          -0.13300
146B ->158B          -0.11684
147B ->152B           0.55710
148B ->157B           0.12735
150B ->152B          -0.13395

Excited State   36:   2.625-A        4.5747 eV   271.02 nm   f=0.0252   <S**2>=1.473
138A ->152A          -0.20517
141A ->153A          -0.10808
142A ->152A           0.13597
144A ->152A          -0.11395
144A ->153A           0.11941
145A ->153A          -0.17691
147A ->152A          -0.25085
148A ->153A          -0.10102
148A ->157A          -0.12524
151A ->164A           0.16185
138B ->152B          -0.35062
141B ->152B           0.19867
141B ->153B           0.10811
142B ->152B          -0.10257
143B ->152B          -0.12061
144B ->152B           0.40296
145B ->152B          -0.38599
148B ->157B           0.20635

Excited State   38:   2.533-A        4.6394 eV   267.24 nm   f=0.0496   <S**2>=1.354
138A ->152A           0.30048
141A ->152A          -0.10772
142A ->152A          -0.26624
144A ->152A           0.56680
146A ->152A           0.15689
147A ->152A           0.23325
148A ->152A          -0.10867
148A ->153A          -0.10076
148A ->157A           0.16631
138B ->152B          -0.14451
141B ->153B          -0.14873
144B ->152B           0.21946
144B ->153B          -0.10131
145B ->152B          -0.23087
145B ->153B           0.13152
148B ->153B           0.15230

Excited State  108:   2.525-A        6.1338 eV   202.13 nm   f=0.0270   <S**2>=1.344
139A ->153A           0.11002
141A ->153A           0.10494
144A ->153A           0.10945
146A ->154A           0.16913
147A ->154A           0.42636
147A ->155A          -0.10367
```

148A ->157A	0.11530
150A ->154A	0.10603
143B ->153B	-0.15503
145B ->153B	-0.23972
146B ->154B	-0.21292
147B ->154B	0.13108
148B ->156B	-0.10665
151B ->164B	0.13355
151B ->166B	0.37027
151B ->168B	0.32757
151B ->169B	0.25933

Table S34. Electronic transitions computed by TD-DFT for the triplet state of the Asp-based $(MV^+)_2$ given in a *slipped* fashion, for which part of the Gaussian output is shown.

Excitation energies and oscillator strengths ($\lambda > 200$ nm, f > 0.02 only):

Excited State   4:   3.016-A   2.3705 eV   523.03 nm   f=0.5117   <S**2>=2.025
   151A ->153A   -0.18963
   151A ->154A   0.64309
   152A ->153A   -0.55179
   152A ->154A   -0.16964
   152A ->155A   0.30873
   150B ->151B   0.21958
   150B ->152B   -0.10524

Excited State   14:   3.137-A   3.4405 eV   360.36 nm   f=1.0228   <S**2>=2.210
   151A ->154A   -0.15293
   152A ->153A   0.15631
   142B ->153B   0.14058
   143B ->152B   0.14960
   144B ->152B   -0.15849
   145B ->154B   0.12596
   146B ->151B   -0.12559
   146B ->152B   -0.12379
   147B ->151B   0.14936
   147B ->152B   0.11677
   150B ->151B   0.74272
   150B ->152B   -0.34325

Excited State   16:   3.088-A   3.9391 eV   314.75 nm   f=0.0234   <S**2>=2.133
   143A ->154A   -0.10939
   139B ->151B   0.16566
   139B ->152B   -0.17682
   140B ->152B   0.19336
   142B ->151B   -0.26359
   142B ->152B   0.21822
   143B ->152B   -0.13409
   145B ->152B   0.79639
   145B ->156B   -0.10576
   146B ->152B   0.14594

Excited State   17:   3.068-A   4.0026 eV   309.76 nm   f=0.0206   <S**2>=2.103
   139B ->151B   0.15661
   140B ->151B   -0.43042

```
140B ->152B        -0.18542
142B ->151B         0.42613
142B ->152B         0.12794
144B ->151B         0.10406
145B ->151B         0.24727
145B ->152B         0.18453
146B ->151B        -0.19886
147B ->151B         0.44932
147B ->152B         0.11939
149B ->151B        -0.18110
150B ->151B        -0.24698
150B ->152B        -0.13164
```

Excited State   19:   3.078-A   4.0317 eV   307.52 nm   f=0.0455   <S**2>=2.119
```
140B ->152B        -0.28139
142B ->151B         0.34206
142B ->152B        -0.28844
143B ->151B        -0.22000
143B ->152B        -0.13367
144B ->151B         0.36256
145B ->152B         0.20637
146B ->151B         0.25516
146B ->152B         0.14017
147B ->151B        -0.30812
147B ->152B        -0.16292
149B ->151B         0.10302
150B ->151B         0.35896
150B ->152B         0.14018
```

Excited State   21:   3.092-A   4.1126 eV   301.47 nm   f=0.0300   <S**2>=2.140
```
143B ->152B         0.22007
144B ->151B         0.11978
144B ->152B        -0.37675
145B ->152B         0.20139
146B ->152B        -0.40135
147B ->151B        -0.16592
147B ->152B         0.50833
149B ->151B         0.25774
150B ->151B        -0.17742
150B ->152B         0.31970
```

Excited State   31:   3.451-A   4.4156 eV   280.79 nm   f=0.0721   <S**2>=2.728
```
139A ->158A        -0.11999
140A ->156A         0.12359
140A ->157A        -0.15302
141A ->155A        -0.17034
143A ->156A        -0.12436
143A ->157A        -0.11451
139B ->151B        -0.18615
139B ->152B        -0.11427
139B ->158B         0.12241
140B ->154B         0.11943
140B ->155B        -0.15276
142B ->151B         0.32151
142B ->152B         0.17471
142B ->153B         0.22632
144B ->151B        -0.34440
```

145B ->154B	0.11859
145B ->155B	0.12232
146B ->151B	0.42204
146B ->152B	0.19152

Excited State   34:   3.457-A   4.4885 eV   276.23 nm   f=0.1380   <S**2>=2.738

139A ->158A	0.12441
140A ->156A	-0.13228
140A ->157A	0.15263
141A ->153A	0.14156
141A ->155A	0.16443
142A ->155A	0.11336
143A ->156A	0.14957
143A ->157A	0.12689
151A ->160A	0.28017
152A ->160A	0.12421
138B ->151B	0.12162
139B ->151B	-0.26030
139B ->158B	-0.12129
140B ->152B	0.14149
140B ->154B	-0.11504
140B ->155B	0.15426
142B ->151B	0.35952
142B ->153B	-0.24076
143B ->152B	0.11099
144B ->151B	-0.33248
144B ->152B	-0.29440
145B ->152B	0.11250
145B ->154B	-0.12272
145B ->155B	-0.11833

Table S35. Electronic transitions computed by TD-DFT for the closed-shell singlet state of the Asp-based $(MV^+)_2$ in a staggered fashion, for which part of the Gaussian output is shown.

Excitation energies and oscillator strengths ($\lambda > 200$ nm, f > 0.02 only):

Excited State 1:	Singlet-A	1.4423 eV	859.64 nm	f=0.1800	<S**2>=0.000
151 ->152	0.74138				
151 <-152	-0.22934				

Excited State 3:	Singlet-A	2.4416 eV	507.80 nm	f=0.1358	<S**2>=0.000
151 ->153	0.59315				
151 ->155	-0.15961				
151 ->156	-0.33832				

Excited State 5:	Singlet-A	2.9190 eV	424.75 nm	f=0.3158	<S**2>=0.000
149 ->152	-0.11118				
150 ->152	-0.12324				
151 ->153	0.35161				
151 ->155	0.22853				
151 ->156	0.54320				

Excited State 7:	Singlet-A	3.3072 eV	374.89 nm	f=0.1575	<S**2>=0.000
151 ->154	-0.10572				
151 ->157	0.68099				

Excited State 9:	Singlet-A	4.0143 eV	308.86 nm	f=0.8444	<S**2>=0.000
149 ->152	0.43663				
150 ->152	0.51134				
151 ->153	0.14684				

Excited State 10:	Singlet-A	4.1373 eV	299.68 nm	f=0.1382	<S**2>=0.000
147 ->152	0.54848				
148 ->152	0.11453				
149 ->152	0.29770				
150 ->152	-0.26153				

Excited State 12:	Singlet-A	4.2864 eV	289.25 nm	f=0.0440	<S**2>=0.000
143 ->152	0.16187				
144 ->152	0.21698				
145 ->152	0.40921				
146 ->152	-0.14703				
149 ->152	0.18229				
150 ->152	-0.18815				
151 ->160	0.38570				

Excited State 13:	Singlet-A	4.3113 eV	287.58 nm	f=0.0523	<S**2>=0.000
143 ->152	-0.10554				
144 ->152	-0.12925				
145 ->152	-0.26011				
146 ->152	0.10432				
147 ->152	0.10833				
148 ->152	0.10793				
149 ->152	-0.12258				
151 ->160	0.57852				

Excited State 17:	Singlet-A	4.6689 eV	265.55 nm	f=0.0248	<S**2>=0.000

141 ->152	0.57694
143 ->152	0.35545
144 ->152	-0.14650

Excited State 41: Singlet-A 5.9168 eV 209.55 nm f=0.1650 <S**2>=0.000
145 ->154	0.26744
147 ->154	0.34652
148 ->154	-0.12675
149 ->154	-0.32589
149 ->156	0.12010
150 ->154	0.29962

Excited State 42: Singlet-A 5.9812 eV 207.29 nm f=0.1200 <S**2>=0.000
140 ->153	0.11566
143 ->154	0.15623
144 ->154	0.24230
145 ->154	0.37777
146 ->153	-0.13675
146 ->154	-0.13066
147 ->154	0.11707
149 ->154	0.24017
150 ->154	-0.20671
151 ->168	0.15340

Excited State 43: Singlet-A 6.0012 eV 206.60 nm f=0.0290 <S**2>=0.000
142 ->153	-0.11867
143 ->153	0.10252
144 ->153	-0.16824
145 ->153	0.29505
146 ->153	0.43710
147 ->156	-0.12009
150 ->154	-0.10372
150 ->156	0.14268
151 ->168	0.16005

Excited State 44: Singlet-A 6.0038 eV 206.51 nm f=0.0507 <S**2>=0.000
141 ->154	0.13983
147 ->153	-0.14754
147 ->156	-0.16085
149 ->154	-0.13481
149 ->155	0.24685
149 ->156	-0.20975
149 ->157	0.21015
150 ->155	0.29479
150 ->156	-0.14710
150 ->157	0.24087

Excited State 46: Singlet-A 6.0420 eV 205.21 nm f=0.0348 <S**2>=0.000
135 ->152	-0.17494
140 ->153	-0.10682
141 ->154	-0.11284
145 ->153	-0.11614
146 ->153	0.19790
147 ->155	0.17944
147 ->156	0.11367
149 ->155	0.25240
149 ->157	-0.21225

150 ->155	0.25991
150 ->157	-0.24340
151 ->168	0.16661

Excited State   52:   Singlet-A   6.1438 eV   201.81 nm   f=0.0230   <S**2>=0.000

141 ->153	-0.30300
143 ->153	-0.26482
149 ->156	0.15785
151 ->168	-0.12780
151 ->169	0.13407
151 ->170	0.37763
151 ->172	0.16197

Table S36. Electronic transitions computed by TD-DFT for the open-shell singlet state of the Asp-based $(MV^+)_2$ in a staggered fashion, for which part of the Gaussian output is shown.

Excitation energies and oscillator strengths ($\lambda > 200$ nm, f > 0.02 only):

Excited State   2:   0.571-A   1.3689 eV   905.69 nm   f=0.1081   <S**2>=-0.169

151A ->152A	-0.70755
151B ->152B	0.72007
151A <-152A	0.10814
151B <-152B	-0.10580

Excited State   3:   2.666-A   2.0005 eV   619.77 nm   f=0.0336   <S**2>=1.527

151A ->153A	-0.63167
151A ->154A	-0.28896
151B ->153B	0.63433
151B ->154B	-0.30284

Excited State   5:   2.208-A   2.2026 eV   562.91 nm   f=0.0266   <S**2>=0.969

151A ->153A	-0.25105
151A ->154A	0.63763
151A ->155A	0.32073
151A ->157A	-0.15723
151B ->153B	0.29173
151B ->154B	0.46906
151B ->155B	0.23492
151B ->157B	-0.11885

Excited State   6:   2.177-A   2.3971 eV   517.22 nm   f=0.3465   <S**2>=0.935

150A ->152A	-0.13382
151A ->153A	0.65072
151A ->157A	-0.22780
150B ->152B	-0.12317
151B ->153B	0.63241
151B ->157B	0.22997

Excited State   10:   2.195-A   2.8525 eV   434.64 nm   f=0.0236   <S**2>=0.955

151A ->155A	-0.42584
151A ->157A	-0.24182
151B ->153B	-0.11323
151B ->154B	-0.14089
151B ->155B	0.78279

```
151B ->156B          0.23125
151B ->157B          0.21415

Excited State   11:   2.148-A      3.1397 eV   394.89 nm   f=0.0304   <S**2>=0.903
   150A ->152A          0.13900
   151A ->153A         -0.20124
   151A ->154A         -0.10231
   151A ->155A          0.19071
   151A ->157A         -0.60044
   150B ->152B          0.13515
   151B ->153B         -0.19756
   151B ->155B         -0.24262
   151B ->157B          0.60323

Excited State   15:   2.156-A      3.4686 eV   357.45 nm   f=0.1433   <S**2>=0.912
   149A ->152A         -0.17353
   150A ->152A          0.33539
   151A ->157A          0.52636
   149B ->152B         -0.22698
   150B ->152B         -0.33042
   151B ->157B          0.53915
   151B ->158B          0.14653

Excited State   16:   2.550-A      3.5801 eV   346.32 nm   f=0.5488   <S**2>=1.376
   144A ->152A          0.10528
   145A ->152A          0.19945
   146A ->152A          0.12514
   147A ->152A         -0.25729
   149A ->152A         -0.14581
   150A ->152A          0.46400
   151A ->153A          0.14686
   151A ->157A          0.12323
   144B ->152B         -0.11957
   145B ->152B         -0.14648
   147B ->152B          0.36179
   149B ->152B          0.21932
   150B ->152B          0.41883
   151B ->153B          0.14658

Excited State   19:   2.231-A      4.0188 eV   308.51 nm   f=0.1304   <S**2>=0.995
   139A ->152A          0.16212
   144A ->152A          0.17932
   145A ->152A          0.23111
   146A ->152A         -0.28450
   149A ->152A          0.14556
   150A ->152A         -0.19047
   139B ->152B         -0.14530
   141B ->152B          0.18217
   142B ->152B          0.18462
   144B ->152B         -0.19730
   145B ->152B         -0.10590
   146B ->152B          0.13579
   147B ->152B          0.56402
   149B ->152B         -0.17307
   150B ->152B         -0.18178
   151B ->159B         -0.24518
```

Excited State   21:   2.338-A   4.0619 eV   305.23 nm   f=0.1675   <S**2>=1.117
     141A ->152A   0.30289
     142A ->152A   -0.31186
     143A ->152A   0.20015
     145A ->152A   0.42272
     146A ->152A   0.36723
     147A ->152A   -0.39854
     148A ->152A   -0.13254
     149A ->152A   0.25739
     140B ->152B   0.12939
     140B ->153B   0.13952
     147B ->152B   -0.10989
     149B ->152B   -0.10783
     150B ->152B   -0.18146

Excited State   22:   2.329-A   4.0800 eV   303.88 nm   f=0.0440   <S**2>=1.106
     140A ->152A   -0.25437
     140A ->153A   -0.12471
     144A ->152A   0.16642
     145A ->152A   0.27849
     146A ->152A   -0.29893
     150A ->152A   0.11549
     140B ->152B   -0.19986
     141B ->152B   -0.24455
     142B ->152B   -0.12802
     143B ->152B   0.14618
     144B ->152B   0.46887
     145B ->152B   0.44726
     149B ->152B   0.10125

Excited State   27:   2.867-A   4.3755 eV   283.36 nm   f=0.1382   <S**2>=1.805
     139A ->152A   0.22760
     139A ->158A   -0.11833
     140A ->154A   -0.23204
     141A ->152A   0.12891
     141A ->156A   0.15005
     142A ->152A   -0.22944
     144A ->155A   -0.11532
     145A ->155A   -0.10548
     146A ->155A   0.19338
     147A ->152A   0.12531
     149A ->152A   -0.20601
     150A ->152A   0.23252
     150A ->156A   -0.11544
     151A ->160A   0.12229
     139B ->152B   -0.17836
     139B ->154B   0.12013
     139B ->158B   0.10645
     140B ->154B   0.22029
     141B ->152B   0.13029
     141B ->156B   0.13192
     142B ->152B   0.16034
     144B ->155B   0.15169
     145B ->155B   0.15404
     147B ->155B   0.12968
     149B ->152B   0.11499
     150B ->152B   0.24090

```
150B ->156B           -0.11229

Excited State   29:   3.165-A      4.4110 eV   281.08 nm   f=0.0229   <S**2>=2.254
    139A ->156A           -0.16969
    140A ->154A           -0.10973
    140A ->155A           -0.16481
    141A ->158A            0.15153
    144A ->154A           -0.14437
    145A ->154A           -0.14442
    146A ->154A            0.24866
    146A ->155A           -0.10096
    149A ->152A            0.13379
    150A ->152A           -0.11776
    151A ->160A            0.33732
    139B ->156B           -0.19109
    140B ->154B           -0.13959
    140B ->155B           -0.17935
    141B ->158B           -0.15000
    144B ->154B           -0.13815
    145B ->154B           -0.17878
    145B ->155B            0.10559
    147B ->153B           -0.10603
    147B ->154B           -0.20059
    147B ->156B            0.14884
    147B ->158B           -0.10283
    149B ->152B            0.11401
    151B ->160B            0.22975

Excited State   92:   2.807-A      5.9002 eV   210.13 nm   f=0.0228   <S**2>=1.719
    134A ->152A           -0.13929
    135A ->152A            0.10157
    146A ->154A            0.16159
    147A ->154A           -0.19086
    149A ->154A            0.14609
    150A ->154A            0.16178
    150A ->155A            0.13360
    144B ->154B           -0.14397
    145B ->154B            0.14666
    146B ->153B           -0.10154
    147B ->154B            0.19505
    148B ->153B           -0.16326
    148B ->154B           -0.27641
    149B ->154B            0.56169
    149B ->157B           -0.10292
    150B ->153B           -0.10153
    150B ->154B           -0.31805

Excited State   93:   2.539-A      5.9327 eV   208.98 nm   f=0.0494   <S**2>=1.361
    141A ->153A           -0.10112
    144A ->154A            0.12373
    145A ->154A            0.25432
    147A ->154A           -0.10309
    148A ->154A           -0.14618
    149A ->154A            0.45228
    149A ->155A           -0.12719
    150A ->154A            0.30574
    150A ->155A            0.15096
```

150A ->157A	-0.12347
151A ->168A	-0.12013
146B ->154B	-0.11164
147B ->154B	-0.38901
149B ->154B	-0.16831
150B ->155B	-0.14942

Excited State   97:   2.793-A   5.9903 eV   206.97 nm   f=0.0334   <S**2>=1.700

142A ->153A	-0.11663
143A ->154A	-0.11273
144A ->153A	0.11623
146A ->154A	-0.25896
147A ->154A	0.30652
148A ->153A	-0.10783
148A ->154A	-0.12957
149A ->154A	0.43934
150A ->154A	0.17591
150A ->155A	-0.25385
151A ->168A	0.14116
141B ->153B	0.12256
141B ->154B	-0.10818
142B ->153B	0.12024
144B ->153B	-0.13295
144B ->154B	-0.16453
145B ->153B	0.10867
145B ->154B	-0.20059
146B ->153B	0.15515
147B ->156B	0.11404
147B ->157B	-0.12389
149B ->154B	0.17664
150B ->155B	0.12085
151B ->168B	0.10224

Excited State   98:   2.401-A   6.0069 eV   206.40 nm   f=0.0764   <S**2>=1.192

141A ->154A	-0.11508
144A ->154A	0.15747
145A ->154A	0.15740
146A ->154A	-0.19736
147A ->155A	-0.10045
149A ->154A	-0.20287
150A ->154A	-0.10343
150A ->156A	-0.10344
150A ->157A	0.14685
141B ->153B	-0.12089
141B ->154B	0.10805
144B ->153B	-0.13471
144B ->154B	-0.27513
145B ->154B	-0.25658
146B ->153B	0.39541
147B ->153B	-0.14867
147B ->154B	-0.13229
147B ->155B	-0.12054
149B ->154B	0.10420
149B ->157B	-0.16906
150B ->155B	-0.10212
150B ->157B	-0.27023
151B ->165B	0.12369

151B ->168B	0.11887

Excited State 99: 2.558-A 6.0172 eV 206.05 nm f=0.0372 <S**2>=1.385

140A ->153A	0.16267
142A ->153A	-0.11075
143A ->154A	-0.15832
145A ->153A	0.16202
145A ->154A	-0.22693
146A ->153A	0.20517
146A ->154A	0.17632
147A ->153A	0.25718
149A ->154A	0.32285
149A ->157A	-0.17378
150A ->156A	-0.15364
150A ->157A	0.33479
141B ->153B	-0.11526
141B ->154B	0.12302
142B ->153B	-0.12759
144B ->154B	0.12713
145B ->153B	-0.12702
145B ->154B	0.22622
145B ->156B	0.10097
146B ->153B	0.24053
149B ->154B	-0.15135
150B ->154B	0.11952

Excited State 102: 2.438-A 6.0424 eV 205.19 nm f=0.0393 <S**2>=1.236

140A ->154A	-0.11164
141A ->153A	0.14771
142A ->153A	-0.11588
145A ->153A	-0.13943
146A ->154A	-0.15635
147A ->153A	-0.14764
149A ->156A	-0.15453
150A ->156A	0.25412
150A ->157A	0.14270
140B ->153B	-0.13677
141B ->153B	-0.12695
142B ->153B	-0.19765
144B ->153B	0.42148
145B ->153B	-0.19800
146B ->153B	0.23935
147B ->156B	0.18074
148B ->153B	-0.15865
149B ->156B	-0.19863
150B ->155B	0.14516
150B ->156B	-0.22322
150B ->157B	0.12693
151B ->165B	-0.10044
151B ->167B	-0.20644

Excited State 108: 2.268-A 6.1089 eV 202.96 nm f=0.0332 <S**2>=1.036

140A ->153A	0.39723
141A ->153A	0.15376
145A ->154A	0.10898
145A ->156A	-0.15857
146A ->153A	0.19763

146A ->156A	-0.12041
147A ->156A	0.16651
148A ->154A	-0.19244
150A ->158A	0.14417
140B ->153B	0.42999
141B ->153B	0.16035
141B ->154B	-0.10573
145B ->153B	-0.19634
147B ->154B	-0.17409
147B ->156B	-0.24195
150B ->156B	-0.21817
151B ->167B	-0.10420
151B ->168B	0.15459

Table S37. Electronic transitions computed by TD-DFT for the triplet state of the Asp-based $(MV^+)_2$ in a staggered fashion, for which part of the Gaussian output is shown.

Excitation energies and oscillator strengths ($\lambda > 200$ nm, f > 0.02 only):

Excited State   3:   3.018-A   2.2209 eV   558.27 nm   f=0.0720   <S**2>=2.028
   151A ->153A   0.35413
   151A ->154A   0.25166
   151A ->156A   -0.14515
   152A ->153A   0.69279
   152A ->154A   -0.47384
   152A ->155A   -0.16256
   149B ->152B   -0.10282
   150B ->151B   -0.11820

Excited State   4:   3.016-A   2.3508 eV   527.41 nm   f=0.3555   <S**2>=2.024
   151A ->153A   0.18541
   151A ->154A   -0.25730
   151A ->155A   -0.20093
   152A ->153A   0.48684
   152A ->154A   0.69074
   152A ->156A   -0.19056
   149B ->151B   -0.14688
   150B ->152B   -0.17466

Excited State   5:   3.026-A   2.4751 eV   500.93 nm   f=0.0344   <S**2>=2.039
   151A ->153A   0.71638
   151A ->154A   0.18216
   151A ->157A   0.16558
   151A ->158A   -0.25823
   152A ->153A   -0.36312
   152A ->156A   -0.10646
   152A ->157A   0.20008
   152A ->158A   0.36323

Excited State   6:   3.037-A   2.5007 eV   495.79 nm   f=0.0393   <S**2>=2.056
   151A ->153A   -0.31002
   151A ->154A   0.56014
   151A ->157A   0.46906
   152A ->154A   0.17127

```
     152A ->155A        -0.12334
     152A ->157A         0.51011
     152A ->158A        -0.13227

Excited State   12:   3.030-A      3.3274 eV   372.62 nm   f=0.0213   <S**2>=2.045
     151A ->158A         0.71291
     152A ->158A         0.49728
     148B ->152B         0.11863
     149B ->152B        -0.17524
     150B ->151B        -0.35097
     150B ->152B         0.12441

Excited State   13:   3.090-A      3.3746 eV   367.41 nm   f=0.0867   <S**2>=2.138
     151A ->158A         0.36930
     152A ->158A         0.26715
     148B ->152B        -0.18502
     149B ->151B         0.30740
     149B ->152B         0.33761
     150B ->151B         0.63401

Excited State   14:   3.151-A      3.4621 eV   358.12 nm   f=0.7833   <S**2>=2.233
     151A ->153A         0.14491
     151A ->154A        -0.10624
     151A ->158A        -0.10458
     152A ->154A         0.13371
     142B ->154B         0.10907
     148B ->151B        -0.34405
     149B ->151B         0.59996
     150B ->151B        -0.15675
     150B ->152B         0.50318

Excited State   15:   3.069-A      3.7732 eV   328.59 nm   f=0.0557   <S**2>=2.104
     142B ->151B         0.27691
     142B ->152B        -0.20450
     144B ->151B        -0.16485
     145B ->151B         0.14252
     148B ->151B         0.20193
     148B ->152B        -0.17069
     149B ->151B        -0.37358
     149B ->152B         0.53902
     150B ->151B        -0.12965
     150B ->152B         0.46553

Excited State   16:   3.063-A      3.8146 eV   325.03 nm   f=0.0338   <S**2>=2.096
     140B ->151B        -0.22385
     140B ->152B        -0.12322
     141B ->151B        -0.10789
     142B ->151B        -0.12143
     143B ->151B         0.11506
     144B ->151B        -0.24622
     144B ->152B        -0.13782
     146B ->151B         0.11367
     148B ->151B         0.22069
     148B ->152B         0.32833
     149B ->151B        -0.14477
     149B ->152B        -0.38257
     150B ->151B         0.44884
```

| 150B ->152B | 0.43837 |

Excited State   18:   3.083-A   3.9891 eV   310.81 nm   f=0.0304   <S**2>=2.126
141B ->151B	0.31945
141B ->152B	0.29881
142B ->152B	-0.11886
143B ->151B	-0.18616
144B ->151B	0.42400
145B ->151B	-0.40317
145B ->152B	-0.20361
146B ->151B	-0.11704
147B ->151B	-0.14264
148B ->151B	-0.12748
149B ->151B	-0.25688
150B ->151B	0.22803
150B ->152B	0.28041

Excited State   19:   3.090-A   4.0281 eV   307.80 nm   f=0.0344   <S**2>=2.137
141A ->154A	0.10794
139B ->151B	-0.13956
140B ->152B	0.29993
141B ->151B	-0.37676
141B ->152B	-0.13699
142B ->151B	0.26577
142B ->152B	-0.13839
143B ->151B	-0.30317
143B ->152B	0.19559
144B ->151B	0.39480
144B ->152B	-0.32490
145B ->152B	0.22196
146B ->151B	-0.18657
146B ->152B	0.10621
147B ->151B	0.10268
148B ->152B	0.12523

Excited State   21:   3.131-A   4.1276 eV   300.38 nm   f=0.0447   <S**2>=2.201
151A ->159A	-0.26270
139B ->151B	-0.15313
139B ->152B	-0.10059
140B ->151B	0.39655
141B ->151B	-0.22927
141B ->152B	-0.19035
142B ->151B	-0.19449
142B ->152B	0.23052
143B ->152B	-0.28730
144B ->151B	0.22769
144B ->152B	0.38913
146B ->151B	-0.12833
146B ->152B	-0.14788
148B ->151B	0.11638
149B ->151B	-0.10529
150B ->151B	0.16549
150B ->152B	0.18777

Excited State   27:   3.574-A   4.3845 eV   282.78 nm   f=0.0229   <S**2>=2.944
| 139A ->158A | 0.11260 |
| 140A ->155A | -0.12809 |

```
141A ->156A       -0.18480
142A ->155A       -0.16308
142A ->158A       -0.10972
152A ->160A        0.13978
139B ->152B        0.10133
140B ->151B        0.18459
140B ->154B        0.13623
140B ->158B        0.12361
141B ->151B        0.24442
141B ->152B        0.15449
141B ->153B        0.14326
141B ->157B        0.10640
142B ->151B        0.15785
142B ->152B        0.19041
142B ->153B        0.11931
142B ->154B       -0.21207
144B ->152B       -0.10511
144B ->153B        0.12625
147B ->151B        0.36457
148B ->152B        0.27675

Excited State   30:   3.760-A      4.4548 eV   278.32 nm  f=0.1037  <S**2>=3.284
139A ->157A        0.16175
140A ->156A        0.13087
140A ->157A       -0.15570
141A ->155A        0.17679
141A ->157A       -0.10746
142A ->155A        0.14204
142A ->156A        0.17142
146A ->155A        0.12887
152A ->160A        0.29497
140B ->151B        0.13148
140B ->152B       -0.14169
140B ->153B       -0.10893
140B ->157B        0.16897
141B ->152B       -0.11978
141B ->153B       -0.16683
141B ->154B       -0.11457
141B ->156B       -0.11702
141B ->157B       -0.13869
142B ->153B        0.12390
142B ->154B       -0.14932
144B ->153B       -0.14689
144B ->154B       -0.11321
145B ->152B        0.10962
145B ->153B        0.15133
146B ->151B        0.16569
147B ->152B        0.10864
148B ->151B       -0.15372
148B ->153B        0.11391
149B ->151B        0.11450
149B ->153B       -0.11036
150B ->152B        0.17964

Excited State   31:   3.298-A      4.4981 eV   275.63 nm  f=0.0444  <S**2>=2.469
141A ->155A       -0.10866
151A ->160A        0.13873
```

152A ->160A	0.11278
137B ->152B	0.10890
138B ->151B	0.13793
138B ->152B	-0.10243
139B ->151B	-0.14053
141B ->152B	-0.19696
142B ->154B	0.11358
143B ->151B	-0.18425
145B ->151B	-0.27078
145B ->152B	0.11941
146B ->151B	0.56139
147B ->152B	0.28564
148B ->152B	0.12476

Excited State   34:   3.165-A   4.5564 eV   272.11 nm   f=0.0235   <S**2>=2.255

148A ->154A	-0.12208
151A ->160A	-0.16948
137B ->151B	0.12982
138B ->152B	0.15867
140B ->151B	-0.16128
140B ->152B	0.36548
141B ->152B	0.17003
142B ->151B	0.16051
142B ->152B	0.19044
143B ->152B	-0.14314
144B ->152B	0.17840
145B ->151B	0.12075
146B ->151B	0.50170
146B ->152B	0.19091
147B ->151B	-0.11416
147B ->152B	0.31902
150B ->156B	0.10887

Excited State   81:   3.337-A   5.8315 eV   212.61 nm   f=0.0211   <S**2>=2.533

139A ->153A	0.12183
140A ->153A	-0.16658
141A ->153A	-0.18267
145A ->153A	0.10523
146A ->155A	-0.22651
147A ->160A	0.10142
148A ->155A	0.16500
149A ->159A	0.10878
149A ->160A	0.12020
150A ->153A	-0.18313
150A ->154A	0.15057
150A ->155A	0.10690
151A ->162A	0.11063
151A ->164A	0.12990
151A ->166A	-0.12867
152A ->166A	-0.11442
152A ->167A	0.35767
137B ->151B	0.14296
141B ->155B	0.11781
146B ->159B	0.10058
146B ->160B	0.14483
147B ->159B	0.11889
147B ->160B	0.12485

```
148B ->153B          0.12238
149B ->153B         -0.18332
149B ->154B          0.22261
150B ->154B          0.15753
150B ->158B         -0.11999

Excited State   93:  3.318-A      5.9788 eV   207.37 nm   f=0.0211   <S**2>=2.503
   139A ->155A          0.11312
   141A ->156A         -0.11741
   142A ->155A         -0.17755
   146A ->153A         -0.11668
   146A ->154A          0.18027
   146A ->155A          0.18176
   146A ->156A          0.13105
   147A ->154A         -0.11646
   147A ->155A         -0.13731
   148A ->154A          0.22170
   148A ->155A          0.22781
   150A ->155A         -0.15909
   151A ->166A          0.15982
   151A ->167A         -0.16510
   152A ->166A         -0.14699
   152A ->167A          0.15296
   137B ->151B          0.21125
   137B ->152B          0.13363
   144B ->154B          0.14167
   148B ->153B         -0.13118
   148B ->156B          0.15245
   149B ->156B         -0.23185
   150B ->153B          0.15059
   150B ->156B          0.26061
   150B ->157B         -0.14311

Excited State   95:  3.633-A      6.0067 eV   206.41 nm   f=0.0236   <S**2>=3.049
   148A ->156A         -0.12569
   149A ->154A          0.12714
   150A ->155A         -0.11362
   137B ->152B          0.18529
   143B ->153B         -0.12348
   145B ->153B          0.10189
   147B ->153B          0.24282
   148B ->153B          0.69013
   148B ->156B          0.10752
   149B ->153B          0.32930
   150B ->153B         -0.12399
   150B ->155B          0.12517
   150B ->157B         -0.12224

Excited State  104:  3.515-A      6.1280 eV   202.32 nm   f=0.0247   <S**2>=2.839
   140A ->153A          0.11749
   142A ->153A         -0.22305
   143A ->153A         -0.18033
   145A ->153A          0.20143
   145A ->154A         -0.11610
   146A ->154A          0.14923
   146A ->155A          0.13327
   146A ->156A         -0.16406
```

146A ->157A	-0.14900
147A ->153A	-0.16408
148A ->154A	0.23842
148A ->156A	0.13903
152A ->169A	0.10379
137B ->151B	-0.12707
148B ->155B	0.24639
149B ->155B	-0.28596
149B ->157B	0.15603
150B ->155B	0.39255
150B ->156B	-0.21943
150B ->158B	-0.19197

Table S38. Electronic transitions computed by TD-DFT for the double state of non-derivatized MV$^+\bullet$ radical, for which part of the Gaussian output is shown.

Excitation energies and oscillator strengths (λ > 200 nm, f > 0.02 only):

Excited State   2: 2.018-A   2.3588 eV 525.62 nm f=0.3056 <S**2>=0.768
    50A -> 51A   0.95473
    49B -> 50B   -0.27746

Excited State   4: 2.201-A   3.5208 eV 352.14 nm f=0.5794 <S**2>=0.961
    50A -> 51A   0.23039
    46B -> 52B   0.12216
    47B -> 53B   0.15804
    48B -> 51B   -0.20886
    49B -> 50B   0.90902

Excited State   6: 2.151-A   4.1236 eV 300.67 nm f=0.0595 <S**2>=0.906
    48A -> 51A   -0.19678
    49A -> 53A   -0.10003
    47B -> 50B   0.95098
    48B -> 52B   -0.18229

Excited State   8: 3.334-A   4.5449 eV 272.80 nm f=0.0962 <S**2>=2.529
    47A -> 53A   0.38447
    48A -> 52A   0.51083
    50A -> 51A   0.16279
    47B -> 53B   -0.41051
    48B -> 51B   0.53915
    49B -> 50B   0.25656

Table S39. Geometry optimized for the staggered π-dimer of non-derivatized MV^+, i.e., $(MV^+)_2$, in its closed-shell singlet state. Optimized at the M06/6-311+G(2d,p) level under water solvated model (PCM, polarizable continuum model).[a]

Atom	X	Y	Z
N1	-3.032149	-1.791117	-1.535145
N2	-3.033500	1.791135	1.534022
N3	3.033496	1.794841	-1.530607
N4	3.032124	-1.794842	1.531676
C5	-0.658843	-1.784942	-1.496521
C6	-3.030456	-0.432548	-1.561547
C7	-0.611233	-0.361769	-1.518810
C8	-1.842859	-2.448214	-1.490071
C9	-1.874695	0.280111	-1.565664
C10	0.612580	0.365546	-1.518138
C11	1.876024	-0.276285	-1.565424
C12	0.660180	1.788671	-1.493510
C13	1.844235	2.451906	-1.485313
C14	3.031804	0.436321	-1.559494
C15	4.297657	2.508338	-1.418999
C16	-4.296160	-2.504992	-1.424522
C17	-1.876085	-0.280095	1.565257
C18	-1.844195	2.448232	1.489535
C19	-0.612616	0.361779	1.518883
C20	-3.031841	0.432582	1.560563
C21	-0.660184	1.784940	1.496526
C22	0.611197	-0.365546	1.518375
C23	1.874632	0.276286	1.566024
C24	0.658814	-1.788685	1.493760
C25	1.842866	-2.451905	1.485929
C26	3.030415	-0.436312	1.560492
C27	4.296210	-2.508398	1.419770
C28	-4.297519	2.504987	1.423175
H29	-1.898689	-3.529721	-1.463139
H30	-1.960412	1.358844	-1.608182
H31	-4.004559	0.043466	-1.593941
H32	-0.240663	2.388503	-1.485650
H33	1.900094	3.533360	-1.456600
H34	4.005927	-0.039645	-1.592204
H35	4.137209	3.564472	-1.629013
H36	5.012137	2.104905	-2.137472
H37	-4.697263	-2.400515	-0.412161
H38	-4.136532	-3.559903	-1.641287
H39	-5.012232	-2.097103	-2.138851
H40	-1.961824	-1.358827	1.607799
H41	-4.005968	-0.043409	1.592532
H42	-1.900012	3.529737	1.462594
H43	-0.242011	-2.388532	1.485581
H44	1.898738	-3.533361	1.457187
H45	4.004515	0.039674	1.593508
H46	4.698360	-2.400124	0.408229

H47	4.136253	-3.564105	1.632335
H48	-4.699053	2.399430	0.411104
H49	-4.137698	3.560120	1.638690
H50	-5.013328	2.097947	2.138257
H51	1.961727	-1.354963	-1.609476
H52	0.242031	-2.384729	-1.488937
H53	0.240727	2.384688	1.489638
H54	1.960327	1.354962	1.610076
H55	5.011607	-2.103278	2.136361
H56	4.701246	2.397946	-0.408270

[a]Part of the Gaussian output file:

SCF Done: E(RM06) =   -1149.51126094   A.U. after   9 cycles

	1	2	3
	A	A	A
Frequencies --	34.3269	40.6756	62.6214
Red. masses --	4.4354	4.8726	2.9089

Zero-point correction=   0.476157 (Hartree/Particle)
Thermal correction to Energy=   0.502301
Thermal correction to Enthalpy=   0.503245
Thermal correction to Gibbs Free Energy=   0.421145
Sum of electronic and zero-point Energies=   -1149.035103
Sum of electronic and thermal Energies=   -1149.008960
Sum of electronic and thermal Enthalpies=   -1149.008016
Sum of electronic and thermal Free Energies=   -1149.090116

| Item	Value	Threshold	Converged?
Maximum Force	0.000006	0.000450	YES
RMS Force	0.000001	0.000300	YES

Table S40. Electronic transitions computed by TD-DFT for the closed-shell singlet state of the non-derivatized $(MV^+)_2$ in a staggered fashion using the M06/6-311+G(2d,p) level under water solvated model (PCM):

Excitation energies and oscillator strengths ($\lambda > 200$ nm, f > 0.02 only):

Excited State   1:   Singlet-A   1.3748 eV   901.82 nm   f=0.1774   <S**2>=0.000
        99 ->100   0.73833
        99 <-100   -0.21892

Excited State   3:   Singlet-A   2.2553 eV   549.74 nm   f=0.0844   <S**2>=0.000
        99 ->101   0.60748

```
99 ->103           0.35550

Excited State    5:      Singlet-A      2.7883 eV  444.67 nm  f=0.3109  <S**2>=0.000
      98 ->100        -0.14961
      99 ->101        -0.33936
      99 ->103         0.60167

Excited State    7:      Singlet-A      3.0777 eV  402.85 nm  f=0.1280  <S**2>=0.000
      99 ->102        -0.11994
      99 ->106         0.68886

Excited State   10:      Singlet-A      3.2538 eV  381.04 nm  f=0.0212  <S**2>=0.000
      99 ->108         0.70169

Excited State   15:      Singlet-A      3.8763 eV  319.85 nm  f=0.0897  <S**2>=0.000
      98 ->100        -0.35975
      99 ->114         0.58465

Excited State   18:      Singlet-A      4.0119 eV  309.04 nm  f=0.6017  <S**2>=0.000
      98 ->100         0.56420
      99 ->101        -0.10459
      99 ->114         0.38121

Excited State   20:      Singlet-A      4.0717 eV  304.50 nm  f=0.0289  <S**2>=0.000
      99 ->118         0.69529

Excited State   22:      Singlet-A      4.1723 eV  297.16 nm  f=0.2802  <S**2>=0.000
      97 ->100         0.67336
      99 ->113        -0.15878

Excited State   30:      Singlet-A      4.6346 eV  267.52 nm  f=0.0207  <S**2>=0.000
      95 ->100         0.69466

Excited State   47:      Singlet-A      5.5923 eV  221.70 nm  f=0.0221  <S**2>=0.000
      94 ->100         0.12823
      97 ->102         0.55935
      98 ->103        -0.24789
      99 ->138         0.12542
      99 ->141         0.24234

Excited State   54:      Singlet-A      5.7966 eV  213.89 nm  f=0.2969  <S**2>=0.000
      94 ->101        -0.13022
      96 ->102         0.66660
      97 ->104        -0.10319

Excited State   56:      Singlet-A      5.8899 eV  210.50 nm  f=0.0669  <S**2>=0.000
      96 ->101         0.22882
      98 ->104         0.61153
      98 ->105        -0.18693

Excited State   68:      Singlet-A      6.1007 eV  203.23 nm  f=0.1833  <S**2>=0.000
      96 ->103         0.60705
      98 ->105         0.29565
```
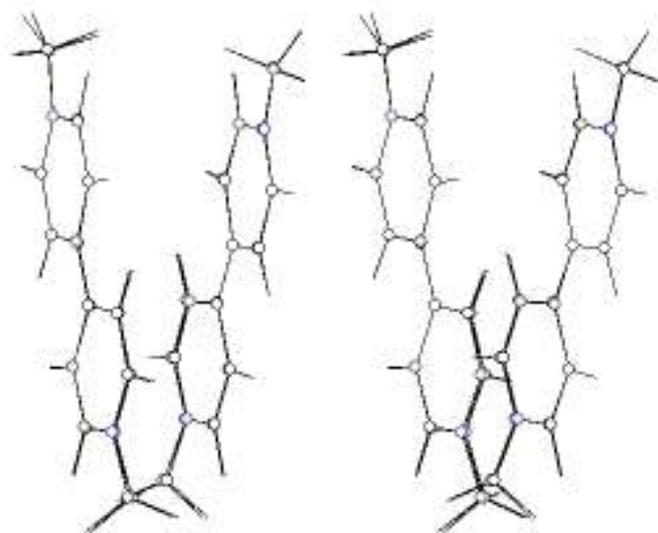
Figure S19. Geometries of non-derivatized $(MV^+)_2$ (closed-shell singlet) optimized using the M06/6-31G**/PCM and M06/6-311+G(2d,p)/PCM level of DFT are superimposed in a stereo mode.
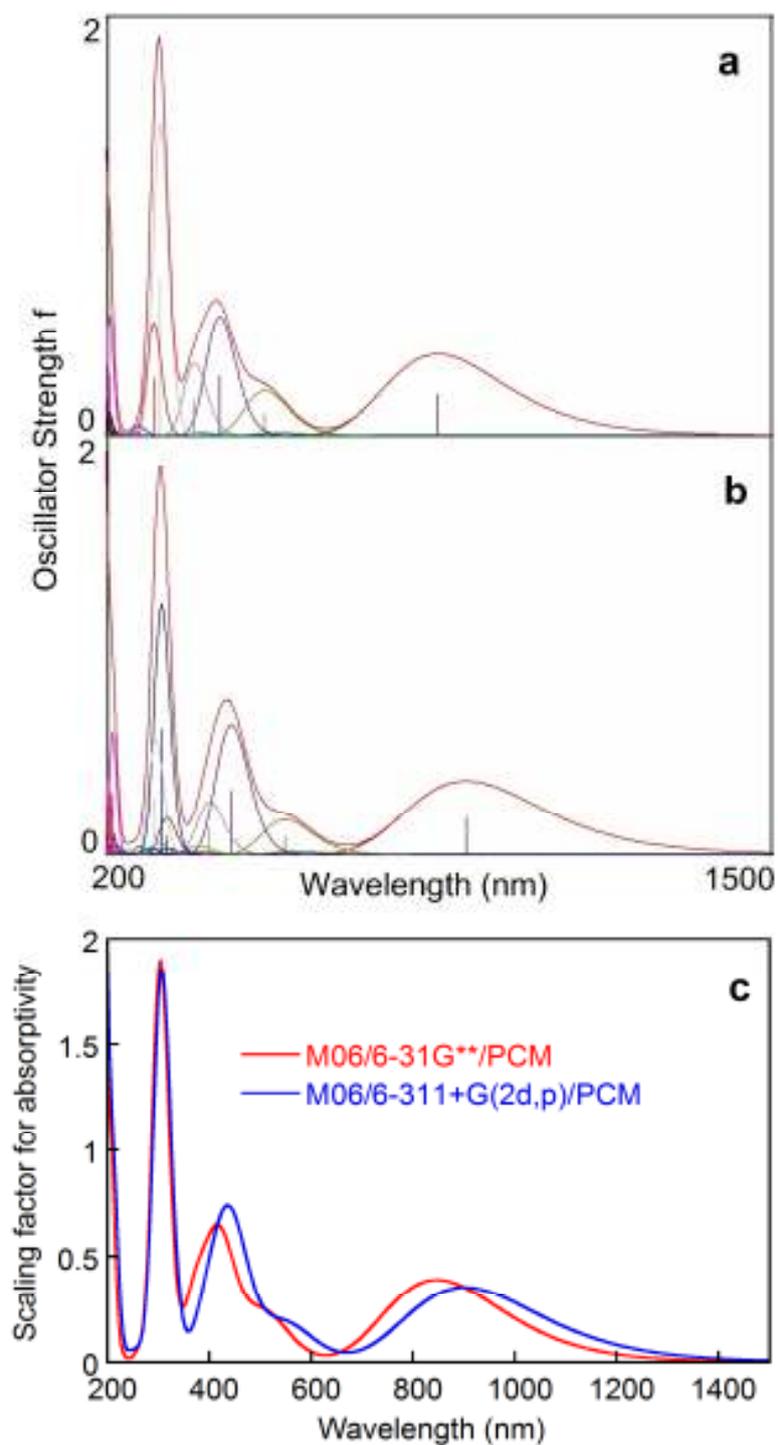
Figure S20. Calculated absorption spectra of the staggered π-dimers of non-derivatized MV^+, i.e., $(MV^+)_2$, in its closed-shell singlet state, optimized using (a) M06/6-31G** or (b) M06/6-311+G(2d,p) level under water solvated model (PCM, polarizable continuum model). (c) Comparison of calculated absorption spectra.
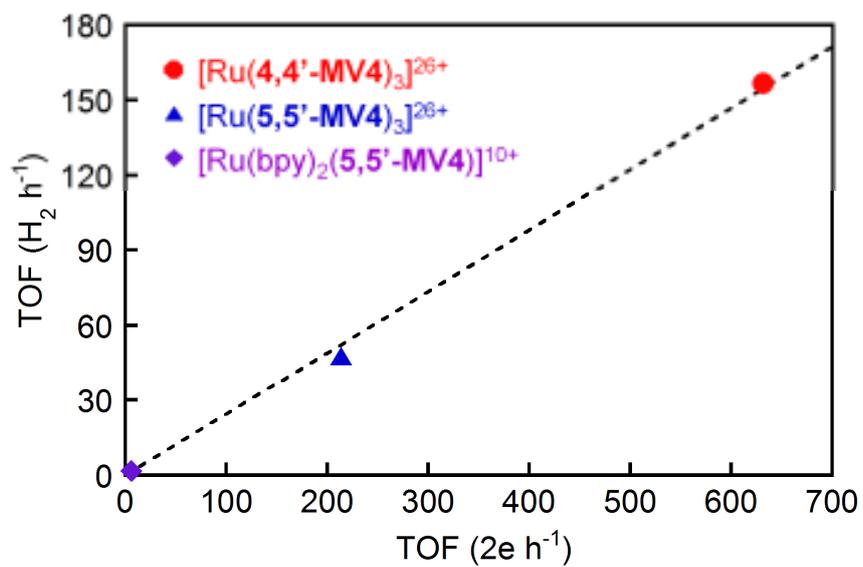
Figure S21. Linear relationship between the rate of H_2 evolution shown in Fig. 9A and the rate of electron charging shown in Fig. 5.
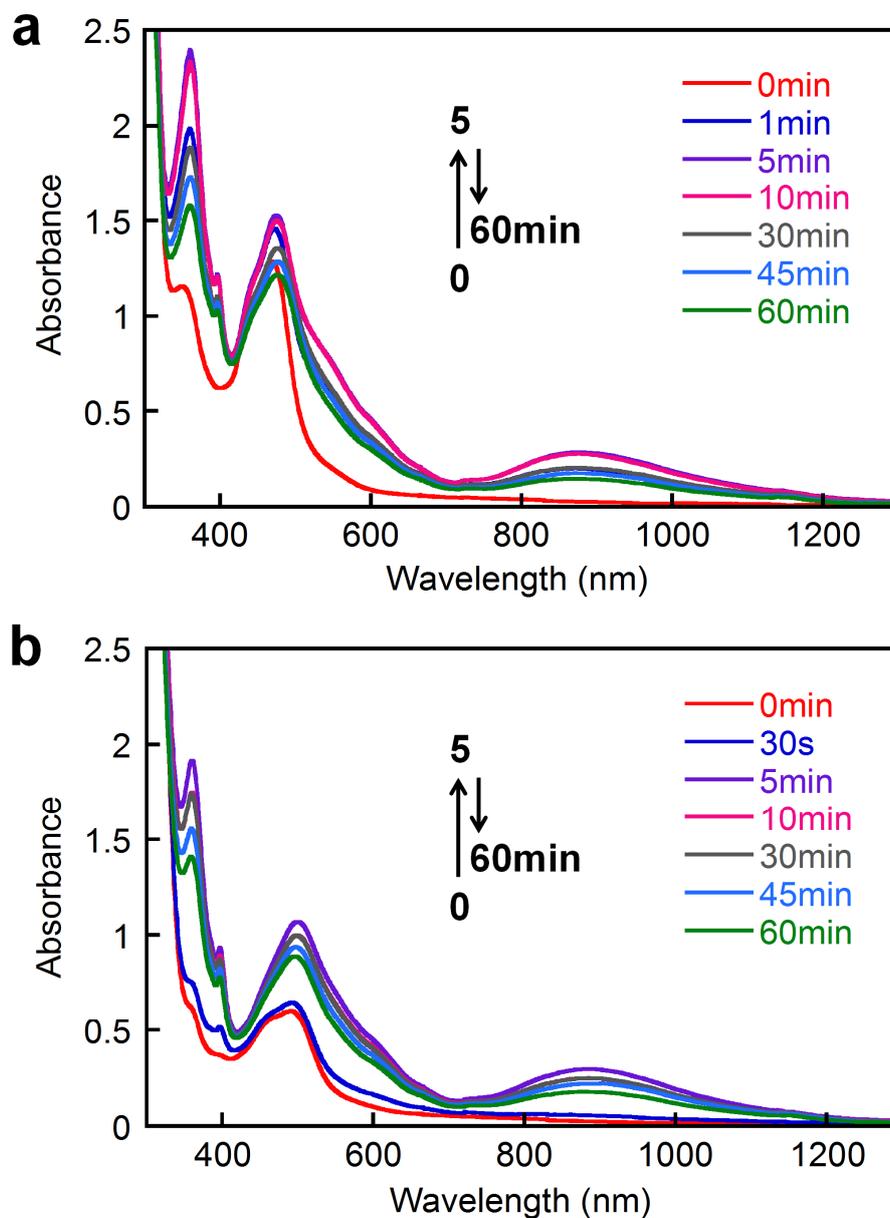
Figure S22. Spectral changes during the photolysis of an aqueous acetate buffer solution (0.03 M CH$_3$COOH, 0.07 M CH$_3$COONa; pH = 5.0) containing 30 mM EDTA and PVP-protected colloidal Pt (0.1 mM on the basis of the net Pt atom concentration) in the presence of (a) 0.04 mM [Ru(**4,4'-MV4**)$_3$](PF$_6$)$_{26}$ and (b) 0.04 mM [Ru(**5,5'-MV4**)$_3$](PF$_6$)$_{26}$ at 20 °C under Ar atmosphere.
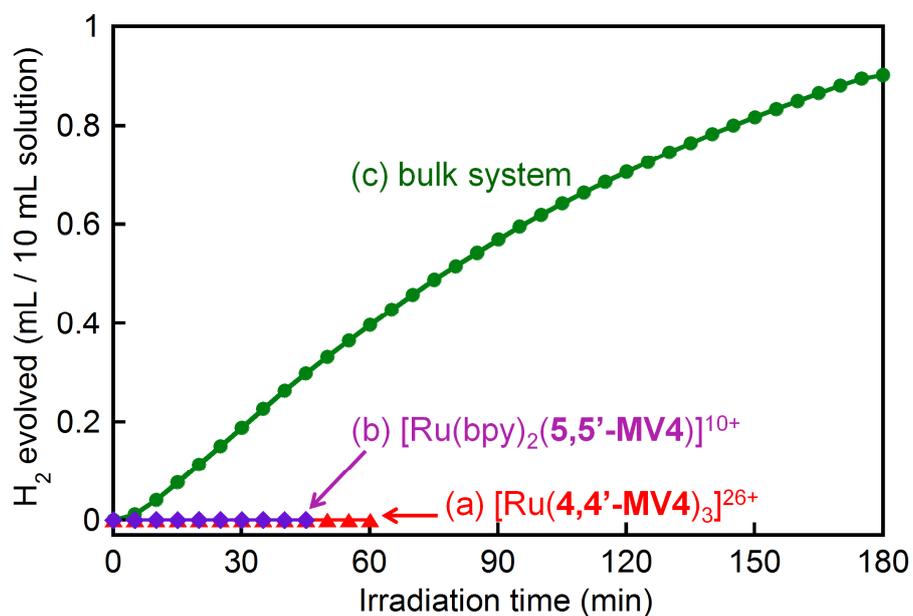
Figure S23. Photochemical H_2 evolution from an aqueous acetate buffer solution (0.1 M, pH = 5.0) containing TEOA (30 mM) and PVP-protected colloidal Pt (0.1 mM on the basis of the net Pt atom concentration) in the presence of (a) 0.04 mM [Ru(**4,4'-MV4**)$_3$](PF$_6$)$_{26}$, (b) 0.04 mM [Ru(bpy)$_2$(**5,5'-MV4**)](PF$_6$)$_{10}$, or (c) 0.04 mM [Ru(bpy)$_3$](NO$_3$)$_2$ and 2 mM MV(NO$_3$)$_2$, under Ar atmosphere at 20 °C under visible light irradiation (300 W Xe; λ > 400 nm).

Supplementary References

1. K. Kitamoto and K. Sakai, *Angew. Chem. Int. Ed.*, 2014, **53**, 4618.

2. M. Ogawa, B. Balan, G. Ajayakumar, S. Masaoka, H.-B. Kraatz, M. Muramatsu, S. Ito, Y. Nagasawa, H. Miyasaka and K. Sakai, *Dalton Trans.*, 2010, **39**, 4421.

3. A. R. Oki and R. J. Morgan, *Synth. Commun.* 1995, **25**, 4093.

4. H. Ishida, M. Kyakuno and S. Oishi, *Biopolymers*, 2004, **76**, 69.

5. I. P. Evans, A. Spencer and G. Wilkinson, *J. Chem. Soc., Dalton Trans.*, 1973, **9**, 204.

6. K. Sakai, Y. Kizaki, T. Tsubomura and K. Matumoto, *J. Mol. Catal.*, 1993, **79**, 141.

7. M. Kobayashi, S. Masaoka and K. Sakai, *Dalton Trans.*, 2012, **41**, 4903.

8. H. Goto and E. Osawa, *J. Chem. Soc., Perkin Trans. 2*, 1993, **2**, 187.

9. N. L. Allinger, *J. Am. Chem. Soc.*, 1977, **99**, 8127.

10. N. L. Allinger, Y. H. Yuh and J.-H. Lii, *J. Am. Chem. Soc.*, 1989, **111**, 8551.

11. J. P. Bowen and J.-Y. Shim, *J. Comp. Chem.*, 1998, **19**, 1370.

12. M. J. Frisch, *et al.* Gaussian 09 Revision C.01 (Gaussian Inc., Wallingford CT, 2009).

13. Y. Zhao and D. G. Truhlar, *Theor. Chem. Acc.*, 2008, **120**, 215.

14. Y. Zhao and D. G. Truhlar, *J. Phys. Chem. A*, 2008, **112**, 1095.

15. Y. Zhao and D. G. Truhlar, *Acc. Chem. Res.*, 2008, **41**, 157.

16. V. Barone, M. Cossi and J. Tomasi, *J. Comp. Chem.*, 1998, **19**, 404.

17. M. Cossi, G. Scalmani, N. Rega and V. Barone, *J. Chem. Phys.*, 2002, **117**, 43.

18. J. Tomasi, B. Mennucci and R. Cammi, *Chem. Rev.*, 2005, **105**, 2999.

19. M. E. Casida, C. Jamorski, K. C. Casida and D. R. Salahub, *J. Chem. Phys.*, 1998, **108**, 4439.

20. R. E. Stratmann, G. E. Scuseria and M. J. Frisch, *J. Chem. Phys.*, 1998, **109**, 8218.

21. R. Bauernschmitt and R. Ahlrichs, *Chem. Phys. Lett.*, 1996, **256**, 454.

22. GaussView, Version 5, R. Dennington, T. Keith, and J. Millam, *Semichem Inc.*, Shawnee Mission, KS, 2009.

23. A. Juris and V. Balzani, *Coord. Chem. Rev.*, 1988, **84**, 85.

24. M. Ogawa, G. Ajayakumar, S. Masaoka, H.-B. Kraatz and K. Sakai, *Chem.–Eur. J.*, 2011, **17**, 1148.

25. J. W. Park, N. H. Choi and J. H. Kim, *J. Phys. Chem.*, 1996, **100**, 769.